UNIVERSITÄT OSNABRÜCK

Isothermal quantum dynamics: Investigations for the harmonic oscillator

Dem Fachbereich Physik der Universität Osnabrück
zur Erlangung des Grades eines

Doktors der Naturwissenschaften

vorgelegte Dissertation von

Dipl.–Phys. Detlef Mentrup

aus Georgsmarienhütte

Osnabrück, Januar 2003

Betreuer	:	PD Dr. J. Schnack
Zweitgutachter	:	Prof. Dr. M. Luban

The key principle of statistical mechanics is as follows:

If a system in equilibrium can be in one of N states, then the probability of the system having energy E_n is $(1/Q)\, e^{-E_n/k_BT}$, where $Q = \sum_{n=1}^{N} e^{-E_n/k_BT}$. (...)

If we take $|\, i\,\rangle$ as a state with energy E_i and $\underset{\sim}{A}$ as a quantum mechanical operator for a physical observable, then the expected value of the observable is $\langle\langle\, \underset{\sim}{A}\,\rangle\rangle = 1/Q \sum_{|\, i\,\rangle} \langle\, i\,|\, \underset{\sim}{A}\,|\, i\,\rangle e^{-E_i/k_BT}$.

This fundamental law is the summit of statistical mechanics, and the entire subject is either the slide-down from this summit, as the principle is applied to various cases, or the climb-up to where the fundamental law is derived and the concepts of thermal equilibrium and temperature clarified.

R. P. Feynman, *Statistical mechanics* [1, ch. 1]

Contents

List of Figures

1. Introduction

In a macroscopic system, the number of particles or degrees of freedom is extremely large, such that it is impossible to obtain a complete physical description of the system, both experimentally and theoretically. For example, the microscopic state of a classical gas includes all positions and momenta of $\sim 10^{23}$ particles. However, the detailed behaviour of the constituents is not reflected on a macroscopic scale, where one is only interested in a few properties of a system, e. g., we only require that a given system has N particles, a volume V and an energy in a small interval around the value E. These macroscopic conditions are met by a large number of microscopic states. The mental collection of systems that are in these states is called an ensemble. The typical problem in statistical physics is the determination of averages over such ensembles.

The three ensembles that are usually dealt with in standard textbooks on statistical physics are the microcanonical (constant number of particles N, volume V, energy E), the canonical (constant N, V, temperature T) and the grand-canonical (constant chemical potential μ, V, T) ensemble. Each of the ensembles is characterised by a distribution function that describes the probability for a macroscopically prepared system to be in a given microscopical state, which is, in classical physics, given by a point in the phase space of the system, whereas in quantum physics it is given by a state vector in Hilbert space. The determination of this distribution function is the fundamental question that is answered by statistical mechanics. The distribution function permits the calculation of ensemble averages and, more generally, of the partition function, which is of outstanding importance in statistical mechanics since it contains the whole thermodynamics of a system.

If $f(q,p)$ denotes the classical unnormalised distribution function on the phase space Γ (with configuration coordinates $(q_1, \dots q_N) = q$ and conjugate momenta $(p_1, \dots p_N) = p$), a classical statistical ensemble average $\langle\langle\, B \,\rangle\rangle$ of an observable $B(q,p)$ (which in classical mechanics is a function on phase space) is given by the phase space integral

$$\langle\langle\, B \,\rangle\rangle = \frac{1}{Z_{cl}} \int_\Gamma \mathrm{d}q\mathrm{d}p\, B(q,p) f(q,p) \;, \tag{1.1}$$

i. e. the phase space function corresponding to the macroscopic observable has to be averaged over properly weighted microstates. The quantity

$$Z_{cl} = \int_\Gamma \mathrm{d}q\mathrm{d}p\, f(q,p) \;, \tag{1.2}$$

which is used to normalise the above expression, is called the classical partition function.

A direct evaluation of the high-dimensional integrals (1.1) and (1.2) is possible only in very particular cases, such as the ideal gas. In more general cases, e. g. for interacting many-particle systems, it is usually impossible. In order to be able to investigate the wide variety of physically interesting phenomena of these systems, a large number of techniques has been developed for the evaluation of ensemble averages, which can basically be divided into two groups: The stochastic or Monte Carlo methods that make use of random numbers, and the deterministic methods.

The latter are used in the context of molecular dynamics simulations and will be in the focus of the present work.

The basic idea of molecular dynamics (MD) simulations is to solve Hamilton's equations of motion for the particles of a given system numerically to obtain the temporal trajectories $q(t)$, $p(t)$ of all particles in phase space. This is, despite the large number of particles and possibly complicated interactions, usually possible given the availability of both accurate numerical methods and fast computers. Now, in order to calculate an ensemble average, one averages over the time evolution, and hopes that the *ergodic hypothesis* is satisfied. Loosely speaking, this means that the trajectory runs through the allowed region of phase space[1] with the correct weight such that the average over the time evolution of the system is equivalent to the average over the corresponding statistical ensemble:

$$\lim_{\tau\to\infty}\frac{1}{\tau}\int_0^\tau \mathrm{d}t\, B(q(t),p(t)) = \frac{1}{Z_{cl}}\int_\Gamma \mathrm{d}q\mathrm{d}p\, B(q,p)f(q,p)\ . \tag{1.3}$$

In Monte Carlo (MC) methods, one introduces an artificial dynamics on phase space which is based on random numbers. MC simulations are very powerful and popular for static properties. The most common type of MC simulations, the Metropolis Monte Carlo method [2], is naturally adapted to the canonical ensemble. It allows a direct sampling of the Boltzmann distribution by generating a Markov chain with a suitable transition rule and using rejections to achieve detailed balance. The dynamics obtained in an MC simulation also needs to be ergodic in the sense that the random walk needs to sample the entire allowed phase space such that MC averages and ensemble averages coincide. However, since in MC one does not rely on a "real" (i. e., physically meaningful) dynamics, this is less of a problem. In case of non-ergodic behaviour, one has to invent more elaborate transition rules.

Usually molecular dynamics calculations are performed with a fixed number of particles in a given volume of constant shape. In addition, as a consequence of Hamilton's equations, the energy of the system is conserved during time evolution. Therefore, if the trajectory passes uniformly through all parts of phase space that have the specified energy, the time average one obtains from an MD simulation corresponds to a microcanonical ensemble average. Only phase space points which lie on the hypersurface described by the condition of constant energy $H(q,p) = E$ contribute to the equilibrium ensemble average, and they contribute with equal weight according to the principle of equal *a priori* probability. The corresponding probability density in phase space is therefore given by

$$f(q,p) = \delta(H(q,p) - E)\ . \tag{1.4}$$

As a conclusion, the microcanonical ensemble may be considered as the *natural* ensemble for MD simulations.

However, if this approach to the calculation of ensemble averages were limited to the microcanonical ensemble, it would be practically useless. Experiments are usually carried out at constant temperature (and pressure), and therefore it is desirable to have techniques to realise different types of thermodynamic ensembles in MD simulations. More specifically, in order to obtain a canonical ensemble average, the above technique is inadequate, since in the canonical ensemble, the condition of constant energy is replaced by a *condition of constant temperature*, and the distribution function (1.4) is replaced by a Boltzmann distribution[2],

$$f(q,p) = \exp(-\beta H(q,p))\ . \tag{1.5}$$

[1] The term "allowed" refers to the constraints imposed on the system.

[2] In this work, we will use the notation T for the temperature, and $\beta = 1/k_B T$ in parallel, k_B being Boltzmann's constant.

The total energy of the system is allowed to fluctuate around its mean value by thermal contact with an external heat reservoir which allows for energy exchange. The physical effect of the heat bath upon the system of interest is to impose a constant temperature condition, while the details of the thermal interactions are usually unknown. How can this modified situation be described on the level of the equations of motion, such that the temperature value can be given beforehand as a fixed parameter? Clearly, a mechanism is needed that introduces suitable energy fluctuations. We will call such a mechanism a thermostat.

The constant temperature condition is certainly fulfilled for a Brownian particle which is a macroscopic particle immersed into a liquid of a given temperature. Energy transfer takes place via the ceaseless random collisions between the Brownian particle and the constituents of the liquid. The motion of the particle is described by the so-called Langevin equation, and it has been shown in 1945 that under appropriate conditions, the long-time limit of a time average over the solution of the Langevin equation corresponds to a canonical ensemble average [3]. The Langevin equation involves a stochastic force that mimics directly the collisions mentioned above, therefore we call this approach a stochastic thermostat. In contrast to pure MC sampling, this phenomenological equation is based on Newton's equation of motion and includes only a "moderate" amount of randomness.

It is surprising that beyond this direct modelling of the heat bath interaction, a different technique which is *completely deterministic* has been initiated by Nosé in 1984 [4]. His original method was based on the idea of a scaling of the particle momenta, allowing energy fluctuations and thereby temperature control by a control of the kinetic energy. Although formally correct, the original formulation featured ergodicity problems and therefore was not applied very much in practice. Later on, numerous extensions and refinements have been added that turned out to be more efficient and easier to handle. These modified techniques are known as extended system methods. Their common underlying idea is to append additional degrees of freedom to the original physical system that act as pseudofriction terms, thereby destroying energy conservation and, moreover, the overall Hamiltonian structure of the dynamics. The equations of motion of the enlarged system are designed in such a way that in the subspace belonging to the original physical system, the temporal average corresponds to a canonical average. To ensure this, the equipartition theorem of classical statistical mechanics is implicitly exploited. Extended system methods are commonly used nowadays in classical MD simulations [5, 6] and have turned out to be extremely powerful.

The main advantage a molecular dynamics approach has over Monte Carlo is that in the course of an MD simulation, physically reasonable dynamical equations are integrated. This makes dynamical information available, even though one can argue that the particular constant temperature methods appear somewhat artificial. Consequently, dynamical properties such as time correlation functions may be calculated. Monte Carlo simulations are not suitable for the determination of dynamical physical properties and allow only the calculation of static properties, unless one accepts that the random walk generated by MC is an interesting physical dynamical model.

In the field of finite-temperature simulations of *quantum systems*, the most successful approach is based on the path-integral formulation by Feynman [1]. The power of the method is due to the fact that it allows to relate the quantum density matrix at arbitrary temperature, $e^{-\beta \underset{\sim}{H}}$, where $\underset{\sim}{H}$ is the Hamiltonian of the system, to integrals over paths in coordinate space,

$$\langle R | \, e^{-\beta \underset{\sim}{H}} \, | R' \rangle = \int \cdots \int \mathrm{d}R_1 \ldots \mathrm{d}R_M \, \exp(-S(R_1, \ldots R_M)) \; . \tag{1.6}$$

S is the so-called *action* of the path and is real, and thus (1.6) involves a basically classical

distribution function, such that one can use classical molecular dynamics [7] or Monte Carlo techniques [8] to evaluate the integral. The latter have been applied very successfully to the interacting boson system ^{4}He that undergoes the famous λ-transition at $T = 2.18\,K$ [8], and to bosons in a magnetic trap [9]. However, for fermions, the contributions of even and odd permutations to the density matrix involve opposite signs due to the required antisymmetry of the wave function. The cancellation of contributions usually causes the signal/noise ratio to approach zero rapidly and rules out a straightforward MC evaluation of the integrand. This is known as the "fermion sign problem".

The main obstacle to an approach to the calculation of ensemble averages via time averaging over the quantum time development is the fact that the solution of the Schrödinger equation is *not* readily available for complicated systems. Contrary to the classical case, quantum dynamics itself is a very hard computational problem. In essence, the quantum time evolution implies to calculate an exponential of the Hamiltonian, which is practically equivalent to treating the canonical density operator directly. On this level, the ansatz of time averaging does not lead to substantial computational advantages. Nevertheless, the question whether it is possible to determine canonical averages for a quantum system by averaging over trajectories generated by an appropriate dynamics is challenging.

The interest for techniques comparable to the classical extended system methods in the realm of finite-temperature quantum MD simulations has different sources. On the one hand, even for relatively simple quantum systems constisting of a very small number of particles, it is usually impossible to determine the full set of eigenfunctions and eigenvalues. Given the availability of various efficient approximate quantum MD schemes (for a review of techniques for fermions, see [10]), the following question is interesting from a methodological point of view: Does a generalisation of the classical methods to quantum dynamics permit to make the power of approximate quantum MD schemes available for the calculation of equilibrium averages without diagonalising the full many-body Hamiltonian? The present work may be considered a first step towards an affirmative answer to this demanding question. Beyond, given the fact that quantum MC has a non-physical time evolution, it is highly desirable to have an isothermal quantum MD method at hand that depicts the physical dynamics of the system at a given finite temperature more realistically. This would enlarge the variety of techniques available in many-body theory and possibly extend their overall range of applicability.

Apart from permitting the determination of equilibrium ensemble averages, the classical extended system methods also offer a model scenario for the dynamical evolution of a non-equilibrium state towards thermal equilibrium. Although it is not clear whether the specific approach using pseudofriction terms is a faithful physical picture of the real dynamical evolution of a system enroute to thermal equilibrium, this view is a natural interpretation of the methods that permit "cooling" and "heating" of non-equilibrium initial states. Consequently, one may hope that a quantum analogue of the classical methods models the approach of a quantum system to equilibrium.

On the other hand, real physical systems such as ultracold trapped gases are in the focus of modern research for which such a method appears to be tailor-made and may allow for the direct theoretical analysis of systems in a constant temperature condition. Recently, investigations of ultracold magnetically trapped atomic gases have led to the discovery of intriguing physical phenomena, among them the spectacular evidence for Bose-Einstein condensation in weakly interacting Bose gases [11, 12]. On the fermionic side, researchers study the large impact of Fermi-Dirac statistics on the behaviour of so-called degenerate Fermi gases [13, 14]. It is remarkable that these systems constitute dilute gases in which the interparticle interactions are *weak*. For fermions, the quantum statistical suppression of s-wave interactions makes an

ultracold trapped gas of fermionic atoms even an *excellent* realisation of an ideal gas. In addition, we note that the confinement by the magnetical trap may approximately be considered as harmonic [15]. Beyond, from a theorist's point of view, the ideal gas forms the starting point for perturbative treatments of interacting many-particle assemblies, and motion in a common harmonic oscillator potential is of special interest because of its importance for low-excitation dynamics. Therefore, it appears reasonable to start with this tractable case. In *interacting* fermion systems, a number of other fascinating effects is discussed, e. g., theorists have studied the prospects of observing a superfluid phase based on the BCS concept of Cooper-pair formation [16].

First ideas for a translation of classical constant temperature MD methods to quantum mechanics have been discussed by Grilli and Tosatti in 1989 [17], but their approach has turned out to have serious shortcomings [18] some of which are discussed in appendix A. An alternate method due to Kusnezov [19] is limited to quantum systems of finite dimensionality and has only been applied to a two-level system. Schnack has investigated a quantum system at constant temperature using a thermometer and a feedback mechanism to drive the system to the desired temperature value by complex time steps [20]. The main drawback of this ansatz is the fact that an interaction is needed to equilibrate the system of interest and the thermometer, which leads to a perturbation of the original system and thereby excludes simulations at very low temperatures. This illustrates a main difficulty encountered in quantum mechanics: While in classical mechanics, the equipartition theorem provides a direct and infallible "thermometer", such a useful a priori relation between the average value of some observable and temperature is not readily at hand in quantum mechanics. Instead, it needs to be implemented in a sophisticated manner, involving a number of difficulties, like the perturbation due to the interaction and the insecurity about correct equilibration between system and thermometer.

In view of this unsatisfactory situation, the major goal of the present work has been to devise a quantum thermostat following the lines of the methods successfully employed in classical mechanics. We will show that in the case of an ideal quantum gas enclosed in an external harmonic oscillator potential, the framework of coherent states permits new, far-reaching methodological developments. For a single quantum particle, the analogy to classical physics is very close, whereas for two non-interacting indistinguishable quantum particles genuine quantum features have been found and investigated. It turns out that the approach based on the classical Langevin equation is not suitable for identical particles, whereas the extended system methods can successfully be translated to quantum mechanics.

The outline of the present work is as follows. Chapter 2 deals with temperature control methods in classical mechanics, namely the Langevin equation and the extended system method of Nosé and Hoover along with its refinements. Chapter 3 gives a brief introduction to coherent states and their properties. Chapter 4 contains the main outcome of this work, presenting the unprecedented quantum thermostat methods for one and two particles, and N fermions in an external harmonic oscillator potential. In chapter 5, the results obtained with the new methods are presented. Chapter 6 summarises the work and gives a critical analysis of the chances and limits of the quantum thermostat method devised in this work.

2. Methods of isothermal classical dynamics

2.1. Stochastic temperature control: The classical Langevin equation

The Langevin equation may be regarded as a phenomenological approach to temperature control in classical mechanics. It has been developed to describe the irregular motion of a macrosopic (so-called *Brownian*) particle immersed into a liquid of absolute temperature T. The main idea is to describe the action of the liquid that acts as a heat bath upon the particle by two additional forces that are introduced in Newton's equation of motion: Firstly, a slowly varying frictional force proportional to the velocity of the particle, $-m\gamma \frac{d}{dt}q$, where m is the mass of the particle and γ is a constant frictional coefficient, and secondly, a rapidly fluctuating random force $F(t)$ that describes the disordered collisions of the particles of the liquid with the Brownian particle and that vanishes on average. If in addition the particle moves in an external potential $V(q)$, the resulting equation describing its motion on the spatial q-axis reads

$$m\frac{d^2q}{dt^2} = -\frac{\partial V}{\partial q} - m\gamma\frac{dq}{dt} + F(t) \ . \tag{2.1}$$

Equivalently, one can study the set of equations of first order in time,

$$\frac{dq}{dt} = \frac{p}{m} \ , \qquad \frac{dp}{dt} = -\frac{\partial V}{\partial q} - \gamma\, p + F(t) \ . \tag{2.2}$$

The time average of $F(t)$ vanishes,

$$\lim_{\tau\to\infty}\frac{1}{\tau}\int_0^\tau F(t)\mathrm{d}t = 0 \ , \tag{2.3}$$

and $F(t)$ shall be purely random, which means that it has a vanishingly short correlation time[1]. Moreover, the amplitude of the random force is related to the temperature T and the friction coefficient γ by the second fluctuation-dissipation theorem, which together is expressed as

$$\langle\langle\ F(t_1)F(t_2)\ \rangle\rangle = 2\,m\gamma k_B T\delta(t_1 - t_2) \ . \tag{2.4}$$

In addition, for technical reasons, one must assume that the random force is Gaussian, i. e. one assumes that the coefficients of the Fourier series of $F(t)$ (which are random variables) are distributed according to a Gaussian distribution.

Equation (2.4) guarantees that the temperature is kept at a constant value by the balance between the thermal agitation due to the random force and the slowing down due to the friction. Under the assumptions made above, it has been shown that in the limit $t \to \infty$, the probability density $P(q,p;t|q_0,p_0)$ at the phase space point (q,p) given that at time $t = 0$ the particle was

[1] As a result of the Wiener-Khintchine-theorem that relates the correlation function of a stochastic function to its power spectrum [21], the spectral density of the fluctuating force is constant under this condition. Therefore, the spectrum of $F(t)$ is frequently said to be *white*.

situated at q_0 with initial momentum p_0 is the canonical Maxwell-Boltzmann density [3]. This limiting probability distribution is independent of the initial state of the system. Therefore, a time average over a sufficiently long period will be equivalent to a canonical ensemble average.

The proof that the limiting probability distribution of the Langevin equation (2.1) is a Maxwell-Boltzmann distribution uses a Fokker-Planck equation associated to (2.1) [3, 21]. In general, for a one-dimensional Markov process $y(t)$, the Fokker-Planck equation is a partial differential equation for the probability density $P(y,t|y_0)$ that is derived from the obvious condition

$$P(y,t+\Delta t|y_0) = \int \mathrm{d}z\; P(y,\Delta t|z)P(z,t|y_0)\;, \tag{2.5}$$

which is called the Smoluchowski equation, in the limit of small Δt and a small difference $y-y_0$. The resulting Fokker-Planck equation for a one-dimensional Markov process,

$$\frac{\partial P}{\partial t} = -\frac{\partial}{\partial y}(M_1(y)P) + \frac{1}{2}\frac{\partial^2}{\partial y^2}(M_2(y)P)\;, \tag{2.6}$$

contains the first and second moment of the change of the random variable y, the nth moment being defined as

$$M_n(y) = \lim_{\Delta t\to 0}\frac{1}{\Delta t}\int \mathrm{d}z\,(z-y)^n P(z,\Delta t|y)\;. \tag{2.7}$$

Equation (2.6) is derived assuming that the moments M_n vanish for $n>2$ which expresses the fact that in a short period of time, the spatial coordinate can only change by small amounts.

The Fokker-Planck equation for an n-dimensional Markov process $\mathbf{y}=(y_1,\ldots,y_n)$ reads

$$\frac{\partial P}{\partial t} = -\sum_{i=1}^{n}\frac{\partial}{\partial y_i}(M_1(\mathbf{y})P) + \frac{1}{2}\sum_{k,l=1}^{n}\frac{\partial^2}{\partial y_k\partial y_l}(M_{2kl}(\mathbf{y})P)\;. \tag{2.8}$$

The case of the harmonic oscillator, $V(q)=\frac{1}{2}m\omega^2q^2$, is particularly simple. The moments required in the Fokker-Planck equation can be determined, and the resulting equation for the probability density $P(q,p;t)$ reads explicitly

$$\frac{\partial P}{\partial t} = -\frac{p}{m}\frac{\partial P}{\partial q} + \frac{\partial}{\partial p}\Big(\big(\gamma\, p + m\omega^2 q\big)P\Big) + m\gamma k_BT\,\frac{\partial^2 P}{\partial p^2} \tag{2.9}$$

and may be solved analytically with the initial conditions

$$P(q,p,t{=}0) = \delta(q-q_0)\delta(p-p_0)\;. \tag{2.10}$$

The result is a two-dimensional Gaussian distribution in q and p with time-dependent average values and widths. In the limit $t\to\infty$, one obtains the Maxwell-Boltzmann distribution (C is a normalisation constant),

$$\lim_{t\to\infty}P(q,p;t|q_0,p_0) = C\exp\left(-\frac{1}{k_BT}\Big(\frac{p^2}{2m}+\frac{1}{2}m\omega^2q^2\Big)\right)\;, \tag{2.11}$$

which is a Gaussian distribution both in positions and momenta, independent of the initial conditions. Note that the amplitude of the random force (2.4) which contains the temperature T determines the width of the limiting Gaussian distribution.

We summarise the main points of this section. The long-time limit of a time average over the solution of the classical Langevin equation corresponds to a canonical ensemble average. In the simplest case of the harmonic oscillator, the solution of the Langevin equation provides an average with Gaussian distribution functions. This statement is verified by an explicit solution of the associated Fokker-Planck equation. The width of the Gaussians is determined by the amplitude of the fluctuating force via the fluctuation-dissipation relation.

2.2. Deterministic temperature control methods

While the Langevin approach is readily comprehensible and physically intuitive, it is less evident that a *completely deterministic* time development may also provide canonical averages. Such an alternate technique has originally been proposed by Nosé [4], and has been refined by Hoover [22], Kusnezov, Bulgac, and Bauer [23], and Martyna, Klein, and Tuckerman [24]. A review of these and various other constant temperature molecular dynamics methods can be found in [25]. Only recently [26], the theory of these methods was put on a firm theoretical ground, providing a valuable deeper view that we present in section 2.2.4.

In the original method of Nosé, temperature control in a molecular dynamics simulation is achieved by the introduction of an additional degree of freedom s that is used to scale time and thereby the particle velocities. This is reasonable since temperature is related to the average of the kinetic energy. However, Nosé's original formulation, although formally correct, features substantial problems in practice, and therefore, the method has been modified and refined. The so-called classical Nosé-Hoover thermostat with the extension to chains of thermostats and the so-called demon method have turned out to be most successful and reliable. Simply speaking, these methods exploit the equipartition theorem to determine the equations of motion of pseudofriction coefficients that are introduced in the equations of motion of the original system. These methods may be transferred to the quantum harmonic oscillator, which is why the functionality of these classical deterministic thermostats is the subject of the following paragraphs and will be outlined in detail.

2.2.1. The Nosé-Hoover method

Consider an isolated classical N-particle system in one dimension described by a Hamiltonian,

$$H(q,p) = \sum_{i=1}^{N} \frac{p_i^2}{2m} + V(q) \ . \tag{2.12}$$

As usual, the ith particle is located at position q_i with momentum p_i, and q (resp. p) is the N-tuple of all positions (momenta). The motion of the system in phase space is governed by Hamilton's equations,

$$\frac{d}{dt}\, q_i = \frac{\partial H}{\partial p_i} = \frac{p_i}{m} \ , \qquad \frac{d}{dt}\, p_i = -\frac{\partial H}{\partial q_i} = -\frac{\partial V(q)}{\partial q_i} \ . \tag{2.13}$$

In the Nosé-Hoover method, the equations of motion of the momenta p_i are supplemented by a term similar to a frictional force. In order to permit energy fluctuations, the frictional coefficient is regarded as time-dependent and can assume both positive and negative values. In contrast to the Langevin approach, a stochastic force is not employed. One wants to obtain canonical time averages solely from varying the frictional coefficient suitably in time.

In the original notation introduced by Hoover [22], the modified equations of motion read

$$\frac{d}{dt}\, q_i = \frac{p_i}{m}\ , \qquad \frac{d}{dt}\, p_i = -\frac{\partial V(q)}{\partial q_i} - \zeta(t)\, p_i\ , \tag{2.14}$$

where $\zeta(t)$ is a time-dependent supplementary degree of freedom added to the system to drive the energy fluctuations required in the canonical ensemble. Therefore, the Nosé-Hoover and related methods are frequently referred to as *extended system methods*.

From (2.14) it can be inferred that ζ acts as a pseudofriction coefficient. Both the value and the sign of ζ vary in time. Accordingly, the momenta of the original system either decrease or increase, which leads to a change of the kinetic energy of the system. This mechanism is used for temperature control. The key point is to determine the time dependence of ζ such that the energy fluctuations correspond to the canonical ensemble. More precisely, we demand that the weight with which the phase space of the original system is sampled in time is the canonical distribution function,

$$\exp\big(-\beta H(q,p)\big)\ . \tag{2.15}$$

On the level of the phase space of the extended system we postulate the distribution function

$$f(q,p,\zeta) = \exp\left(-\beta\Big(H(q,p) + \frac{1}{2}Q\zeta^2\Big)\right)\ . \tag{2.16}$$

Note that the Boltzmann distribution (2.15) is a marginal of f. The choice of the distribution function for ζ is related to the linear coupling $-\zeta p_i$ in the equation of motion (2.14). A different coupling would entail a different distribution function, as will become evident in the discussion of the demon method.

In order to make sure that f is sampled during time evolution, the time dependence of ζ is determined by the condition that f is the stationary solution of a generalised Liouville equation which we derive now. To fix the notation, let x denote a point in a (possibly enlarged) phase space. A distribution function $f(x)$ satisfies a continuity equation that expresses conservation of probability,

$$\frac{\partial f}{\partial t} + \mathrm{div}_x(f\dot{x}) = 0\ . \tag{2.17}$$

This equation is obtained by equating the local change of a conserved quantity inside a given volume and the flow of this quantity through the surface of this volume. On the other hand, the total time derivative of f along a phase space trajectory is defined by

$$\frac{d}{dt}\, f = \frac{\partial f}{\partial t} + \dot{x}\cdot\frac{\partial f}{\partial x}\ . \tag{2.18}$$

With this identity, (2.17) can be reexpressed as

$$\frac{d}{dt}\, f = -f\left(\frac{\partial}{\partial x}\cdot\dot{x}\right)\ . \tag{2.19}$$

Note the modified notation $\mathrm{div}_x\dot{x} \equiv \frac{\partial}{\partial x}\cdot\dot{x}$.

Now, if $x = (q,p)$ is an element of the phase space of a Hamiltonian system and the time evolution of the system is determined by Hamilton's equations of motion (2.13), the right hand side of this equation vanishes identically and Liouville's theorem $df/dt = 0$ holds. Its meaning

is that given an initial distribution in phase space, the local density of representative points does not change if we follow the solution of Hamilton's equations.

In the case of the Nosé-Hoover equations (2.14) on the enlarged phase space, i. e. with $x = (q, p, \zeta)$, we use this equation to determine an equation of motion for ζ so as to reproduce the postulated thermal distribution (2.16). In order to obtain an explicit equation, we impose the constraint $\partial\dot{\zeta}/\partial\zeta = 0$, and along with (2.14) we easily get for the right hand side of (2.19)

$$-f\left(\frac{\partial\dot{x}}{\partial x}\right) = -f\left(\sum_{i=1}^{N}\left(\frac{\partial}{\partial q_i}\dot{q}_i + \frac{\partial}{\partial p_i}\dot{p}_i\right) + \frac{\partial}{\partial\zeta}\dot{\zeta}\right) = fN\zeta\ . \tag{2.20}$$

Now, we calculate the left hand side of (2.19), employing the equations of motion (2.14),

$$\begin{aligned}\frac{d}{dt}\,f &= \frac{\partial f}{\partial p}\dot{p} + \frac{\partial f}{\partial q}\dot{q} + \frac{\partial f}{\partial\zeta}\dot{\zeta} \\ &= f\cdot\left(-\beta\sum_{i=1}^{N}\left(\frac{p_i}{m}\dot{p}_i + \frac{\partial V}{\partial q_i}\dot{q}_i\right) - \beta Q\zeta\dot{\zeta}\right) \\ &= f\,\beta\,\zeta\cdot\left(\sum_{i=1}^{N}\frac{p_i^2}{m} - Q\dot{\zeta}\right)\ .\end{aligned} \tag{2.21}$$

Equating (2.20) and (2.21) yields the following equation of motion for ζ:

$$\frac{d}{dt}\,\zeta = \frac{1}{Q}\left(\sum_{i=1}^{N}\frac{p_i^2}{m} - Nk_BT\right)\ . \tag{2.22}$$

It is interesting to notice that the time evolution of ζ is determined by the deviation of the momentary value of the kinetic energy $\sum_i p_i^2/2m$ from its canonical average value $N/2\ k_BT$. As a result, temperature control is achieved by a feedback mechanism: In case the momentary kinetic energy is larger than $N/2\ k_BT$, the time derivative of ζ is positive and ζ increases, so that the frictional force $-\zeta p_i$ reduces the momenta, thereby "cooling" the system. In the opposite case, the feedback mechanism heats the system up by accelerating the particles.

Besides, it is noteworthy that the influence of a heat bath may be imitated by adding a *single* supplementary degree of freedom to the original system. This is in striking contrast to the usual attributes of a heat bath, namely, that it is "larger" in comparison to the system of interest, which is usually exposed as "having much more degrees of freedom" [21, ch. 3.6]. Furthermore, we remark that in the Nosé-Hoover method, the canonical distribution in phase space is reproduced from a single thermodynamic average, the average of the kinetic energy.

For reasons of completeness, the following equation

$$\frac{d}{dt}\,\Theta = \zeta \tag{2.23}$$

is also solved in a simulation, since it contributes to the quantity

$$H' = H(q,p) + \frac{1}{2}Q\zeta^2 + Nk_BT\Theta \tag{2.24}$$

that is conserved by the set of equations of motion (2.14) and (2.22). We stress that the quantity (2.24) is *not* a Hamiltonian for the extended system; the equations of motion (2.14), (2.22) along with (2.23) do not have a Hamiltonian form. This is the reason why we considered

the non-Hamiltonian phase space (q, p, ζ) of odd dimensionality. We have abandoned the strict Hamiltonian structure in the present context. The question of a sound generalisation of the Hamiltonian phase space notions to a non-Hamiltonian system will be addressed more closely in section 2.2.4.

By construction, f is the static probability distribution generated by the dynamics (2.14) and (2.22). This condition is necessary, but not sufficient for the equivalence of a trajectory average and an ensemble average. It does not guarantee that the correct limiting distribution will be generated by the dynamics, since it is not clear whether the system actually runs through all phase space points with the correct weight, independent of the initial conditions. In fact, it might be possible that some regions of phase space are unreachable for the dynamics and therefore not sampled. Loosely speaking, the many body system needs to be sufficiently complex such that the dynamics will cover the entire phase space. The analysis by Tuckerman et al. presented in section 2.2.4 allows to expose this point very clearly.

This additional property, the equivalence of time average and ensemble average, is generally referred to as *ergodicity*. A strict proof of ergodic behaviour for a given system can rarely be given, however, it is observed that the more complex the dynamics of a system gets, the more likely ergodic behaviour is observed. This is intuitively understandable since it is clear that the number of unwanted conserved quantities decreases with increasing complexity. When using deterministic methods such as the Nosé-Hoover method, one usually checks the marginals of the additional degrees of freedom and hopes that if these marginals are sampled correctly, the phase space of the entire system is also sampled correctly [6].

There is an important example of apparent non-ergodic behaviour in the case of the Nosé-Hoover method. The classical harmonic oscillator cannot be thermalised by the simple scheme outlined above [22]. The shape of the Poincaré-sections in phase space strongly depends on the choice of the numerical value of Q, and the distributions sampled do in no case correspond to a canonical distribution. For other systems, among them classical spin systems, it was found that the simple Nosé-Hoover scheme may be ergodic for one temperature, but not ergodic for a different value of T [23, 6]. In addition, in all cases of non-ergodic behaviour, a strong dependence of the initial conditions is observed, which is unacceptable. In summary, the Nosé-Hoover method is not capable to reliably create canonical distributions.

However, more general schemes like the demon method or the method of chain thermostats basically resolve this problem by generating a more complex dynamics. A deeper study using the notions of section 2.2.4 sheds light on the problem underlying the non-ergodicity of the harmonic oscillator.

2.2.2. The demon method

In an effort to cure the problem of unpredictable non-ergodic behaviour in the Nosé-Hoover method, Kusnezov, Bulgac, and Bauer [23] have devised a generalised coupling scheme. Two additional degrees of freedom are used to replicate the interaction of the original system with a heat bath. The first one is coupled to the equations of motion of the positions, the second one to the momenta of the particles. This approach appears sensible since it takes into account the equality of positions and momenta in Hamiltonian mechanics. Another advantage of this method is that the Hamilton function of the envisaged system does not have to contain a kinetic energy term for temperature control; instead, the time derivative of the pseudofriction coefficients turns out to be proportional to the difference of two quantities whose ratio of canonical averages is $k_B T$. This extends the range of applicability of the method to, e. g., classical spin systems [27, 6].

Explicitly, the equations of motion of the KBB-scheme read

$$\frac{d}{dt}\, q_i = \frac{\partial H}{\partial p_i} - g_2'(\xi)\, F_i(q,p)\ , \qquad \frac{d}{dt}\, p_i = -\frac{\partial H}{\partial q_i} - g_1'(\zeta)\, G_i(q,p)\ . \tag{2.25}$$

The additional degrees of freedom ζ and ξ are frequently referred to as *demons* which are coupled to the equations of motion with the functions $g_1'(\zeta)$ and $g_2'(\xi)$. $F_i(q,p)$ and $G_i(q,p)$ are arbitrary functions of all coordinates and momenta. Note that the original Nosé-Hoover equations are obtained from (2.25) by the specific choice $G_i = p_i$, $g_1' = \zeta$, and $F_i = g_2' = 0$.

The phase space distribution function in the $(2N+2)$-dimensional extended phase space is chosen to be

$$f(q,p,\zeta,\xi) = C \exp\left(-\beta\Big(H(q,p) + \frac{1}{\kappa_1} g_1(\zeta) + \frac{1}{\kappa_2} g_2(\xi)\Big)\right)\ , \tag{2.26}$$

where C is again a normalisation constant, and κ_1 and κ_2 are, at the moment, free parameters. The functions g_1 and g_2 that determine the thermal distribution of the demons need to be chosen such that the integral of f with respect to ζ and ξ converges. Note that their respective derivatives g_1', g_2' appear in the equations of motion (2.25). This has been the reason for choosing a Gaussian distribution function for ζ in (2.16).

In order to derive equations of motion for ζ and ξ so as to reproduce the postulated thermal distribution (2.26), we substitute the equations of motion (2.25) and the distribution function f into the generalised Liouville equation (2.19) derived in the preceding section. In addition, we have the freedom to impose the constraints

$$\frac{\partial \dot{\zeta}}{\partial \zeta} = 0\ , \qquad \frac{\partial \dot{\xi}}{\partial \xi} = 0\ . \tag{2.27}$$

By comparing the coefficients of the functions g_1', g_2' in the generalised Liouville equation, one obtains the following equations of motion for the demons:

$$\begin{aligned} \frac{d}{dt}\, \zeta &= \kappa_1 \sum_{i=1}^{N} \left(\frac{\partial H}{\partial p_i} G_i - \frac{1}{\beta} \frac{\partial G_i}{\partial p_i}\right)\ , \\ \frac{d}{dt}\, \xi &= \kappa_2 \sum_{i=1}^{N} \left(\frac{\partial H}{\partial q_i} F_i - \frac{1}{\beta} \frac{\partial F_i}{\partial q_i}\right)\ . \end{aligned} \tag{2.28}$$

The equations of motion (2.25) and (2.28) conserve the quantity

$$H' = H(q,p) + \frac{1}{\kappa_1} g_1(\zeta) + \frac{1}{\kappa_2} g_2(\xi) + \frac{1}{\beta} \int^t \mathrm{d}t' \sum_i \left[g_1'(\zeta(t')) \frac{\partial G_i}{\partial p_i} + g_2'(\xi(t')) \frac{\partial F_i}{\partial q_i}\right]\ . \tag{2.29}$$

By partial integration, one easily shows that

$$k_B T \left\langle\!\left\langle\, \frac{\partial G_i}{\partial p_i} \,\right\rangle\!\right\rangle = \left\langle\!\left\langle\, \frac{\partial H}{\partial p_i} G_i \,\right\rangle\!\right\rangle\ , \tag{2.30}$$

and likewise

$$k_B T \left\langle\!\left\langle\, \frac{\partial F_i}{\partial q_i} \,\right\rangle\!\right\rangle = \left\langle\!\left\langle\, \frac{\partial H}{\partial q_i} F_i \,\right\rangle\!\right\rangle\ . \tag{2.31}$$

In fact, the time dependence of the demons is determined by the difference of two quantities whose ratio of canonical averages is k_BT. The control of the kinetic energy in the original Nosé-Hoover thermostat is only a special case. This paves a way for the generalisation of this method to systems whose Hamiltonian does not contain a kinetic energy term. As an example, we mention classical spin systems, where this method has been employed successfully for extensive studies [27, 6].

In principle, since the choice of the functions F, G, g_1, g_2 is arbitrary, this method offers a lot of freedom. Kusnezov, Bulgac, and Bauer have investigated different choices of the various functions and were able to show that the demon method frequently resolves problems of non-ergodic behaviour. The most prominent choice of functions is the following so-called cubic coupling scheme:

$$g_1 = \frac{1}{4}\zeta^4 \ , \qquad g_2 = \frac{1}{2}\xi^2 \ , \qquad F_i = q_i^3 \ , \qquad G_i = p_i \ , \tag{2.32}$$

resulting in the set of equations of motion

$$\begin{aligned} \frac{d}{dt}\, q_i &= \frac{p_i}{m} - \xi q_i^3 \ , \qquad \frac{d}{dt}\, p_i = -\frac{\partial V}{\partial q_i} - \zeta^3 p_i \ , \\ \frac{d}{dt}\zeta &= \kappa_1 \left(\sum_{i=1}^{N} \frac{p_i^2}{m} - N k_B T \right) \ , \\ \frac{d}{dt}\xi &= \kappa_2 \left(\sum_{i=1}^{N} \frac{\partial V}{\partial q_i} q_i^3 - 3 k_B T \sum_{i=1}^{N} q_i^2 \right) \ . \end{aligned} \tag{2.33}$$

These equations provide ergodic behaviour in all examples given in [23], see also section 2.2.5. The problems of the simple Nosé-Hoover scheme – dependence of the choices of Q, T, and the initial conditions – are reliably resolved. The choice of the numerical values of κ_1 and κ_2 may still influence ergodicity, but rules of thumb have been found empirically that will be discussed in chapter 5.

2.2.3. The chain thermostat

Another variation of the Nosé-Hoover method has been proposed by Martyna, Klein, and Tuckerman [24]. The main idea of this technique is to impose on the first thermalising pseud-ofriction coefficient a second one which may be coupled to yet a third one, and so on, thereby forming a chain of thermostats. This approach of recursive thermalisation increases the size of the phase space and thus makes the dynamical evolution of the system more complex, thereby leading to ergodicity.

In a modified notation ($\zeta \equiv p_\eta/Q$), the set of dynamical equations

$$\begin{aligned} \frac{d}{dt}\, q_i &= \frac{p_i}{m} \ , \qquad \frac{d}{dt}\, p_i = -\frac{\partial V(q)}{\partial q_i} - p_i \frac{p_\eta}{Q} \ , \\ \frac{d}{dt}\, p_\eta &= \sum_{i=1}^{N} \frac{p_i^2}{m} - N k_B T \ , \\ \frac{d}{dt}\, \eta &= \frac{p_\eta}{Q} \ , \end{aligned} \tag{2.34}$$

defines Nosé-Hoover dynamics. The fact that the temporal evolution of p_η is governed by the deviation of the kinetic energy of the system from its canonical average value is displayed very

obviously. The variable η which is not coupled to the dynamics is again included for reasons of completeness. The stationary distribution function reads

$$f(q,p,p_\eta) = \exp\left(-\beta\Big(H(q,p) + \frac{p_\eta^2}{2Q}\Big)\right) \ , \tag{2.35}$$

and the conserved quantity is

$$H'(q,p,p_\eta,\eta) = H(q,p) + \frac{p_\eta^2}{2Q} + Nk_BT\eta \ . \tag{2.36}$$

The desired distribution (2.35) has a Gaussian dependence on the particle momenta as well as on the thermostat momentum p_η. While the Gaussian fluctuations of the particle momenta are driven by p_η, there is nothing to equilibrate p_η itself. Therefore, it appears sensible to couple another pseudofriction coefficient to the first one, and so on. As a result, one obtains the equations of motion of the Nosé-Hoover chain method,

$$\begin{aligned}
\frac{d}{dt}\, q_i &= \frac{p_i}{m} \ , \qquad \frac{d}{dt}\, p_i = -\frac{\partial V(q)}{\partial q_i} - p_i \frac{p_{\eta_1}}{Q_1} \ , \\
\frac{d}{dt}\, p_{\eta_1} &= \left(\sum_{i=1}^{N} \frac{p_i^2}{m} - Nk_BT\right) - p_{\eta_1}\frac{p_{\eta_2}}{Q_2} \ , \\
\frac{d}{dt}\, p_{\eta_j} &= \left(\frac{p_{\eta_{j-1}}^2}{Q_{j-1}} - k_BT\right) - p_{\eta_j}\frac{p_{\eta_{j+1}}}{Q_{j+1}} \ , \\
\frac{d}{dt}\, p_{\eta_M} &= \frac{p_{\eta_{M-1}}^2}{Q_{M-1}} - k_BT \ , \\
\frac{d}{dt}\, \eta_i &= \frac{p_{\eta_i}}{Q_i} \ ,
\end{aligned} \tag{2.37}$$

where a chain of M thermostats has been implemented. These equations have the stationary phase space distribution

$$f(q,p,p_\eta) = C\exp\left(-\beta\Big(H(q,p) + \sum_{j=1}^{M}\frac{p_{\eta_j}^2}{2Q_j}\Big)\right) \tag{2.38}$$

and the conserved quantity

$$H'(q,p,\eta_j,p_{\eta_j}) = H(q,p) + \sum_{j=1}^{M}\frac{p_{\eta_j}^2}{2Q_j} + Nk_BT\eta_1 + k_BT\sum_{j=2}^{M}\eta_j \ . \tag{2.39}$$

Although the number of degrees of freedom added in this approach is usually larger than in the demon method, the addition of the successive thermostats is numerically inexpensive as they form a simple one-dimensional chain. Only the first thermostat interacts with all N particles. A thorough analysis of the method has shown that it reliably leads to ergodicity, see section 2.2.5, and that it is competitive with the demon method with regard to the speed of convergence.

2.2.4. Non-Hamiltonian phase space as a manifold

Tuckerman, Mundy, and Martyna have pointed out that all derivations outlined above do not properly take into account that the equations of motion such as (2.14) along with (2.22), (2.33), or (2.37) describe non-Hamiltonian systems. In [26], a consistent classical statistical mechanical theory for such systems is presented. It is based on the concepts of differential geometry as applied to dynamical systems and provides a sound generalisation of the usual Hamiltonian based statistical mechanical phase space principles to non-Hamiltonian systems. Using these notions, a procedure is developed that leads to the phase space counterpart of the time averages generated by a non-Hamiltonian system. Besides, this approach reveals and surmounts a number of weaknesses of the original formulation, e. g., it permits to explore the reason for the apparent non-ergodicity of certain systems, notably the classical harmonic oscillator [28].

We shall briefly outline the basic ideas presented in [26]. Traditional classical statistical mechanics is based on a Hamiltonian function. A point in the phase space of a system is given by the coordinates and momenta $x = (q, p)$. Given a time-dependent phase space distribution function $f(x, t)$, the average of an observable $B(x)$ in the ensemble described by f is given by

$$\langle\langle\ B\ \rangle\rangle(t) = \frac{\int \mathrm{d}^n x\, B(x) f(x,t)}{\int \mathrm{d}^n x\, f(x,t)}\ . \tag{2.40}$$

The measure $\mathrm{d}q\,\mathrm{d}p \equiv \mathrm{d}^n x$, which is used for the calculation of phase space averages, is preserved by Hamiltonian dynamics. This means that a subset of systems with initial conditions contained in a phase space volume element $\mathrm{d}^n x_0$ will at a later time occupy a volume element of the same size[2]: $\mathrm{d}^n x_0 = \mathrm{d}^n x_t$. This property of Hamiltonian dynamics is frequently referred to as the incompressibility of phase space flow. It is tantamount to the statement that the coordinate transformation specified by the solution of Hamilton's equations of motion $x_t(t; x_0)$ has a Jacobian of absolute value 1. The existance of this time-invariant measure implies that (2.40) can be computed with respect to the phase space variables x at *any* time t.

In the case of a general non-Hamiltonian dynamical system,

$$\dot{x} = \xi(x, t)\ , \tag{2.41}$$

the situation becomes more complicated. The time evolution generated by the set of differential equations (2.41) is in general compressible and the usual phase space measure $\mathrm{d}^n x$ is no longer invariant under the dynamical evolution. Therefore, in a more refined analysis of the situation, one must treat the phase space of the system as a general Riemannian manifold. The metric on this manifold has to be taken into account in the formulation of a continuity equation for the distribution function and in the expression of a phase space average which is given in terms of an integral over the manifold.

Moreover, if one wants to relate a phase space average to a time average, the question of the integration measure needs to be considered carefully. Analogous to the Hamiltonian case, an expression for an ensemble average is needed that uses a measure on phase space that is invariant under time evolution. If such an *invariant measure* is found, the phase space average of some property (expressed in terms of an integral over the manifold with the preserved measure) corresponds to the time average of the same property over the trajectories of the system under the usual assumption of ergodicity.

[2] Together with the statement that trajectories of identical systems do not intersect (since the solution of Hamilton's equations of motion is unique), one easily proves the theorem of Liouville, $\frac{d}{dt}\ f = 0$.

In order to derive an invariant measure on this manifold, consider the solution of (2.41),

$$x_t^i = x_t^i(t; x_0^1, \dots x_0^n) \ , \quad i = 1, \dots n \ , \tag{2.42}$$

as a coordinate transformation from the initial coordinates at time $t = 0$ to the coordinates at time t. It can be shown that the Jacobian $J(x_t; x_0)$ of this transformation,

$$J(x_t; x_0) = \det \frac{\partial(x_t^1, \dots x_t^n)}{\partial(x_0^1, \dots x_0^n)} \tag{2.43}$$

obeys the equation of motion

$$\frac{d}{dt} \, J = J\kappa(x_t) \ , \tag{2.44}$$

where the quantity $\kappa(x_t) = \sum_{i=1}^n \partial \dot{x}^i / \partial x^i$ is called the phase space compressibility of the dynamical system[3]. Since equation (2.44) may be rewritten as

$$\frac{d}{dt} \, \ln J = \kappa \ , \tag{2.45}$$

it can be integrated easily. If we introduce the variable $w(x)$ related to κ by $\dot{w} = \kappa$, the solution reads

$$J(x_t; x_0) = \exp\big(w(x_t) - w(x_0)\big) \ . \tag{2.46}$$

The infinitesimal volume element transforms under a coordinate transformation according to

$$\mathrm{d}^n x_t = J(x_t; x_0) \mathrm{d}^n x_0 \ . \tag{2.47}$$

Rearranging this equation such that quantities at time t appear on one side and quantities at $t = 0$ appear on the other, we get

$$e^{-w(x_t)} \mathrm{d}^n x_t = e^{-w(x_0)} \mathrm{d}^n x_0 \ . \tag{2.48}$$

This equation shows that the measure $e^{-w(x_t)} d^n x_t$ is conserved by the dynamics. The metric determinant of the transformation can be identified as $\sqrt{g} = \exp(-w(x))$. Due to the general transformation law of the metric tensor, it is clear that the values of $\sqrt{g}$ at times 0 and t are related by the Jacobian,

$$\sqrt{g_0} = \sqrt{g_t} \, J(x_t; x_0) \ . \tag{2.49}$$

Consequently, $\sqrt{g}$ satisfies the following differential equation,

$$\frac{d}{dt} \, \sqrt{g} = -\sqrt{g} \, \kappa \ . \tag{2.50}$$

Note that the same equation is fulfilled by the inverse J^{-1} of the Jacobian J as can easily be seen from equation (2.44) and the relation $J \, J^{-1} = 1$.

Next, if an ensemble of systems on phase space is considered, a continuity equation that accounts for number conservation must be expressed. It may be regarded as a generalisation of the theorem of Liouville. The change of local density is balanced by a flux through the

[3] This same quantity already occured on the right hand side of (2.19)

boundary surface taking into account the geometry of the space. As a result, the following equation is obtained [26]:

$$\frac{\partial(f\sqrt{g})}{\partial t} + \nabla \cdot (f\sqrt{g}\,\dot{x}) = 0 \ . \tag{2.51}$$

This equation can be put into the form of equation (2.17) by defining a new function $\tilde{f} = \sqrt{g}f$, but such an identification is not general, since it entails problems with a coherent notion of the entropy of a system [26]. Finally, note that equations (2.50) and (2.51) together imply that even in the case of a non-Hamiltonian system, $f(x,t)$ is conserved,

$$\frac{d}{dt}\, f = 0 \ . \tag{2.52}$$

The notion of ergodicity may now be exposed more clearly. Suppose that the set of dynamical equations (2.41) possesses a set of n_c conserved quantities $\Lambda_k(x)\,,\ k = 1, \ldots n_c$, satisfying

$$\frac{d}{dt}\, \Lambda_k = 0 \ . \tag{2.53}$$

As a consequence, the trajectories generated by equation (2.41) will only sample the intersection of the hypersurfaces $\{\Lambda_k(x) = C_k\}$, where C_k is a set of constants. If all points on a given hypersurface have the same probability of being visited by a trajectory, then the system is said to be *ergodic*. In this case, a time average corresponds to a microcanonical average of the extended system which is a phase space average with the distribution function

$$f(x) = \prod_{k=1}^{n_c} \delta(\Lambda_k - C_k) \ , \tag{2.54}$$

which is a product of δ-functions expressing the conservation laws. It is evident that $f(x)$ satisfies the generalised Liouville equation (2.51), which is inferred most easily from its modified form (2.52).

It is worth noting that a distribution constructed from a subset of the conservation laws,

$$f(x) = \prod_{k=1}^{n_c^{'}} \delta(\Lambda_k - C_k) \ , \tag{2.55}$$

with $n_c^{'} < n_c$, also satisfies equation (2.52). However, this solution does not describe the correct microcanonical distribution function. Therefore, satisfying the generalised Liouville equation (2.51) is a necessary but not sufficient condition for a dynamical system to generate a particular phase space distribution. It is essential to determine all the conservation laws satisfied by the equations of motion. This clarifies the limitations of relying solely on the generalised Liouville equation to determine the distribution function as in the precedent approaches presented in sections 2.2.1, 2.2.2, and 2.2.3.

In those derivations, the desired distribution function f is used to deduce equations of motion for the pseudofriction coefficients on the basis of the generalised Liouville equation. Now, following Tuckerman's analysis outlined above, one can start the other way round from the Nosé-Hoover equations of motion (2.34) and show that the microcanonical average in the extended system corresponds to a canonical average in the original physical system.

Assuming that the quantity

$$H' = H(q,p) + \frac{p_\eta^2}{2Q} + Nk_BT\eta \tag{2.56}$$

is the only quantity conserved by the dynamics (2.34), the microcanonical distribution function that is sampled in case of ergodicity reads

$$\delta(H' - C_1) \ . \tag{2.57}$$

We want to investigate the microcanonical partition function[4] of the enlarged system,

$$\Omega_T = \int \mathrm{d}q\mathrm{d}p\mathrm{d}p_\eta\mathrm{d}\eta\sqrt{g}\ \delta\big(H(q,p) + \frac{p_\eta^2}{2Q} + Nk_BT\eta - C_1\big) \ , \tag{2.58}$$

and show that the marginal of the distribution function (2.57) in the subspace of the physical variables corresponds to a canonical distribution function. In the next step, the compressibility of the equations of motion (2.34) must be calculated (cf. (2.44)):

$$\kappa(x) = \sum_{i=1}^{n} \frac{\partial \dot{x}^i}{\partial x^i} = -N\dot{\eta} \ . \tag{2.59}$$

Thus, we obtain $\sqrt{g} = \exp(N\eta)$. By integration over the non-physical variables in (2.58) the distribution function in the physical subspace may be determined. Using the δ-function to perform the integration over η requires that

$$\eta = \frac{1}{Nk_BT}\Big(C_1 - H(q,p) - \frac{p_\eta^2}{2Q}\Big) \ . \tag{2.60}$$

Substituting this result into equation (2.58), one obtains

$$\Omega_T = \frac{e^{\beta C_1}}{Nk_BT} \int \mathrm{d}p_\eta\, e^{-\beta\frac{p_\eta^2}{2Q}} \int \mathrm{d}q\mathrm{d}p\, e^{-\beta H(q,p)} \ . \tag{2.61}$$

The integration over p_η is separated, and the distribution function in the physical subspace is, as desired, the canonical one. This illustrates that the Nosé-Hoover method works since the microcanonical distribution function (2.57) is designed such that its marginal in the original physical subspace is the canonical distribution function. Furthermore, the proof implies that the Nosé-Hoover equations generate a canonical distribution in the subspace of the physical variables provided that H' is the *only* conserved quantity.

In the case of the harmonic oscillator, however, Tuckerman et al. [28] have investigated the slightly modified equations (all constants have been set equal to 1)

$$\dot{x} = p - p_\eta x \ , \quad \dot{p} = -x - p_\eta p \ , \quad \dot{\eta} = p_\eta \ , \quad \dot{p}_\eta = x^2 + p^2 - 2 \ . \tag{2.62}$$

These equations create Poincaré sections in phase space that bear great resemblance to the case of the usual Nosé-Hoover dynamics for the harmonic oscillator that features apparent ergodicity problems. The well-known first conserved quantity reads

$$H' = \frac{1}{2}(x^2 + p^2 + p_\eta^2) + 2\eta \ . \tag{2.63}$$

[4]The subscript T indicates that the microcanonical partition function depends parametrically on temperature.

In [28], the authors have demonstrated that the distribution function resulting from a time average over the solution of (2.62) agrees with a microcanonical distribution,

$$\delta(H' - C_1)\, \delta(K - C_2) \;, \tag{2.64}$$

that contains a *second* conserved quantity, namely

$$K = \frac{1}{2}(x^2 + p^2)e^{2\eta} \;. \tag{2.65}$$

To show this, the compressibility associated with (2.62) needs to be evaluated in order to calculate the metric in phase space. Subsequently, a numerical analysis reveals that the time evolution (2.62) samples marginals of (2.64).

This clearly shows that one needs to include *all* conservation laws in order to determine the precise distribution that is sampled by the trajectories of a non-Hamiltonian system. In a sense, the Nosé-Hoover method is ergodic even in the case of the harmonic oscillator; however, the term ergodicity is now used in view of two conservation laws, (2.63) and (2.65), and means that the *accessible* portion of phase space is correctly sampled. The statement that the Nosé-Hoover method is not ergodic for the harmonic oscillator is right if only the first conservation law is taken into account, or if the term is used loosely in the sense of the equivalence of time averages and (canonical) ensemble averages[5]. The extensions of the Nosé-Hoover method, the demon method and the chain thermostat, create the desired canonical distribution in phase space since they violate the second conservation law. It is a merit of the phase space analysis that the issue of apparent non-ergodicity of the Nosé-Hoover method for the classical harmonic oscillator may be illuminated more deeply.

2.2.5. Note on deterministic chaos and ergodicity

Generally speaking, for a given deterministic system it is hard to determine whether it is ergodic or not; however, it is possible to find indications of when a system may or may not behave well in this respect.

Consider a point in phase space with

$$\frac{\partial V(q)}{\partial q_i} = 0 \;, \qquad p_i = 0 \;. \tag{2.66}$$

At such a point, the Nosé-Hoover chain dynamics (2.37) effectively stops in the original system since all temporal derivatives of the physical variables vanish. These so-called Hoover holes are fixed points of the dynamics. If a fixed point is stable, then in its vicinity, the equations will drive the system into the point, which is unacceptable if an ergodic system is required. The stability of a fixed point can be examined by investigating the linearised equations of motion about the point. It has been shown that neither the Nosé-Hoover chain dynamics [24] nor the demon method with the cubic coupling scheme [23] have stable fixed points.

The preceding analysis cannot determine whether the system is ergodic. Therefore, in order to obtain numerical evidence for ergodic behaviour, brute force methods have also been applied to the chain thermostat and the cubic coupling scheme.

In more detail, a necessary condition for ergodicity is that the system be chaotic [29], by which we mean that the time development of the system sensitively depends on the initial conditions. In a chaotic system, adjacent trajectories in phase space diverge exponentially.

[5] This is the meaning usually implied in this work, notably in chapter 5.

This is characterised by a positive so-called Liapunov exponent, whereas a negative Liapunov exponent indicates that the trajectories converge to a fixed point. The Liapunov exponent vanishes in case the system is recurrent and moves periodically on a stable orbit. Both for the chain thermostat and the demon method, extensive investigations of the Liapunov exponents have been performed, yielding positive values in all cases.

Another property encountered in this context is *mixing* [29, 30]. If a dynamics is mixing, it distorts any volume element of phase space so strongly that it is eventually spread over the entire phase space, just as a drop of ink (which is supposed to correspond to a given phase space volume element) is homogeneously distributed within a glass of water after stirring. Mixing guarantees the spontaneous evolution of a non-equilibrium distribution function to equilibrium and is therefore a sufficient condition for ergodicity. This property has numerically been verfied for the cubic coupling scheme [23].

3. Coherent states

In the preceding chapter, we have described two different techniques to incorporate the influence of a heat bath on a classical system on the level of the dynamical equations. The resulting equations of motion have the property that under certain conditions a time average is equivalent to a canonical ensemble average.

With the original Langevin equation and the Nosé-Hoover method being techniques of classical molecular dynamics, it seems difficult to directly translate them to quantum mechanics. Position and momentum of a particle in quantum mechanics are described by operators $\underset{\sim}{r}$ and $\underset{\sim}{p}$ with a non-vanishing commutator, and consequently, there is no common eigenbasis of the operators. The time evolution of a quantum state is governed by Schrödinger's equation which describes a unitary transformation in the Hilbert space of state vectors. So there is no immediate correspondence in quantum mechanics to Hamilton's classical equations of motion on phase space.

However, it appears natural to start an attempt of translation to quantum dynamics with a system that features properties that allow a direct linking to classical mechanics. In this chapter, we will show that for the quantum harmonic oscillator, it is possible to construct state vectors with very special properties, the so-called coherent states. For these states, the time evolution of the expectation values $r = \langle\, \underset{\sim}{r} \,\rangle$, $p = \langle\, \underset{\sim}{p} \,\rangle$ (which always obey quasi-classical equations of motion according to Ehrenfest's theorem) describes the *full* quantum mechanical time evolution. This will allow the desired access to isothermal quantum dynamics.

Quantum mechanical operators are denoted by an underlying tilde, e. g., we write $\underset{\sim}{\mathbb{1}}$ for the unit operator. While quantum mechanical expectation values are denoted by $\langle\, . \,\rangle$, quantum canonical ensemble averages are denoted by $\langle\langle\, . \,\rangle\rangle$, just as classical phase space averages (1.1). There should be no confusion since the averaged quantity indicates which kind of average is implied.

3.1. Introduction

In one dimension, the quantum Hamiltonian of one particle in an external harmonic oscillator reads

$$\begin{aligned} \underset{\sim}{H}^{(1)} &= \frac{1}{2m}\underset{\sim}{p}^2 + \frac{1}{2}m\omega^2\underset{\sim}{r}^2 = \frac{1}{2}\hbar\omega(\underset{\sim}{\hat{p}}^2 + \underset{\sim}{\hat{r}}^2) \\ &= \hbar\omega\,\left(\underset{\sim}{a}^\dagger\underset{\sim}{a} + \frac{1}{2}\right)\,, \end{aligned} \tag{3.1}$$

with $\underset{\sim}{\hat{r}} = \sqrt{\frac{m\omega}{\hbar}}\underset{\sim}{r}$ and $\underset{\sim}{\hat{p}} = \frac{1}{\sqrt{m\hbar\omega}}\underset{\sim}{p}$ being defined as dimensionless operators of position and momentum, and $\underset{\sim}{a} = \frac{1}{\sqrt{2}}(\underset{\sim}{\hat{r}} + i\underset{\sim}{\hat{p}})$, $\underset{\sim}{a}^\dagger = \frac{1}{\sqrt{2}}(\underset{\sim}{\hat{r}} - i\underset{\sim}{\hat{p}})$ being the so-called annihilation and creation operators. $\underset{\sim}{a}^\dagger\underset{\sim}{a}$ is called the number operator and has eigenstates $|\, n \,\rangle$,

$$\underset{\sim}{a}^\dagger\underset{\sim}{a}\,|\, n \,\rangle = n\,|\, n \,\rangle\,, \tag{3.2}$$

n being a non-negative integer. $\underset{\sim}{a}^\dagger$ and $\underset{\sim}{a}$ act upon the eigenstates $|\,n\,\rangle$ of the Hamiltonian (3.1) in the well-known way

$$\begin{aligned} \underset{\sim}{a}^\dagger\,|\,n\,\rangle &= \sqrt{n+1}\,|\,n+1\,\rangle\ , \\ \underset{\sim}{a}\,|\,n\,\rangle &= \sqrt{n}\,|\,n-1\,\rangle\ . \end{aligned} \tag{3.3}$$

$\underset{\sim}{a}$ and $\underset{\sim}{a}^\dagger$ are non-hermitian operators that satisfy the basic commutation relation $[\underset{\sim}{a}, \underset{\sim}{a}^\dagger] = \underset{\sim}{1}$.

The term "coherent states" was initially used by R. Glauber (see, e. g., [31]) in the field of quantum optics. Following him, we define coherent states as eigenstates of the annihilation operator $\underset{\sim}{a}$,

$$\underset{\sim}{a}\ \,|\,\alpha\,\rangle = \alpha\ \,|\,\alpha\,\rangle\ . \tag{3.4}$$

Since $\underset{\sim}{a}$ is not hermitian, we cannot expect that its eigenvalues are real and that the appendant eigenstates $|\,\alpha\,\rangle$ are mutually orthogonal. α can take on any complex value, and we write

$$\alpha = \sqrt{\frac{m\omega}{2\hbar}}\ r + \frac{i}{\sqrt{2m\hbar\omega}}\ p\ , \tag{3.5}$$

with $r,\ p \in \mathbb{R}$. Note that $\hbar\omega|\alpha|^2 = p^2/2m + m\omega^2 r^2/2$.

The expansion of $|\,\alpha\,\rangle$ in terms of the number states $|\,n\,\rangle$,

$$|\,\alpha\,\rangle = \sum_{n=0}^{\infty} w_n\,|\,n\,\rangle\ , \tag{3.6}$$

is found by inserting the expression (3.6) into the eigenvalue equation (3.4). This yields the recurrence relation

$$w_{n+1} = \frac{\alpha}{\sqrt{n+1}} w_n \tag{3.7}$$

for the expansion coefficients. From this we can infer

$$w_n = \frac{\alpha^n}{\sqrt{n!}} w_0\ . \tag{3.8}$$

The coefficient w_0 is determined from the normalisation condition,

$$\langle\,\alpha\,|\,\alpha\,\rangle = 1 = \sum_{n=0}^{\infty} |w_n|^2 = \sum_{n=0}^{\infty} \frac{|\alpha|^{2n}}{n!} |w_0|^2 = e^{|\alpha|^2} |w_0|^2\ , \tag{3.9}$$

which means

$$|w_0| = e^{-\frac{1}{2}|\alpha|^2}\ . \tag{3.10}$$

In the standard definition of coherent states, w_0 is arbitrarily chosen to be real. Hence, the expansion of $|\,\alpha\,\rangle$ in eigenstates of the harmonic oscillator $|\,n\,\rangle$ reads

$$|\,\alpha\,\rangle = e^{-\frac{1}{2}|\alpha|^2} \sum_{n=0}^{\infty} \frac{\alpha^n}{\sqrt{n!}}\,|\,n\,\rangle\ . \tag{3.11}$$

Note that the probability $P_n(\,|\,\alpha\,\rangle)$ of finding the nth eigenstate $|\,n\,\rangle$ in a coherent state, which is a measure of the energy distribution, is given by a Poisson distribution,

$$P_n(\,|\,\alpha\,\rangle) = \frac{|\alpha|^{2n}}{n!} e^{-|\alpha|^2} \ . \tag{3.12}$$

Alternatively, coherent states are frequently introduced using the so-called displacement[1] or Weyl operator,

$$\underset{\sim}{D}(\alpha) = e^{\alpha \underset{\sim}{a}^\dagger - \alpha^* \underset{\sim}{a}} \ , \tag{3.13}$$

by the relation

$$|\,\alpha\,\rangle = \underset{\sim}{D}(\alpha)\,|\,0\,\rangle \ , \tag{3.14}$$

where $|\,0\,\rangle$ is the harmonic oscillater ground state. The equivalence of this definition and equation (3.11) can easily be inferred with the help of the equation [32, p.40]

$$e^{\underset{\sim}{A}+\underset{\sim}{B}} = e^{-\frac{1}{2}[\underset{\sim}{A},\underset{\sim}{B}]} e^{\underset{\sim}{A}} e^{\underset{\sim}{B}} \ , \tag{3.15}$$

valid whenever $[\underset{\sim}{A}, \underset{\sim}{B}]$ commutes with both $\underset{\sim}{A}$ and $\underset{\sim}{B}$. Since we have $[\alpha \underset{\sim}{a}^\dagger, \alpha^* \underset{\sim}{a}] = |\alpha|^2$, which is a c-number, this requirement is fulfilled, and we find from (3.14)

$$|\,\alpha\,\rangle = e^{-\frac{1}{2}|\alpha|^2} e^{\alpha \underset{\sim}{a}^\dagger} e^{-\alpha^* \underset{\sim}{a}}\,|\,0\,\rangle \ . \tag{3.16}$$

The relation $\underset{\sim}{a}\,|\,0\,\rangle = 0$ implies $e^{-\alpha^* \underset{\sim}{a}}\,|\,0\,\rangle = |\,0\,\rangle$, which allows the simplification

$$|\,\alpha\,\rangle = e^{-\frac{1}{2}|\alpha|^2} e^{\alpha \underset{\sim}{a}^\dagger}\,|\,0\,\rangle \ . \tag{3.17}$$

By expanding the operator $e^{\alpha \underset{\sim}{a}^\dagger}$, we easily arrive at the desired form (3.11).

The expansion (3.11) allows the calculation of the scalar product of two coherent states. One obtains

$$\langle\,\alpha_2\,|\,\alpha_1\,\rangle = e^{-\frac{1}{2}|\alpha_2|^2} e^{-\frac{1}{2}|\alpha_1|^2} e^{\alpha_2^* \alpha_1} \ . \tag{3.18}$$

This expression does not vanish for any pair (α_1, α_2), i. e., as anticipated earlier, there is no pair of mutually orthogonal coherent states. The overlap between two coherent states,

$$|\langle\,\alpha_1\,|\,\alpha_2\,\rangle|^2 = e^{-|\alpha_1 - \alpha_2|^2} \ , \tag{3.19}$$

is given by a Gaussian.

Inserting the definitions of $\underset{\sim}{a}$, $\underset{\sim}{a}^\dagger$ and α, α^*, the following equation is obtained from (3.14),

$$|\,\alpha\,\rangle = e^{\frac{i}{\hbar}(p \underset{\sim}{r} - r \underset{\sim}{p})}\,|\,0\,\rangle \ , \tag{3.20}$$

which transforms into

$$|\,\alpha\,\rangle = e^{-\frac{i}{\hbar}\frac{1}{2}pr}\, e^{\frac{i}{\hbar} p \underset{\sim}{r}}\, e^{-\frac{i}{\hbar} r \underset{\sim}{p}}\ |\,0\,\rangle \tag{3.21}$$

[1] The displacement operator indeed performs a displacement of the wavefunction both in coordinate and momentum space, as will become clear later on.

using equation (3.15). This expression for the state vector $|\,\alpha\,\rangle$ has the advantage that its coordinate representation $\langle\, x\,|\,\alpha\,\rangle$ may be inferred easily. Starting from the coordinate representation of the ground state $|\,0\,\rangle$,

$$\langle\, x\,|\,0\,\rangle = \left(\frac{m\omega}{\hbar\pi}\right)^{1/4} e^{-\frac{1}{2}\frac{m\omega}{\hbar}x^2}\ , \tag{3.22}$$

which is a Gaussian situated at the origin of the x-axis, the effect of the operators in (3.21) is straightforward. The operator $e^{-\frac{i}{\hbar}r\underset{\sim}{p}}$ shifts the argument x of the wavefunction to $(x-r)$ since $\underset{\sim}{p}$ is the generator of spatial translations. Subsequently, the operator $e^{\frac{i}{\hbar}p\underset{\sim}{r}}$ describes a translation in momentum space by the multiplication with the phase factor $e^{\frac{i}{\hbar}px}$. The factor $e^{-\frac{i}{\hbar}\frac{1}{2}pr}$ is an additional overall phase factor. On the whole we obtain

$$\langle\, x\,|\,\alpha\,\rangle = \left(\frac{m\omega}{\hbar\pi}\right)^{1/4} \exp\left(-\frac{1}{2}\frac{m\omega}{\hbar}(x-r)^2 + \frac{i}{\hbar}p(x-\frac{1}{2}r)\right)\ . \tag{3.23}$$

That means that a coherent state, in coordinate representation, corresponds to a displaced Gaussian wavepacket with mean position $\langle\,\alpha\,|\,\underset{\sim}{r}\,|\,\alpha\,\rangle = r$ and mean momentum $\langle\,\alpha\,|\,\underset{\sim}{p}\,|\,\alpha\,\rangle = p$. Therefore, another common notation for a coherent state is

$$|\,r,p\,\rangle \equiv\ |\,\alpha\,\rangle\ . \tag{3.24}$$

In this work, we will make use of both notations, depending on the respective context.

It is known from standard quantum mechanics that Gaussian wavepackets minimise Heisenberg's uncertainty relation for the operators of position and momentum. Therefore, coherent states are also frequently referred to as minimum uncertainty states.

3.2. General properties of coherent states

The expansion (3.11) of coherent states in the basis of eigenstates of the harmonic oscillator entails very advantageous consequences. The action of the time evolution operator upon a coherent state and the matrix elements of the statistical operator may be calculated analytically. Both operators are exponentials of the Hamiltonian.

Time evolution

Perhaps the most prominent property of coherent states is their stability under time evolution in a harmonic oscillator potential. The elementary calculation

$$\begin{aligned} e^{-i\omega t\underset{\sim}{a}^\dagger\underset{\sim}{a}}\,|\,\alpha\,\rangle &= e^{-\frac{1}{2}|\alpha|^2}\sum_{n=0}^{\infty}\frac{\alpha^n}{\sqrt{n!}}e^{-in\omega t}\,|\,n\,\rangle \\ &=\ |\,e^{-i\omega t}\alpha\,\rangle \end{aligned} \tag{3.25}$$

implies that a coherent state remains a coherent state for the exact quantum mechanical time evolution generated by the Hamiltonian (3.1). In other words, the time-evolved version of a coherent state is obtained solely by a uniform rotation of its label, α, in a clockwise manner

on a circle of radius $|\alpha|$ in the complex plane. Using the obvious notation $\alpha(t) = \sqrt{\frac{m\omega}{2\hbar}} r(t) + \frac{i}{\sqrt{2m\hbar\omega}} p(t)$, equation (3.25) may be rephrased in terms of $r(t)$ and $p(t)$,

$$\begin{aligned} r(t) &= r_0 \cos(\omega t) + \frac{1}{m\omega} p_0 \sin(\omega t) \ , \\ p(t) &= p_0 \cos(\omega t) - m\omega r_0 \sin(\omega t) \ , \end{aligned} \tag{3.26}$$

with $\alpha_0 = \alpha(t=0) = \sqrt{\frac{m\omega}{2\hbar}} r_0 + \frac{i}{\sqrt{2m\hbar\omega}} p_0$. Consequently, the time evolution of a coherent state in a harmonic oscillator potential can be cast into a form that is familiar from the classical harmonic oscillator, namely

$$\frac{d}{dt} r = \frac{p}{m} \ , \qquad \frac{d}{dt} p = -m\omega^2 r \ . \tag{3.27}$$

This fact will play a decisive role for the translation of the Nosé-Hoover technique to this quantum system. It has been discovered implicitly by Schrödinger in 1926 [33] who in his fundamental work was the first to study the time evolution of a spatially displaced harmonic oscillator ground state.

According to (3.23), the parameters r and p correspond to mean position and mean momentum of the coherent state. Yet we stress that the statement of (3.27) goes far beyond the much weaker theorem of Ehrenfest. This theorem says that the time dependent expectation values of the operators of position and momentum (denoted by $\langle \underset{\sim}{r} \rangle(t) = \langle \psi(t) | \underset{\sim}{r} | \psi(t) \rangle$ and $\langle \underset{\sim}{p} \rangle(t) = \langle \psi(t) | \underset{\sim}{p} | \psi(t) \rangle$) satisfy the equations of motion

$$\begin{aligned} \frac{d}{dt} \langle \underset{\sim}{r} \rangle(t) &= \frac{1}{m} \langle \underset{\sim}{p} \rangle(t) \ , \\ \frac{d}{dt} \langle \underset{\sim}{p} \rangle(t) &= - \langle \nabla \underset{\sim}{V} \rangle(t) \ , \end{aligned} \tag{3.28}$$

as a result of the Schrödinger time evolution of a quantum mechanical state $|\psi(t)\rangle$. These equations again strongly resemble the classical equations of motion. However, contrary to (3.27), this theorem does not contain a statement about the *complete time evolution of a quantum mechanical state*, since a general quantum state $|\psi(t)\rangle$ is not fully parametrised by only two expectation values.

Matrix element of the statistical operator

The foregoing calculation (3.25) is particularly simple since the phase factor $e^{-i\omega t}$ does not change the absolute value of α. This is different in the case of the statistical operator, $e^{-\beta \underset{\sim}{H}}$, for which we find

$$\begin{aligned} e^{-\beta\hbar\omega \underset{\sim}{a}^\dagger \underset{\sim}{a}} |\alpha\rangle &= e^{-\beta\hbar\omega \underset{\sim}{a}^\dagger \underset{\sim}{a}} e^{-\frac{1}{2}|\alpha|^2} \sum_{n=0}^{\infty} \frac{\alpha^n}{\sqrt{n!}} |n\rangle \\ &= e^{-\frac{1}{2}|\alpha|^2} \sum_{n=0}^{\infty} \frac{(e^{-\beta\hbar\omega}\alpha)^n}{\sqrt{n!}} |n\rangle \\ &= e^{-\frac{1}{2}|\alpha|^2} \frac{e^{-\frac{1}{2}|\alpha|^2 e^{-2\beta\hbar\omega}}}{e^{-\frac{1}{2}|\alpha|^2 e^{-2\beta\hbar\omega}}} \sum_{n=0}^{\infty} \frac{(e^{-\beta\hbar\omega}\alpha)^n}{\sqrt{n!}} |n\rangle \\ &= e^{-\frac{1}{2}|\alpha|^2 (1 - e^{-2\beta\hbar\omega})} \, |e^{-\beta\hbar\omega}\alpha\rangle \ . \end{aligned} \tag{3.29}$$

We have inserted the fraction $1 = \frac{e^{-\frac{1}{2}|\alpha|^2 e^{-2\beta\hbar\omega}}}{e^{-\frac{1}{2}|\alpha|^2 e^{-2\beta\hbar\omega}}}$ to simplify the separation of the ket $|\, e^{-\beta\hbar\omega}\alpha\,\rangle$. From this we determine the matrix element of the statistical operator:

$$\begin{aligned}\langle\, \alpha \,|\, e^{-\beta \underset{\sim}{H}} \,|\, \alpha \,\rangle &= e^{-\frac{1}{2}\beta\hbar\omega} \langle\, \alpha \,|\, e^{-\beta\,\hbar\omega\, \underset{\sim}{a}^\dagger \underset{\sim}{a}} \,|\, \alpha \,\rangle \\ &= e^{-\frac{1}{2}\beta\hbar\omega} e^{-|\alpha|^2(1-e^{-\beta\hbar\omega})} \ .\end{aligned} \tag{3.30}$$

Resolution of unity and over-completeness

In order to prove the following resolution of unity,

$$\underset{\sim}{\mathbb{1}} = \int \frac{\mathrm{d}^2\alpha}{\pi} \ |\, \alpha \,\rangle\langle\, \alpha \,| \ , \quad \mathrm{d}^2\alpha = \mathrm{d}\,(\mathrm{Re}\,\alpha)\,\mathrm{d}\,(\mathrm{Im}\,\alpha) \ , \tag{3.31}$$

one inserts again the expansion (3.11) on the right hand side. Introducing subsequently polar coordinates, $\alpha = |\alpha| e^{i\theta}$, one obtains

$$\begin{aligned}&\sum_{n,m=0}^{\infty} \frac{1}{\sqrt{n!m!}} \int \frac{\mathrm{d}^2\alpha}{\pi} \ e^{-|\alpha|^2} \alpha^{*n} \alpha^m \ |\, m \,\rangle\langle\, n \,| \\ &= \sum_{n,m=0}^{\infty} \frac{1}{\sqrt{n!m!}} \int_0^\infty \mathrm{d}|\alpha| |\alpha|^{m+n+1} e^{-|\alpha|^2} \frac{1}{\pi} \int_{-\pi}^{\pi} \mathrm{d}\theta e^{-i(m-n)\theta} \ |\, n \,\rangle\langle\, m \,| \ .\end{aligned} \tag{3.32}$$

With the help of the relation $\frac{1}{2\pi}\int_{-\pi}^{\pi} \mathrm{d}\theta e^{im\theta} = \delta_{m,0}$ the summation over m can be carried out. It then proves useful to change to the new integration variable $\zeta = |\alpha|^2$, and with the integral formula $\int_0^\infty \mathrm{d}\zeta\, \zeta^n e^{-\zeta} = \Gamma(n+1) = n!$ the right hand side finally takes the form

$$\sum_{n=0}^{\infty} \ |\, n \,\rangle\langle\, n \,| \ , \tag{3.33}$$

which is the completeness relation for the eigenstates of the harmonic oscillator. Therefore, (3.31) is in fact a valid representation of the identity operator in terms of coherent states. In the alternative notation of (3.24), we may write

$$\underset{\sim}{\mathbb{1}} = \int \frac{\mathrm{d}r\,\mathrm{d}p}{2\pi\hbar} \ |\, r,p \,\rangle\langle\, r,p \,| \ . \tag{3.34}$$

The set of all coherent states, $\{\ |\, \alpha \,\rangle,\ \alpha \in \mathbb{C}\ \}$, is overcomplete, which implies on the one hand that the coherent states are not mutually orthogonal, on the other hand that certain (even countable) subsets still span the whole Hilbert space [34]. This question has been discussed in great detail in the literature. Moreover, the non-orthogonality leads to a number of remarkable expansion properties, e. g., that a given coherent state may be expanded into a set of coherent states [35].

In Appendix C, we make use of an expansion of an eigenstate $|\, n \,\rangle$ into a circle of coherent states in order to derive the time evolution of an arbitrary displaced eigenfunction of the harmonic oscillator.

3.3. Determination of ensemble averages with coherent states

Since (3.31) is a correct resolution of unity, coherent states are a valid basis for the calculation of traces of operators and, more specifically, for the calculation of statistical ensemble averages. It will be shown that in the case of the quantum harmonic oscillator, it is possible to cast the expression for a canonical average into the form of an integral over the parameter space of coherent states. This is due to the simple form of the matrix element of the canonical statistical operator in the basis of coherent states (3.30). The resulting special form strongly ressembles a classical phase space average, with a modified thermal weight function for the quantum system. The subject of the following section is to determine the quantum thermal weight functions for a single and two indistinguishable particles in an external harmonic oscillator potential, and for an arbitrary number N of fermions. This will pave the way for a translation of the classical thermostats to the quantum harmonic oscillator.

3.3.1. One particle

To start with, we study the case of a single particle in a harmonic oscillator potential. In a manner following Schnack [36], we calculate the trace involved in a quantum canonical ensemble average,

$$\langle\langle\ \underset{\sim}{B}\ \rangle\rangle = \frac{1}{Z^{(1)}(\beta)}\ \mathrm{Tr}\,(\underset{\sim}{B} e^{-\beta \underset{\sim}{H}^{(1)}})\ , \qquad Z^{(1)}(\beta) = \mathrm{Tr}\,(e^{-\beta \underset{\sim}{H}^{(1)}})\ , \tag{3.35}$$

using the basis of coherent states:

$$\begin{aligned}
\langle\langle\ \underset{\sim}{B}\ \rangle\rangle &= \frac{1}{Z^{(1)}(\beta)} \int \frac{\mathrm{d}^2\alpha}{\pi}\ \langle\,\alpha\,|\ \underset{\sim}{B} e^{-\beta \underset{\sim}{H}^{(1)}}\ |\,\alpha\,\rangle \\
&= \frac{1}{Z^{(1)}(\beta)} \int \frac{\mathrm{d}^2\alpha}{\pi}\ \langle\,\alpha\,|\ e^{-\frac{1}{2}\beta \underset{\sim}{H}^{(1)}}\ \underset{\sim}{B} e^{-\frac{1}{2}\beta \underset{\sim}{H}^{(1)}}\ |\,\alpha\,\rangle \\
&= \frac{1}{Z^{(1)}(\beta)} \int \frac{\mathrm{d}^2\alpha}{\pi}\ e^{-\frac{1}{2}\beta\hbar\omega}\ e^{-|\alpha|^2\left(1-e^{-\beta\hbar\omega}\right)}\ \langle\, e^{-\frac{1}{2}\beta\hbar\omega}\alpha\,|\ \underset{\sim}{B}\ |\, e^{-\frac{1}{2}\beta\hbar\omega}\alpha\,\rangle \\
&= \frac{1}{Z^{(1)}(\beta)} \int \frac{\mathrm{d}^2\alpha}{\pi}\ e^{\frac{1}{2}\beta\hbar\omega}\ e^{-|\alpha|^2\left(e^{\beta\hbar\omega}-1\right)}\ \langle\,\alpha\,|\ \underset{\sim}{B}\ |\,\alpha\,\rangle\ ,
\end{aligned} \tag{3.36}$$

where we have used the cyclic invariance of the trace in the first step and equation (3.29) in the second step. A substitution $\alpha \to e^{-\frac{1}{2}\beta\hbar\omega}\alpha$ has been carried out in the final step.

We now define the function

$$w^{(1)}(\alpha) = e^{-|\alpha|^2\left(e^{\beta\hbar\omega}-1\right)} = e^{-\left(\frac{p^2}{2m}+\frac{1}{2}m\omega^2 r^2\right)\left(e^{\beta\hbar\omega}-1\right)/(\hbar\omega)}\ , \tag{3.37}$$

which specifies the weight with which a coherent state $|\,\alpha\,\rangle = |\,r,p\,\rangle$ contributes to a canonical average. In addition, we define

$$\begin{aligned}
\tilde{Z}^{(1)}(\beta) = e^{-\frac{1}{2}\beta\hbar\omega}\ Z^{(1)}(\beta) &= \int \frac{\mathrm{d}^2\alpha}{\pi}\ w^{(1)}(\alpha) \\
&= \frac{1}{e^{\beta\hbar\omega}-1}\ ,
\end{aligned} \tag{3.38}$$

and

$$\mathcal{B}(\alpha) = \langle\,\alpha\,|\ \underset{\sim}{B}\ |\,\alpha\,\rangle\ , \tag{3.39}$$

which enables us to express the canonical average as follows,

$$\langle\langle \underset{\sim}{B} \rangle\rangle = \frac{1}{\tilde{Z}^{(1)}(\beta)} \int \frac{\mathrm{d}^2\alpha}{\pi}\, w^{(1)}(\alpha)\, \mathcal{B}(\alpha) \;, \tag{3.40}$$

or, in (r,p) – notation,

$$\langle\langle \underset{\sim}{B} \rangle\rangle = \frac{1}{\tilde{Z}^{(1)}(\beta)} \int \frac{\mathrm{d}r\,\mathrm{d}p}{2\pi\hbar}\, w^{(1)}(r,p)\, \mathcal{B}(r,p) \;. \tag{3.41}$$

This representation of a quantum canonical ensemble average has obviously the form of a classical phase space average. Therefore, we are led to the following interpretation: The space of the continuous parameters r and p is a phase space, and the quantum canonical ensemble average for a single particle in a harmonic oscillator may be rewritten as a phase space integral with the thermal weight function $w^{(1)}(r,p)$. The term

$$\mathcal{B}(r,p) = \langle\, r,p \,|\, \underset{\sim}{B} \,|\, r,p \,\rangle \;, \tag{3.42}$$

is the corresponding representation of the observable $\underset{\sim}{B}$ as a phase space function. The distribution function $w^{(1)}$ contains all quantum statistical properties of the system. From (3.37) it can be inferred that formally, it differs from the Boltzmann distribution function of the classical harmonic oscillator by the factor $\left(e^{\beta\hbar\omega}-1\right)/(\beta\hbar\omega)$. Note that this factor tends to 1 both in the classical ($\hbar \to 0$) and in the high-temperature ($\beta \to 0$) limit.

We note for the reader familiar with Wigner functions that this approach to the determination of a quantum canonical ensemble average, resulting in the expression (3.41), is entirely based on the properties of coherent states. In particular, the thermal weight function $w^{(1)}(r,p)$ is *not* the Wigner function of the thermal state

$$\underset{\sim}{\rho} = \frac{1}{Z^{(1)}(\beta)} \sum_{n=0}^{\infty} \exp(-\beta E_n)\, |\, n \,\rangle\langle\, n \,| \;\; . \tag{3.43}$$

The matrix element $\langle\, x \,|\, \underset{\sim}{\rho} \,|\, x' \,\rangle$ can be calculated elegantly with the aid of (3.41), see appendix B. The Wigner function is now defined by the Fourier transform of this matrix element with respect to the "quantum jump" from $x - \frac{1}{2}\xi$ to $x + \frac{1}{2}\xi$,

$$W(x,p) = \frac{1}{2\pi\hbar} \int_{-\infty}^{\infty} \mathrm{d}\xi\; e^{-\frac{i}{\hbar}p\xi}\, \langle\, x + \frac{1}{2}\xi \,|\, \underset{\sim}{\rho} \,|\, x - \frac{1}{2}\xi \,\rangle \;, \tag{3.44}$$

with the result

$$W(x,p) = \frac{1}{\pi\hbar} \tanh\left(\frac{1}{2}\beta\hbar\omega\right) \exp\left(-\frac{2}{\hbar\omega}\tanh\left(\frac{1}{2}\beta\hbar\omega\right)\left(\frac{p^2}{2m} + \frac{1}{2}m\omega^2x^2\right)\right) \;. \tag{3.45}$$

If we compare $W(x,p)$ to the normalised thermal weight function,

$$\frac{1}{2\pi\hbar}\frac{1}{\tilde{Z}^{(1)}(\beta)} w^{(1)}(r,p) = \frac{1}{2\pi\hbar}(e^{\beta\hbar\omega}-1) \exp\left(-\frac{1}{\hbar\omega}(e^{\beta\hbar\omega}-1)\Big(\frac{p^2}{2m} + \frac{1}{2}m\omega^2r^2\Big)\right) \;, \tag{3.46}$$

we find that they may be converted into one another by the formal substitution of the expression $2\tanh(\frac{1}{2}\beta\hbar\omega)$ by $e^{\beta\hbar\omega}-1$. These terms, corresponding to the inverse width (i. e., the

"narrowness") of $W(x,p)$ and $w^{(1)}(r,p)$, respectively, deviate considerably at low temperatures ($\beta \to \infty$), since we have

$$\lim_{\beta\to\infty}\left(2\tanh\left(\frac{1}{2}\beta\hbar\omega\right)\right) = 2 \ ,$$

while $e^{\beta\hbar\omega}-1$ grows exponentially with β. In the high temperature limit ($\beta \to 0$) or equivalently in the classical limit ($\hbar \to 0$), both terms tend towards the same limiting expression, namely $\beta\hbar\omega$. In these limits both resulting weight functions correspond to the classical Boltzmann distribution.

Nevertheless, for any finite temperature, (3.45) and (3.46) are Gaussian distributions with unequal widths, $w^{(1)}$ being always narrower than $W(x,p)$. Therefore there is no equivalence of $w^{(1)}$ to the Wigner function $W(x,p)$.

Eventually, we mention that the thermal weight function for a system of distinguishable quantum particle is simply the product of one-particle thermal weight functions. The case of indistinguishable quantum particles is of course much more interesting.

3.3.2. Two identical particles

In precise analogy to the case of a single particle, we are able to determine a thermal weight function $w_\varepsilon^{(2)}(\alpha_1,\alpha_2)$ for the system of two identical quantum particles.

The case of two identical particles, i. e. two fermions or bosons, contains already the basic principle of quantum mechanical indistinguishability[2]. We define the operators of symmetrisation and antisymmetrisation in the two-particle Hilbert space,

$$\underset{\sim}{S}_+ = \frac{1}{2}(\underset{\sim}{\mathbb{1}} + \underset{\sim}{P}_{12}) \ , \quad \underset{\sim}{S}_- = \frac{1}{2}(\underset{\sim}{\mathbb{1}} - \underset{\sim}{P}_{12}) \ . \tag{3.47}$$

In a general notation, we will use $\underset{\sim}{S}_\varepsilon$, implicating $\varepsilon = +$ or $-$. The operators $\underset{\sim}{S}_\varepsilon$ are defined such that they are projection operators, and therefore they are hermitian and idempotent. Recall that in a system of identical particles, all valid observables commute with $\underset{\sim}{S}_\varepsilon$. In order to have a common notation for both fermions and bosons, we use

$$|\, A_\varepsilon \,\rangle = \begin{cases} \underset{\sim}{S}_- \,|\, \alpha_1,\alpha_2 \,\rangle & \text{if } \varepsilon = - \\ \underset{\sim}{S}_+ \,|\, \alpha_1,\alpha_2 \,\rangle & \text{if } \varepsilon = + \end{cases} \tag{3.48}$$

for the (anti-)symmetrised two-particle state vector. The norms of these vectors may easily be calculated, and we get

$$\langle\, A_\varepsilon \,|\, A_\varepsilon \,\rangle = \frac{1}{2}(1 + \varepsilon e^{-|\alpha_1-\alpha_2|^2}) \ . \tag{3.49}$$

The completeness relation for the two-fermion (two-boson) Hilbert space is obtained by an (anti-)symmetrisation of a tensor product of two identity operators,

$$\underset{\sim}{\mathbb{1}}_\varepsilon = \iint \frac{\mathrm{d}^2\alpha_1}{\pi}\frac{\mathrm{d}^2\alpha_2}{\pi}\, \underset{\sim}{S}_\varepsilon \,|\, \alpha_1,\alpha_2 \,\rangle\langle\, \alpha_1,\alpha_2 \,|\, \underset{\sim}{S}_\varepsilon^\dagger \ . \tag{3.50}$$

[2]Note that throughout this work, we do not consider spin degrees of freedom.

In order to get an expression with normalised state vectors, we multiply and divide the integrand by $\langle\, A_\varepsilon \,|\, A_\varepsilon \,\rangle$:

$$\underset{\sim}{\mathbb{1}}_\varepsilon = \iint \frac{\mathrm{d}^2\alpha_1}{\pi}\frac{\mathrm{d}^2\alpha_2}{\pi}\langle\, A_\varepsilon \,|\, A_\varepsilon \,\rangle \frac{\underset{\sim}{S}_\varepsilon \,|\, \alpha_1, \alpha_2 \,\rangle\langle\, \alpha_1, \alpha_2 \,|\, \underset{\sim}{S}_\varepsilon^\dagger}{\langle\, A_\varepsilon \,|\, A_\varepsilon \,\rangle} \tag{3.51}$$

This resolution of unity may now be used for the calculation of a trace and, more specifically, for the evaluation of a thermal expectation value.

We write down the Hamilton operator of two non-interacting quantum particles in an external harmonic oscillator potential,

$$\underset{\sim}{H}^{(2)} = \underset{\sim}{H}^{(1)} \otimes \underset{\sim}{\mathbb{1}} + \underset{\sim}{\mathbb{1}} \otimes \underset{\sim}{H}^{(1)} \ . \tag{3.52}$$

The starting point for the calculation of $w_\varepsilon^{(2)}$ is the following expression for the calculation of a thermal expectation value $\langle\langle\, \underset{\sim}{B} \,\rangle\rangle$ as a phase space integral,

$$\begin{aligned}\langle\langle\, \underset{\sim}{B} \,\rangle\rangle &= \frac{1}{Z_\varepsilon^{(2)}(\beta)}\ \mathrm{Tr}\left(\underset{\sim}{B} e^{-\beta \underset{\sim}{H}^{(2)}}\right) \\ &= \frac{1}{Z_\varepsilon^{(2)}(\beta)} \iint \frac{\mathrm{d}^2\alpha_1}{\pi}\frac{\mathrm{d}^2\alpha_2}{\pi}\langle\, \alpha_1, \alpha_2 \,|\, \underset{\sim}{S}_\varepsilon^\dagger \underset{\sim}{B} e^{-\beta \underset{\sim}{H}^{(2)}} \underset{\sim}{S}_\varepsilon \,|\, \alpha_1, \alpha_2 \,\rangle \ ,\end{aligned} \tag{3.53}$$

with $Z_\varepsilon^{(2)}(\beta)$ being the respective two-particle partition function. Note that we may drop the projector $\underset{\sim}{S}_\varepsilon$ acting upon the ket using the cyclic invariance of the trace and the idempotency of the projector $\underset{\sim}{S}_\varepsilon$. Decomposition of $e^{-\beta \underset{\sim}{H}^{(2)}} = e^{-\beta \underset{\sim}{H}^{(2)}/2}\ e^{-\beta \underset{\sim}{H}^{(2)}/2}$ and a cyclic shift of the operators under the trace enables further simplification, taking advantage of the specific properties of coherent states in a harmonic oscillator potential, (3.29). After the following calculation,

$$\begin{aligned}\langle\langle\, \underset{\sim}{B} \,\rangle\rangle &= \frac{1}{Z_\varepsilon^{(2)}(\beta)} \iint \frac{\mathrm{d}^2\alpha_1}{\pi}\frac{\mathrm{d}^2\alpha_2}{\pi}\, \langle\, \alpha_1, \alpha_2 \,|\, e^{-\frac{1}{2}\beta \underset{\sim}{H}^{(2)}} \underset{\sim}{S}_\varepsilon^\dagger \underset{\sim}{B} \underset{\sim}{S}_\varepsilon e^{-\frac{1}{2}\beta \underset{\sim}{H}^{(2)}} \,|\, \alpha_1, \alpha_2 \,\rangle \\ &= \frac{1}{Z_\varepsilon^{(2)}(\beta)} \iint \frac{\mathrm{d}^2\alpha_1}{\pi}\frac{\mathrm{d}^2\alpha_2}{\pi}\, e^{-\frac{1}{2}\beta\hbar\omega - |\alpha_1|^2(1-e^{\beta\hbar\omega})} e^{-\frac{1}{2}\beta\hbar\omega - |\alpha_2|^2(1-e^{\beta\hbar\omega})} \\ &\qquad \cdot \langle\, e^{-\frac{1}{2}\beta\hbar\omega}\alpha_1, e^{-\frac{1}{2}\beta\hbar\omega}\alpha_2 \,|\, \underset{\sim}{S}_\varepsilon^\dagger \underset{\sim}{B} \underset{\sim}{S}_\varepsilon \,|\, e^{-\frac{1}{2}\beta\hbar\omega}\alpha_1, e^{-\frac{1}{2}\beta\hbar\omega}\alpha_2 \,\rangle \\ &= \frac{1}{Z_\varepsilon^{(2)}(\beta)} \iint \frac{\mathrm{d}^2\alpha_1}{\pi}\frac{\mathrm{d}^2\alpha_2}{\pi}\, e^{\beta\hbar\omega} e^{-|\alpha_1|^2(e^{\beta\hbar\omega}-1)} e^{-|\alpha_2|^2(e^{\beta\hbar\omega}-1)} \\ &\qquad \cdot \langle\, \alpha_1, \alpha_2 \,|\, \underset{\sim}{S}_\varepsilon^\dagger \underset{\sim}{B} \underset{\sim}{S}_\varepsilon \,|\, \alpha_1, \alpha_2 \,\rangle \\ &= \frac{1}{Z_\varepsilon^{(2)}(\beta)} \iint \frac{\mathrm{d}^2\alpha_1}{\pi}\frac{\mathrm{d}^2\alpha_2}{\pi}\, e^{\beta\hbar\omega} \underbrace{e^{-|\alpha_1|^2(e^{\beta\hbar\omega}-1)} e^{-|\alpha_2|^2(e^{\beta\hbar\omega}-1)} \langle\, A_\varepsilon \,|\, A_\varepsilon \,\rangle}_{w_\varepsilon^{(2)}(\alpha_1,\alpha_2)} \frac{\langle\, A_\varepsilon \,|\, \underset{\sim}{B} \,|\, A_\varepsilon \,\rangle}{\langle\, A_\varepsilon \,|\, A_\varepsilon \,\rangle} \ ,\end{aligned} \tag{3.54}$$

we identify $w_\varepsilon^{(2)}(\alpha_1, \alpha_2)$ as the *thermal weight of the expectation value* $\frac{\langle\, A_\varepsilon \,|\, \underset{\sim}{B} \,|\, A_\varepsilon \,\rangle}{\langle\, A_\varepsilon \,|\, A_\varepsilon \,\rangle}$. With the definition $\tilde{Z}_\varepsilon^{(2)}(\beta) = e^{-\beta\hbar\omega} Z_\varepsilon^{(2)}(\beta)$, we may finally write

$$\langle\langle\, \underset{\sim}{B} \,\rangle\rangle = \frac{1}{\tilde{Z}_\varepsilon^{(2)}(\beta)} \iint \frac{\mathrm{d}^2\alpha_1}{\pi}\frac{\mathrm{d}^2\alpha_2}{\pi}\, w_\varepsilon^{(2)}(\alpha_1, \alpha_2) \frac{\langle\, A_\varepsilon \,|\, \underset{\sim}{B} \,|\, A_\varepsilon \,\rangle}{\langle\, A_\varepsilon \,|\, A_\varepsilon \,\rangle} \ . \tag{3.55}$$

$w_\varepsilon^{(2)}(\alpha_1, \alpha_2)$ is not merely the product of two one-particle thermal weight functions (as it would be the case for two distinguishable particles), but contains in addition the factor $\langle A_\varepsilon | A_\varepsilon \rangle$ that accounts for the quantum effects of indistinguishability. Moreover, $w_\varepsilon^{(2)}(\alpha_1, \alpha_2)$ cannot be written as a product of two functions depending only on α_1 and α_2, respectively, since the term $\langle A_\varepsilon | A_\varepsilon \rangle$ does not have this separation property. This is a manifest consequence of the quantum mechanical principle of indistinguishability. In more detail, the state $| A_\varepsilon \rangle$ describing two identical particles is *entangled*, which means that $| A_\varepsilon \rangle$ does not have the form of a tensor product $| \alpha_1 \rangle \otimes | \alpha_2 \rangle \equiv | \alpha_1, \alpha_2 \rangle$. On the level of the distribution function, this is reflected by the non-separability (or entanglement) of $w_\varepsilon^{(2)}$.

For fermions, we have $\langle A_- | A_- \rangle = \frac{1}{2}(1 - e^{-|\alpha_1 - \alpha_2|^2})$ (see equation (3.49)). In case $\alpha_1 = \alpha_2$, this expression vanishes along with the thermal weight function $w_-^{(2)}$, independent of temperature. This is understandable since a quantum state with two identical fermions in the same one-particle state is forbidden by the Pauli exclusion principle and therefore does not contribute to a thermal average. In contrast, for bosons we have $\langle A_+ | A_+ \rangle = \frac{1}{2}(1 + e^{-|\alpha_1 - \alpha_2|^2})$, which contains a different sign that enhances the thermal weight of the quantum state with two bosons in the same one-particle state.

The integral over the thermal weight function $w_\varepsilon^{(2)}(\alpha_1, \alpha_2)$ yields the correct partition function $\tilde{Z}_\varepsilon^{(2)}(\beta)$. To show this, we calculate

$$\begin{aligned}
\tilde{Z}_\varepsilon^{(2)}(\beta) &= \langle\langle\, \underset{\sim}{\mathbb{1}} \,\rangle\rangle \qquad (3.56)\\
&= \iint \frac{\mathrm{d}^2\alpha_1}{\pi} \frac{\mathrm{d}^2\alpha_2}{\pi}\, e^{-|\alpha_1|^2(e^{\beta\hbar\omega}-1)} e^{-|\alpha_2|^2(e^{\beta\hbar\omega}-1)} \frac{1}{2}(1 + \varepsilon e^{-|\alpha_1-\alpha_2|^2}) \\
&= \frac{1}{2}\left(\int \frac{\mathrm{d}^2\alpha_1}{\pi}\, e^{-|\alpha_1|^2(e^{\beta\hbar\omega}-1)} \right)^2 \\
&\quad + \varepsilon\, \frac{1}{2}\left(\iint \frac{\mathrm{d}^2\alpha_1}{\pi} \frac{\mathrm{d}^2\alpha_2}{\pi}\, e^{-|\alpha_1|^2(e^{\beta\hbar\omega}-1)} e^{-|\alpha_2|^2(e^{\beta\hbar\omega}-1)}\, e^{-|\alpha_1-\alpha_2|^2} \right) \\
&= \frac{1}{2}\left(\frac{1}{e^{\beta\hbar\omega} - 1} \right)^2 + \varepsilon\, \frac{1}{2}\left(\frac{1}{e^{2\beta\hbar\omega} - 1} \right) \\
&= \frac{1}{2}(\tilde{Z}^{(1)}(\beta)^2 + \varepsilon \tilde{Z}^{(1)}(2\beta)) \ .
\end{aligned}$$

This is a correct, well-known recursion relation [37] for the two-particle partition function. The second integral is solved most easily by a change of variables from α_1, α_2 to $\alpha_+ = \frac{1}{\sqrt{2}}(\alpha_1 + \alpha_2)$, $\alpha_- = \frac{1}{\sqrt{2}}(\alpha_1 - \alpha_2)$, which leads to a separation of the double integral.

To set up the equations of motion of the isothermal dynamics, we stress that in order to replace the phase space average by a time average, *the function $w_\varepsilon^{(2)}$ has to be sampled during time evolution*. The expression

$$\langle\langle\, \underset{\sim}{B} \,\rangle\rangle = \frac{1}{\tilde{Z}_\varepsilon^{(2)}(\beta)} \iint \frac{\mathrm{d}^2\alpha_1}{\pi} \frac{\mathrm{d}^2\alpha_2}{\pi} e^{-|\alpha_1|^2(e^{\beta\omega}-1)} e^{-|\alpha_2|^2(e^{\beta\omega}-1)} \langle A_\varepsilon | \underset{\sim}{B} | A_\varepsilon \rangle \qquad (3.57)$$

that follows from (3.55) by a cancellation of $\langle A_\varepsilon | A_\varepsilon \rangle$ seemingly indicates that for the calculation of $\langle\langle \underset{\sim}{B} \rangle\rangle$ it would suffice to sample the product of two one-particle thermal weight functions during time development and take the temporal average of the phase space function $\langle A_\varepsilon | \underset{\sim}{B} | A_\varepsilon \rangle$. However, this conclusion is wrong, since the role of the normalisation (i. e., the partition function) is not properly taken into account.

This can be outlined more explicitly as follows. In a numerical simulation, a time average is calculated as an algebraic mean of values of the respective phase space function at points that are situated on the trajectory and equidistant in time. Let M be the number of phase space points contributing to the algebraic mean. The normalisation of the algebraic mean with the factor $1/M$ implies a normalisation with the histogram of the contributing phase space points, i. e. the integral of the thermal weight function that has been sampled. The value of this integral is precisely the partition function, see (3.56).

Consequently, if the thermal weight function sampled during a simulation is simply the function for distinguishable particles, $e^{-|\alpha_1|^2(e^{\beta\omega}-1)}e^{-|\alpha_2|^2(e^{\beta\omega}-1)}$, the normalisation will correspond to the Maxwell-Boltzmann partition function for two distinguishable particles, $\tilde{Z}^{(2)}_{MB}(\beta) = \tilde{Z}^{(1)}(\beta)^2$, and the average thus obtained will correspond to the quantity

$$\langle\langle\, \underset{\sim}{B}\,\rangle\rangle_{MB} = \frac{1}{\tilde{Z}^{(2)}_{MB}(\beta)} \iint \frac{\mathrm{d}^2\alpha_1}{\pi}\frac{\mathrm{d}^2\alpha_2}{\pi}\, e^{-|\alpha_1|^2(e^{\beta\omega}-1)}e^{-|\alpha_2|^2(e^{\beta\omega}-1)} \langle\, A_\varepsilon \,|\, \underset{\sim}{B} \,|\, A_\varepsilon\,\rangle \;, \tag{3.58}$$

which is *not* equal to (3.57). With the notation $\langle\langle\,.\,\rangle\rangle_\varepsilon$ for an average according to (3.57), we may write

$$\langle\langle\, \underset{\sim}{B}\,\rangle\rangle_\varepsilon = \frac{\tilde{Z}^{(2)}_{MB}}{\tilde{Z}^{(2)}_\varepsilon} \langle\langle\, \underset{\sim}{S}^\dagger_\varepsilon \underset{\sim}{B}\,\rangle\rangle_{MB} \;. \tag{3.59}$$

This reveals that averages of the type $\langle\langle\,.\,\rangle\rangle_{MB}$ (which could be determined with a simpler thermal weight function) are useless for the calculation of ensemble averages of the type $\langle\langle\,.\,\rangle\rangle_\varepsilon$, since the latter can be obtained from the former only if the complete partition function is known.

3.3.3. Case of N fermions

A calculation analogous to (3.54) in the case of an arbitrary number N of fermions results in

$$\begin{aligned}\langle\langle\, \underset{\sim}{B}\,\rangle\rangle &= \frac{1}{Z^{(N)}_\varepsilon(\beta)} \int \frac{\mathrm{d}^2\alpha_1}{\pi} \cdots \int \frac{\mathrm{d}^2\alpha_N}{\pi}\, e^{\frac{N}{2}\beta\hbar\omega} \underbrace{\prod_{j=1}^{N} e^{-|\alpha_j|^2(e^{\beta\hbar\omega}-1)} \langle\, A_\varepsilon \,|\, A_\varepsilon\,\rangle}_{w^{(N)}_\varepsilon(\alpha_1,\ldots\alpha_N)} \frac{\langle\, A_\varepsilon \,|\, \underset{\sim}{B} \,|\, A_\varepsilon\,\rangle}{\langle\, A_\varepsilon \,|\, A_\varepsilon\,\rangle} \\ &= \frac{1}{\tilde{Z}^{(N)}_\varepsilon(\beta)} \int \frac{\mathrm{d}^2\alpha_1}{\pi} \cdots \int \frac{\mathrm{d}^2\alpha_N}{\pi}\, w^{(N)}_\varepsilon(\alpha_1,\ldots\alpha_N) \frac{\langle\, A_\varepsilon \,|\, \underset{\sim}{B} \,|\, A_\varepsilon\,\rangle}{\langle\, A_\varepsilon \,|\, A_\varepsilon\,\rangle} \;.\end{aligned} \tag{3.60}$$

Note we have moved the factor $e^{\frac{N}{2}\beta\hbar\omega}$ connected to the one-particle ground state energy to the partition function, $\tilde{Z}^{(N)}_\varepsilon(\beta) = e^{-\frac{N}{2}\beta\hbar\omega} Z^{(N)}_\varepsilon(\beta)$.

In order to calculate the explicit form of $\langle\, A_\varepsilon \,|\, A_\varepsilon\,\rangle$ in the case of fermions, consider the general N-particle operator of antisymmetrisation,

$$\underset{\sim}{S}^{(N)}_- = \frac{1}{N!} \sum_\pi \mathrm{sgn}\,(\pi) \underset{\sim}{P}_\pi \;. \tag{3.61}$$

π denotes a permutation of the N-tuple $(1,\ldots N)$, and $\underset{\sim}{P}_\pi$ corresponds to the permutation operator which acts upon a N-particle product state as

$$\underset{\sim}{P}_\pi \,|\, \alpha_1, \alpha_2, \ldots \alpha_N\,\rangle = \,|\, \alpha_{\pi(1)}, \alpha_{\pi(2)}, \ldots \alpha_{\pi(N)}\,\rangle \;. \tag{3.62}$$

Using the properties of hermiticity and idempotency of $\underset{\sim}{S}_{-}^{(N)}$, we can easily calculate

$$\begin{aligned} \langle A_- \,|\, A_- \rangle &= \langle \alpha_1, \alpha_2, \ldots \alpha_N \,|\, \underset{\sim}{S}_{-}^{(N)} \,|\, \alpha_1, \alpha_2, \ldots \alpha_N \rangle \\ &= \frac{1}{N!} \sum_{\pi} \mathrm{sgn}\,(\pi)\, \langle \alpha_1 \,|\, \alpha_{\pi(1)} \rangle \ldots \langle \alpha_N \,|\, \alpha_{\pi(N)} \rangle \\ &= \frac{1}{N!} \det\left(\langle \alpha_k \,|\, \alpha_l \rangle \right) \ . \end{aligned} \tag{3.63}$$

This expression in terms of a determinant will turn out to be extremely advantageous, since it will permit a far-reaching analytical development of the N-fermion Nosé-Hoover method.

In the case of bosons, in contrast, it is not possible to obtain an analogous compact and useful expression for $\langle A_+ \,|\, A_+ \rangle$. Accordingly, it will be impossible to devise the Nosé-Hoover method in the N-boson case.

4. Isothermal quantum dynamics for the harmonic oscillator

After the preparations of the preceding chapter that provided suitable phase-space integral representations of quantum canonical average values, we are now ready to design equations of motion which will be solved by isothermal trajectories in the parameter space of coherent states.

4.1. A quantum Langevin equation

Inspecting expression (3.41) for a canonical average of an arbitrary observable of the quantum harmonic oscillator and expression (3.37) for the quantum thermal weight function, one sees that the time evolution of the parameters of coherent states needs to sample Gaussian distributions in order that time averages equal canonical ensemble averages. This is in complete analogy to the classical case. Therefore, a translation of the classical Langevin equation to an equation of motion for the parameters of coherent states is straightforward, since the distribution functions are Gaussians in both cases and differ only with regard to the respective widths. But it is known that the width of the Gaussians is related to the amplitude of the fluctuating force, see equation (2.4). Therefore, in order to obtain sound equations of motion of first order in time that may be interpreted as equations of motion for the parameters of coherent states, we replace q in the classical Langevin equation (2.2) by the parameter r while keeping the letter p, resulting in

$$\frac{dr}{dt} = \frac{p}{m} \ , \qquad \frac{dp}{dt} = -\frac{\partial V}{\partial q} - \gamma p + F(t) \ . \tag{4.1}$$

We interpret (4.1) as equations of motion for the parameters r and p of coherent states. Moreover, we postulate a modified fluctuation-dissipation theorem for the fluctuating force,

$$\langle\langle \ F(t_1)F(t_2) \ \rangle\rangle = 2m\gamma \frac{\hbar\omega}{e^{\beta\hbar\omega} - 1} \delta(t_1 - t_2) \ . \tag{4.2}$$

From the analysis of the case of the classical harmonic oscillator, it is clear that in the long-time limit, a time average over the solution of (4.1) will correspond to an average over the parameter space with Gaussian distribution functions. While the classical version (2.4) of the fluctuation-dissipation theorem leads to a sampling of the Maxwell-Boltzmann distribution (2.11), the replacement of the term $k_B T$ by $\hbar\omega/(e^{\beta\hbar\omega} - 1)$ will lead to a sampling of the quantum thermal weight function $w^{(1)}$.

To summarise this section, we saw that for a single particle, it is very easy to modify the classical Langevin equation along with the corresponding classical fluctuation-dissipation relation such that equations of motion for the parameters of coherent states are obtained and the time evolution samples the distribution function $w^{(1)}$. Formally, the result differs from the classical case only with regard to the temperature dependence of the amplitude of the fluctuating force. This procedure is possible since both the classical canonical distribution

function on phase space and the quantum thermal weight function on the parameter space of coherent states are Gaussians which differ only with respect to the temperature dependence of their widths.

Hence, we recognise that this stochastic approach is limited to the cases of Gaussian distribution functions, corresponding to a single or distinguishable quantum particles in an external harmonic oscillator potential. The distribution function $w_\varepsilon^{(2)}$ of two undistinguishable bosons or fermions is not a product of Gaussians. Beyond, $w_\varepsilon^{(2)}$ is not even separable into a product of two functions each of which only depends on the parameter of one particle. If it *were* possible to find expressions $V_{\varepsilon 1}(r_1)$, $V_{\varepsilon 2}(r_2)$ such that

$$w_\varepsilon^{(2)} = C \exp\left(\frac{p_1^2}{2m} + V_{\varepsilon 1}(r_1)\right) \exp\left(\frac{p_2^2}{2m} + V_{\varepsilon 2}(r_2)\right) \ , \tag{4.3}$$

a use of a modified version of the classical Langevin equation would be conceivable. But the quantum mechanical entanglement of $w_\varepsilon^{(2)}$ prohibits a transfer of the classical Langevin equation to the case of indistinguishable quantum particles.

4.2. The quantum Nosé-Hoover thermostat

4.2.1. One particle[1]

In the present section, we will show that for a single quantum particle in an external harmonic oscillator potential, it is also possible to develop sets of deterministic dynamical equations for the parameters of coherent states that ressemble closely the classical temperature control schemes that have been the subject of chapter 2. According to the idea of these approaches, we will introduce pseudofriction terms into the equations of motion (3.27) of coherent states. The time dependence of the pseudofriction coefficients will be determined in such a way that the distribution function $w^{(1)}$ for one particle is sampled provided the time evolution is ergodic.

We will start with the simple Nosé-Hoover scheme, extending it to Nosé-Hoover chains in the following. The demon method is also sketched.

4.2.1.1. The Nosé-Hoover thermostat and the Nosé-Hoover chain

Adopting the notation of Martyna et al. [24] that is most suitable for the generalisation to chain thermostats, we investigate the following analogue of the classical Nosé-Hoover dynamics for the quantum dynamics of coherent states:

$$\frac{d}{dt}r = \frac{p}{m} \ , \qquad \frac{d}{dt}p = -m\omega^2 r - p\frac{p_\eta}{Q} \ . \tag{4.4}$$

The equation of motion of the parameter p is supplemented by a term similar to a frictional force, $-p\,p_\eta/Q$. This modification obviously touches the time evolution of the overall phase factor $e^{-\frac{i}{\hbar}\frac{1}{2}pr}$ of a coherent state (see equation (3.23)), but the phase factor does not play a role in the present context of quantum statistical averages where a phase independent expectation value $\mathcal{B}(r,p) = \langle\, r,p \,|\, \underset{\sim}{B} \,|\, r,p \,\rangle$ is averaged (see equation (3.41)).

[1] This section, along with section 5.1, is the main content of the publication [38].

The key point is the time evolution the pseudofriction coefficient p_η. It is determined by the condition that the desired distribution function,

$$f(r,p,p_\eta) = w^{(1)}(r,p)\ \exp\left(-\beta\frac{p_\eta^2}{2Q}\right) \tag{4.5}$$
$$= \exp\left(-\left(\frac{p^2}{2m}+\frac{1}{2}m\omega^2 r^2\right)\frac{e^{\beta\hbar\omega}-1}{\hbar\omega}-\beta\frac{p_\eta^2}{2Q}\right)\ ,$$

is a stationary solution of the following generalised Liouville equation (cf. (2.19)) in the mixed quantum-classical phase space with elements $x=(r,p,p_\eta)$:

$$\frac{d}{dt}\,f = -f\left(\frac{\partial}{\partial x}\cdot\dot{x}\right) \tag{4.6}$$
$$= -f\left(\frac{\partial}{\partial r}\dot{r}+\frac{\partial}{\partial p}\dot{p}+\frac{\partial}{\partial p_\eta}\dot{p_\eta}\right)\ .$$

Note that constant overall prefactors of f cancel in this equation, which means that normalisations of f may be neglected in studies of this equation.

We calculate the left hand side of (4.6), employing the equations of motion of r and p, (4.4):

$$\frac{d}{dt}f = \frac{\partial f}{\partial p}\dot{p}+\frac{\partial f}{\partial r}\dot{r}+\frac{\partial f}{\partial p_\eta}\dot{p}_\eta \tag{4.7}$$
$$= f\cdot\left(-\left(\frac{p}{m}\dot{p}+m\omega^2 r\dot{r}\right)\frac{e^{\beta\hbar\omega}-1}{\hbar\omega}-\beta\frac{p_\eta}{Q}\dot{p}_\eta\right)$$
$$= f\cdot\left(\frac{p^2}{m}\frac{p_\eta}{Q}\frac{e^{\beta\hbar\omega}-1}{\hbar\omega}-\beta\frac{p_\eta}{Q}\dot{p_\eta}\right)\ .$$

On the right hand side of (4.7), we have the freedom to impose the constraint $\partial\dot{p_\eta}/\partial p_\eta = 0$ that is common in this context (cf. equation (2.27)). We obtain

$$-f\left(\frac{\partial}{\partial x}\cdot\dot{x}\right) = f\ \frac{p_\eta}{Q}\ . \tag{4.8}$$

Equating (4.7) and (4.8) yields the following equation of motion for p_η:

$$\frac{d}{dt}p_\eta = \frac{1}{\beta}\left(\frac{p^2}{m}\frac{e^{\beta\hbar\omega}-1}{\hbar\omega}-1\right)\ . \tag{4.9}$$

A comparison of this result with (2.34) shows that as in the case of the quantum distribution function $w^{(1)}$, the only difference between this equation and its classical counterpart is given by the factor $(e^{\beta\hbar\omega}-1)/(\beta\hbar\omega)$. Moreover, (4.9) retains the property of its classical counterpart that the time evolution of the pseudofriction coefficient is governed by the deviation of the actual value of a quantity related to the kinetic energy from its canonical average value. This can be inferred by evaluating the canonical average

$$\frac{e^{\beta\hbar\omega}-1}{\hbar\omega}\ \langle\langle\ \frac{p^2}{m}\ \rangle\rangle = 1 \tag{4.10}$$

using (3.41). In addition, one introduces the equation of motion

$$\frac{d}{dt}\,\eta = \frac{p_\eta}{Q} \tag{4.11}$$

of the variable η that contributes to the conserved quantity

$$H' = \left(\frac{p^2}{2m} + \frac{1}{2}m\omega^2 r^2\right)\frac{e^{\beta\hbar\omega}-1}{\beta\hbar\omega} + \frac{p_\eta^2}{2Q} + k_B T\eta \ . \tag{4.12}$$

The set of dynamical equations (4.4), (4.9) (along with (4.11)) forms a quantum Nosé-Hoover thermostat for a single particle in an external harmonic oscillator potential. It is expressed in terms of equations of motion for the parameters of coherent states. Since the distribution function that needs to be sampled on the parameter space during time evolution is a two-dimensional Gaussian as in the classical case, we anticipate ergodicity problems for the simple Nosé-Hoover scheme. Therefore, in practice, we will employ a chain thermostat that has been described for the classical case in section 2.2.3. The application of the idea of a chain of thermostats to the quantum case does not infer anything new compared to the classical case, since only the first pseudofriction coefficient of the chain interacts with the quantum phase space variables.

4.2.1.2. The demon method

In section 2.2.2, we have introduced and discussed another generalisation of the Nosé-Hoover thermostat that is frequently used in classical molecular dynamics, namely, the so-called demon method proposed by Kusnezov, Bulgac, and Bauer [23]. Two pseudofriction coefficients, so-called demons, are introduced for temperature control. The classical equations of motion both of the positions and the momenta are supplemented by additional terms. Now, we introduce demons into the quantum equations of motion of the parameters of coherent states:

$$\frac{d}{dt}r = \frac{p}{m} - g_2'(\xi)F(r,p) \ , \qquad \frac{d}{dt}p = -m\omega^2 r - g_1'(\zeta)G(r,p) \ . \tag{4.13}$$

$F(r,p)$, $G(r,p)$ are arbitrary functions of the quantum phase space variables. $g_1(\zeta)$, $g_2(\xi)$ are functions of the demon variables which have to be chosen such that the integration of the distribution function converges, and g_1', g_2' are the respective derivatives. The distribution function f on the phase space $(r,p,\zeta,\xi) = x$ reads

$$f(r,p,\xi,\zeta) = \exp\left(-\Big(\frac{p^2}{2m} + \frac{1}{2}m\omega^2 r^2\Big)\frac{e^{\beta\hbar\omega}-1}{\hbar\omega} - \beta\Big(\frac{g_1(\zeta)}{\kappa_1} + \frac{g_2(\xi)}{\kappa_2}\Big)\right) \ , \tag{4.14}$$

and the time evolution of the demons is, as above, deduced from the requirement that f is a solution of the generalised Liouville equation (2.19). The additional constraints (cf. equation (2.27)),

$$\frac{\partial\dot{\zeta}}{\partial\zeta} = 0 \ , \qquad \frac{\partial\dot{\xi}}{\partial\xi} = 0 \ ,$$

are also employed. From a comparison of coefficients of the functions g_1', g_2', we finally obtain

$$\frac{d}{dt}\zeta = \frac{\kappa_1}{\beta}\left(\frac{p}{m}G\frac{e^{\beta\hbar\omega}-1}{\hbar\omega} - \frac{\partial G}{\partial p}\right) \ , \tag{4.15}$$

$$\frac{d}{dt}\xi = \frac{\kappa_2}{\beta}\left(m\omega^2 rF\frac{e^{\beta\hbar\omega}-1}{\hbar\omega} - \frac{\partial F}{\partial r}\right) \ . \tag{4.16}$$

It is interesting to notice that

$$\langle\langle \frac{\partial G}{\partial p} \rangle\rangle = \frac{e^{\beta\hbar\omega}-1}{\hbar\omega} \langle\langle \frac{p}{m} G \rangle\rangle \ , \tag{4.17}$$

i. e., the ratio of the canonical averages of the quantities that determine the time derivative of the demons is $\frac{e^{\beta\hbar\omega}-1}{\hbar\omega}$. A comparison with equation (2.30) shows that here again, a replacement of β by $\frac{e^{\beta\hbar\omega}-1}{\hbar\omega}$ leads from the classical to the quantum case (cf. equation (3.37)).

The quantity

$$H' = \left(\frac{p^2}{2m} + \frac{1}{2}m\omega^2 r^2\right) \frac{e^{\beta\hbar\omega}-1}{\beta\hbar\omega} + \frac{g_1(\zeta)}{\kappa_1} + \frac{g_2(\xi)}{\kappa_2} + \frac{1}{\beta}\int^t \mathrm{d}t' \left(\frac{\partial G}{\partial p} g_1' + \frac{\partial F}{\partial r} g_2'\right) \tag{4.18}$$

is conserved during the time evolution defined by (4.13), (4.15), (4.16).

The cubic coupling scheme (2.32) leads in the quantum case to the special set of equations of motion

$$\begin{aligned} &\frac{d}{dt}r = \frac{p}{m} - \xi r^3 \ , \qquad \frac{d}{dt}p = -m\omega^2 r - \zeta^3 p \ , \\ &\frac{d}{dt}\zeta = \frac{\kappa_1}{\beta}\left(\frac{p^2}{m}\frac{e^{\beta\hbar\omega}-1}{\hbar\omega} - 1\right) \ , \\ &\frac{d}{dt}\xi = \frac{\kappa_2}{\beta}\left(m\omega^2 r^4 \frac{e^{\beta\hbar\omega}-1}{\hbar\omega} - 3r^2\right) \ . \end{aligned} \tag{4.19}$$

that will be investigated in chapter 5.

Finally, we note that the equations (4.15), (4.16) may easily be linked to the equations of motion proposed by Kusnezov [19]. $w^{(1)}$ plays the role of Kusnezov's $\rho(Q,P)$. However, while Kusnezov's scheme is limited to quantum systems of finite dimensionality, the present method works for this system with a Hilbert space of infinite dimensionality because our approach takes advantage of the properties of coherent states.

4.2.2. Two identical particles

Quantum mechanical systems of identical, i. e. indistinguishable particles feature a large number of phenomena which are unknown in classical mechanics. The consequences of indistinguishability reach very far and are extremely important. To name but two, we mention the Pauli exclusion principle for fermions that explains the periodic table of elements, and boson statistics which leads to the recently observed phase transition of a boson gas to a Bose-Einstein condensate [11, 12]. Therefore, the extension of the temperature control methods to a system of more than one quantum particle is highly desirable.

We stress that a priori, it is not clear whether the techniques of the foregoing section may be applied to a many-particle quantum system at all. The structure of the two-particle distribution functions $w_\varepsilon^{(2)}$ does not allow a separation (4.3) into a product of two functions each of which depends on the parameters of only one particle. We have already argued that this entanglement prohibits an approach using an equation of the Langevin type (see 4.1). Consequently, it may appear unlikely that the many-particle quantum thermal weight function can be sampled by a time evolution of the Nosé-Hoover type. In view of this, the following investigations give remarkable results.

4.2.2.1. The simple Nosé-Hoover thermostat

We study the following equations of motion of the coherent states parameters (r_1, p_1, r_2, p_2) of two identical quantum particles:

$$\begin{aligned} \frac{d}{dt}\, r_1 &= \frac{p_1}{m}\ , \qquad \frac{d}{dt}\, r_2 = \frac{p_2}{m}\ , \\ \frac{d}{dt}\, p_1 &= -m\omega^2 r_1 - p_1 \frac{p_{\eta_1}}{Q_1}\ , \\ \frac{d}{dt}\, p_2 &= -m\omega^2 r_2 - p_2 \frac{p_{\eta_2}}{Q_2}\ . \end{aligned} \tag{4.20}$$

The equations of motion of the pseudofriction coefficients p_{η_1}, p_{η_2} have to be determined in a procedure analogue to the case of a single particle, i. e. we require that the desired distribution function

$$\begin{aligned} f_\varepsilon^{(2)}(\alpha_1, \alpha_2, p_{\eta_1}, p_{\eta_2}) &\propto w_\varepsilon^{(2)}(\alpha_1, \alpha_2) \exp\left(-\beta\left(\frac{p_{\eta_1}^2}{2Q_1} + \frac{p_{\eta_2}^2}{2Q_2}\right)\right) \\ &= e^{-(|\alpha_1|^2+|\alpha_2|^2)(e^{\beta\hbar\omega}-1)}\,(1+\varepsilon e^{-|\alpha_1-\alpha_2|^2}) \exp\left(-\beta\left(\frac{p_{\eta_1}^2}{2Q_1} + \frac{p_{\eta_2}^2}{2Q_2}\right)\right) \\ &\stackrel{\text{def}}{=} e^{-U}(1+\varepsilon e^{-V}) \end{aligned} \tag{4.21}$$

is a stationary solution of the generalised Liouville equation (4.6) on the phase space with elements $(\alpha_1, \alpha_2, p_{\eta_1}, p_{\eta_2}) = (r_1, p_1, r_2, p_2, p_{\eta_1}, p_{\eta_2}) = x$. The abbreviations U and V are defined as

$$\begin{aligned} U &= (|\alpha_1|^2 + |\alpha_2|^2)(e^{\beta\hbar\omega} - 1) + \beta\left(\frac{p_{\eta_1}^2}{2Q_1} + \frac{p_{\eta_2}^2}{2Q_2}\right) \\ &= \left(\frac{1}{2}m\omega^2(r_1^2 + r_2^2) + \frac{1}{2m}(p_1^2 + p_2^2)\right)\frac{e^{\beta\hbar\omega}-1}{\hbar\omega} + \beta\left(\frac{p_{\eta_1}^2}{2Q_1} + \frac{p_{\eta_2}^2}{2Q_2}\right)\ , \end{aligned} \tag{4.22}$$

$$\begin{aligned} V &= |\alpha_1 - \alpha_2|^2 \\ &= \frac{m\omega}{2\hbar}(r_1 - r_2)^2 + \frac{1}{2m\hbar\omega}(p_1 - p_2)^2\ . \end{aligned} \tag{4.23}$$

For left hand side of the the Liouville equation, we get

$$\begin{aligned} \frac{d}{dt}\, f_\varepsilon^{(2)}(\alpha_1, \alpha_2, p_{\eta_1}, p_{\eta_2}) &= -\dot{U} - \varepsilon \dot{V} e^{-U} e^{-V} \\ &= -(\dot{U} + \dot{V}) f_\varepsilon^{(2)} + \dot{V} e^{-U} \end{aligned} \tag{4.24}$$

and for the right hand side, we calculate

$$\begin{aligned} -\left(\frac{\partial}{\partial x}\cdot\dot{x}\right) &= -\left(\frac{\partial}{\partial r_1}\dot{r}_1 + \frac{\partial}{\partial r_2}\dot{r}_2 + \frac{\partial}{\partial p_1}\dot{p}_1 + \frac{\partial}{\partial p_2}\dot{p}_2 + \frac{\partial}{\partial p_{\eta_1}}\dot{p}_{\eta_1} + \frac{\partial}{\partial p_{\eta_2}}\dot{p}_{\eta_2}\right) \\ &= \frac{p_{\eta_1}}{Q_1} + \frac{p_{\eta_2}}{Q_2}\ , \end{aligned} \tag{4.25}$$

using the equations of motion (4.20) and imposing, in analogy to the case of a single particle, the constraints

$$\frac{\partial \dot{p}_{\eta_i}}{\partial p_{\eta_i}} = 0\ , \quad i = 1, 2\ . \tag{4.26}$$

We obtain the following form of the Liouville equation:

$$\frac{d}{dt}\, f_\varepsilon^{(2)} = -f_\varepsilon^{(2)} \left(\frac{\partial}{\partial x} \cdot \dot{x} \right) \tag{4.27}$$

$$\iff \quad -(\dot{U} + \dot{V}) f_\varepsilon^{(2)} + \dot{V} e^{-U} = f_\varepsilon^{(2)} \left(\frac{p_{\eta_1}}{Q_1} + \frac{p_{\eta_2}}{Q_2} \right)$$

$$\iff \quad \dot{U} = -\left(\frac{p_{\eta_1}}{Q_1} + \frac{p_{\eta_2}}{Q_2} \right) - \varepsilon \dot{V} \frac{1}{e^V + \varepsilon 1} \ .$$

The explicit expressions for $\dot{U}$ and $\dot{V}$ are given by

$$\dot{U} = -\left(\frac{p_1^2}{m} \frac{p_{\eta_1}}{Q_1} + \frac{p_2^2}{m} \frac{p_{\eta_2}}{Q_2} \right) \frac{e^{\beta\hbar\omega} - 1}{\hbar\omega} + \beta \left(\frac{p_{\eta_1}}{Q_1} \dot{p}_{\eta_1} + \frac{p_{\eta_2}}{Q_2} \dot{p}_{\eta_2} \right) \ , \tag{4.28}$$

$$\dot{V} = \frac{p_1 - p_2}{m\hbar\omega} \left(p_2 \frac{p_{\eta_2}}{Q_2} - p_1 \frac{p_{\eta_1}}{Q_1} \right) \ .$$

Hence, in the Liouville equation, only $\dot{U}$ contains the temporal derivatives of the pseudofriction coefficients. This permits to isolate $\dot{p}_{\eta_1}$ and $\dot{p}_{\eta_2}$ on one side. A comparison of the coefficients of the terms p_{η_1}/Q_1 and p_{η_2}/Q_2 on both sides yields the following equations of motion for the pseudofriction coefficients:

$$\dot{p}_{\eta_1} = \frac{1}{\beta} \left(\frac{p_1^2}{m} \frac{e^{\beta\hbar\omega} - 1}{\hbar\omega} - 1 + \varepsilon p_1 \frac{p_1 - p_2}{m\hbar\omega} \frac{1}{e^V + \varepsilon 1} \right) \ , \tag{4.29}$$

$$\dot{p}_{\eta_2} = \frac{1}{\beta} \left(\frac{p_2^2}{m} \frac{e^{\beta\hbar\omega} - 1}{\hbar\omega} - 1 - \varepsilon p_2 \frac{p_1 - p_2}{m\hbar\omega} \frac{1}{e^V + \varepsilon 1} \right) \ .$$

In fact, these equations of motion for the pseudofriction coefficients fulfill the requirement (4.26). Recall that the value '+' of ε applies for bosons, the value '−' for fermions. The set of equations of motion (4.20), (4.29) conserves the quantity

$$H'_\varepsilon = -\frac{1}{\beta} \ln w_\varepsilon^{(2)}(\alpha_1, \alpha_2) + \frac{p_{\eta_1}^2}{2Q_1} + \frac{p_{\eta_2}^2}{2Q_2} + \frac{1}{\beta} \int^t \mathrm{d}t' \left(\frac{p_{\eta_1}(t')}{Q_1} + \frac{p_{\eta_2}(t')}{Q_2} \right) . \tag{4.30}$$

Considering the equations of motion (4.29), we find that the part $\frac{p_i^2}{m} \frac{e^{\beta\hbar\omega}-1}{\hbar\omega} - 1 \ , \quad i = 1, 2$, is familiar from the dynamics of a single thermalised particle, see equation (4.9). However, in the present case of two identical particles we find additional terms that are direct consequences of the principle of indistiguishability in quantum mechanics. The dynamics of the pseudofriction coefficient of each particle depends on the parameters of *both* particles, which is the result of the entanglement prominent in $w_\varepsilon^{(2)}$. In the following chapter 5, we will extensively study the set of equations (4.20), (4.29), and we will demonstrate how the effects of Bose-attraction and Pauli-blocking are reflected in the thermostated dynamics.

We stress that although the thermal distribution function of two identical quantum particles $w_\varepsilon^{(2)}$ in an external harmonic oscillator potential is not separable in the sense of equation (4.3), it has turned out to be possible to design equations of motion for the pseudofriction coefficients p_{η_i} such that $w_\varepsilon^{(2)}$ is a stationary solution of the generalised Liouville equation. Surprisingly, the entanglement involved in the distribution function does not lead to a failure of the ansatz (4.20). Therefore, the set of dynamical equations (4.20) along with (4.29) constitutes a substantial

enhancement of the applicability of the classical Nosé-Hoover scheme. A detailed analysis of the general question whether the equations of motion (4.20), (4.29) actually lead to an ergodic dynamics will be given later on, see section 5.2.

In comparison to the case of a single particle, where the transition from classical to quantum mechanics essentially reduces to an alternate interpretation of the symbols r and p along with suitable modifications of the widths of Gaussian distribution functions, the present section strikingly demonstrates the flexibility and power of the deterministic Nosé-Hoover scheme. Surprisingly, its range of applicability considerably exceeds that of the stochastic Langevin approach discussed in section (4.1). An additional term in the dynamical equations of the pseudofriction coefficients is sufficient to account for the effects of the quantum mechanical principle of indistinguishability.

4.2.2.2. The demon method

The analogous approach using a KBB-scheme starts with the set of equations

$$\begin{aligned}
\frac{d}{dt}r_1 &= \frac{p_1}{m} - g'_{r_1}(\xi_1)F_{r_1}(r_1,p_1)\ , \\
\frac{d}{dt}p_1 &= -m\omega^2 r_1 - g'_{p_1}(\zeta_1)G_{p_1}(r_1,p_1)\ , \\
\frac{d}{dt}r_2 &= \frac{p_2}{m} - g'_{r_2}(\xi_2)F_{r_2}(r_2,p_2)\ , \\
\frac{d}{dt}p_2 &= -m\omega^2 r_2 - g'_{p_2}(\zeta_2)G_{p_2}(r_2,p_2)\ .
\end{aligned} \tag{4.31}$$

This scheme has the obvious advantage that positions and momenta are treated symmetrically, i. e. pseudofriction coefficients are present in all equations of motion. The functions F_{r_1}, F_{r_2}, G_{p_1}, G_{p_2} are arbitrary. In contrast to the original equations published in [23], we have restricted the set of variables the respective functions depend on. However, our specific choice will turn out to be sufficient to ensure ergodicity so that this simplification is acceptable.

The desired distribution function reads

$$\begin{aligned}
f^{(2)}_{\varepsilon}(\alpha_1,\alpha_2,\xi_1,\xi_2,\zeta_1,\zeta_2) = \\
w^{(2)}_{\varepsilon}(\alpha_1,\alpha_2)\exp\left(-\beta\Big(\frac{g_{r_1}(\xi_1)}{\kappa_{r_1}}+\frac{g_{r_2}(\xi_2)}{\kappa_{r_2}}+\frac{g_{p_1}(\zeta_1)}{\kappa_{p_1}}+\frac{g_{p_2}(\zeta_2)}{\kappa_{p_2}}\Big)\right)\ .
\end{aligned} \tag{4.32}$$

The functions g_{r_1}, g_{r_2}, g_{p_1}, g_{p_2} are chosen such that they provide a normalisable distribution function. The time dependence of the pseudofriction coefficients is derived from a comparison of coefficients of the functions g'_{r_1}, g'_{r_2}, g'_{p_1}, g'_{p_2} in the generalised Liouville equation (4.6) on the phase space with elements $(r_1,p_1,r_2,p_2,\xi_1,\xi_2,\zeta_1,\zeta_2)=x$. We obtain

$$\begin{aligned}
\frac{d}{dt}\zeta_1 &= \frac{\kappa_{p_1}}{\beta}\left(\frac{p_1}{m}G_{p_1}\frac{e^{\beta\hbar\omega}-1}{\hbar\omega} - \frac{\partial G_{p_1}}{\partial p_1} + \varepsilon G_{p_1}\frac{p_1-p_2}{m\hbar\omega}\frac{1}{e^V+\varepsilon 1}\right)\ , \\
\frac{d}{dt}\zeta_2 &= \frac{\kappa_{p_2}}{\beta}\left(\frac{p_2}{m}G_{p_2}\frac{e^{\beta\hbar\omega}-1}{\hbar\omega} - \frac{\partial G_{p_2}}{\partial p_2} - \varepsilon G_{p_2}\frac{p_1-p_2}{m\hbar\omega}\frac{1}{e^V+\varepsilon 1}\right)\ , \\
\frac{d}{dt}\xi_1 &= \frac{\kappa_{r_1}}{\beta}\left(m\omega^2 r_1 F_{r_1}\frac{e^{\beta\hbar\omega}-1}{\hbar\omega} - \frac{\partial F_{r_1}}{\partial r_1} + \varepsilon F_{r_1} m\hbar\omega(r_1-r_2)\frac{1}{e^V+\varepsilon 1}\right)\ , \\
\frac{d}{dt}\xi_2 &= \frac{\kappa_{r_2}}{\beta}\left(m\omega^2 r_2 F_{r_2}\frac{e^{\beta\hbar\omega}-1}{\hbar\omega} - \frac{\partial F_{r_2}}{\partial r_2} - \varepsilon F_{r_2} m\hbar\omega(r_1-r_2)\frac{1}{e^V+\varepsilon 1}\right)\ .
\end{aligned} \tag{4.33}$$

A comparison of this result to the dynamical equations (4.15) and (4.16) reveals that the first two terms in the brackets are familiar from the one-particle case. Again, additional terms that account for the effects of Pauli-blocking and Bose attraction are now present in the pseudo-friction coefficients of all parameters.

The conserved quantity reads

$$H'_\varepsilon = -\frac{1}{\beta}\ln w^{(2)}_\varepsilon(\alpha_1,\alpha_2) + \frac{g_{r_1}(\xi_1)}{\kappa_{r_1}} + \frac{g_{r_2}(\xi_2)}{\kappa_{r_2}} + \frac{g_{p_1}(\zeta_1)}{\kappa_{p_1}} + \frac{g_{p_2}(\zeta_2)}{\kappa_{p_2}} + \frac{1}{\beta}\int^t \mathrm{d}t' \left(\frac{\partial F_{r_1}}{\partial r_1} g'_{r_1} + \frac{\partial F_{r_2}}{\partial r_2} g'_{r_2} + \frac{\partial G_{p_1}}{\partial p_1} g'_{p_1} + \frac{\partial G_{p_2}}{\partial p_2} g'_{p_2} \right) . \quad (4.34)$$

4.2.3. Case of N fermions

In section 3.3.3, we have seen that the thermal distribution function of N fermions may be written in the compact form

$$w^{(N)}_-(\alpha_1,\dots\alpha_N) = \frac{1}{N!}\prod_{j=1}^{N} e^{-|\alpha_j|^2(e^{\beta\hbar\omega}-1)} \det\left(\langle\, \alpha_k \,|\, \alpha_l \,\rangle\right) . \quad (4.35)$$

We use the notation of the Nosé-Hoover chain (cf. equation (4.20)) in the following ansatz for the equations of motion of the coherent states parameters. However, for calculational reasons, it turns out most favourable to use a form in terms of the complex parameters α_m,

$$\begin{aligned} \dot\alpha_m &= -i\omega\alpha_m - \frac{\alpha_m - \alpha^*_m}{2}\frac{p_{\eta_m}}{Q_m} , \\ \dot\alpha^*_m &= i\omega\alpha^*_m + \frac{\alpha_m - \alpha^*_m}{2}\frac{p_{\eta_m}}{Q_m} . \end{aligned} \quad (4.36)$$

Formally, we can treat α_m and α^*_m as independent parameters. The thermal distribution function that we will demand to be a stationary solution of the generalised Liouville equation reads

$$\begin{aligned} f^{(N)}_-(\alpha,\alpha^*,p_{\eta_l}) &\propto w^{(N)}_-(\alpha,\alpha^*)\exp\left(-\beta\sum_{j=1}^{N}\frac{p_{\eta_j}}{2Q_j}\right) \\ &= \underbrace{\prod_{j=1}^{N} e^{-|\alpha_j|^2(e^{\beta\hbar\omega}-1)}}_{X} \underbrace{\det\left(\langle\, \alpha_k \,|\, \alpha_l \,\rangle\right)}_{Y} \underbrace{\exp\left(-\beta\sum_{j=1}^{N}\frac{p_{\eta_j}}{2Q_j}\right)}_{Z} , \end{aligned} \quad (4.37)$$

where we have dropped the constant overall prefactor $1/N!$ that cancels in considerations of the generalised Liouville equation (4.6). For this equation, we need the total time derivative of $f^{(N)}_-$,

$$\frac{d}{dt}\, f^{(N)}_- = \frac{d}{dt}\,(XYZ) = \left(\frac{d}{dt}\,X\right)YZ + X\left(\frac{d}{dt}\,Y\right)Z + XY\left(\frac{d}{dt}\,Z\right) . \quad (4.38)$$

Therefore, we calculate successively the time derivatives of X, Y, and Z.

For the first derivative,

$$\frac{d}{dt}\,X = \sum_{m=1}^{N}\left(\frac{\partial X}{\partial \alpha_m}\dot{\alpha}_m + \frac{\partial X}{\partial \alpha_m^*}\dot{\alpha}_m^*\right)\ , \tag{4.39}$$

we need

$$\begin{aligned}\frac{\partial X}{\partial \alpha_m} &= -\alpha_m^*(e^{\beta\hbar\omega}-1)\prod_{j=1}^{N} e^{-|\alpha_j|^2(e^{\beta\hbar\omega}-1)} \\ &= -\alpha_m^*(e^{\beta\hbar\omega}-1)\,X\ ,\end{aligned} \tag{4.40}$$

and

$$\frac{\partial X}{\partial \alpha_m^*} = -\alpha_m(e^{\beta\hbar\omega}-1)\,X\ . \tag{4.41}$$

We obtain

$$\begin{aligned}\frac{d}{dt}\,X &= -X\,(e^{\beta\hbar\omega}-1)\sum_{m=1}^{N}(\alpha_m^*\dot{\alpha}_m + \alpha_m\dot{\alpha}_m^*) \\ &= -X\,\frac{e^{\beta\hbar\omega}-1}{2}\sum_{m=1}^{N}\frac{p_{\eta_m}}{Q_m}(\alpha_m-\alpha_m^*)^2\ .\end{aligned} \tag{4.42}$$

Next, we consider

$$\frac{d}{dt}\,Y = \sum_{m=1}^{N}\left(\frac{\partial Y}{\partial \alpha_m}\dot{\alpha}_m + \frac{\partial Y}{\partial \alpha_m^*}\dot{\alpha}_m^*\right)\ , \tag{4.43}$$

which requires the expression

$$\frac{\partial Y}{\partial \alpha_m} = \frac{\partial}{\partial \alpha_m}\det\left(\langle\,\alpha_k\,|\,\alpha_l\,\rangle\right) = \sum_{k,l=1}^{N}\frac{\partial\left(\langle\,\alpha_k\,|\,\alpha_l\,\rangle\right)}{\partial \alpha_m}A_{kl}\ , \tag{4.44}$$

where the so-called cofactor A_{kl} of the element $a_{kl} = \langle\,\alpha_k\,|\,\alpha_l\,\rangle$ of the original matrix $A = (a_{kl})$ is given by

$$A_{kl} = (-1)^{k+l}M_{kl}\ . \tag{4.45}$$

Here M_{kl} denotes the $(N-1)$th order determinant that is derived from the original matrix A by deletion of the kth row and the lth column[2]. Note that in the present case, since A is a hermitian matrix, the cofactors satisfy the relation

$$A_{kl} = A_{lk}^*\ . \tag{4.46}$$

This is most easily seen from the following representation of the inverse matrix A^{-1} in terms of cofactors,

$$(A^{-1})_{kl} = \frac{1}{\det A}A_{lk}\ , \tag{4.47}$$

[2]Equation (4.44) is an application of the general theorem: If the elements a_{ij} of a matrix A are functions of x, then the following equation holds: $\frac{d}{dx}\det A = \sum_{i,j}\frac{da_{ij}}{dx}A_{ij}$ (cf. [39, ch. 14]).

taking into account that A^{-1} is also hermitian.

Since we have $\langle\, \alpha_m \,|\, \alpha_m \,\rangle = 1$, it is clear that $\frac{\partial}{\partial \alpha_m} \left(\langle\, \alpha_k \,|\, \alpha_l \,\rangle \right)$ vanishes in case $k = l = m$. If $k \neq l$, we find

$$\frac{\partial}{\partial \alpha_m} \left(\langle\, \alpha_k \,|\, \alpha_l \,\rangle \right) \Big|_{k \neq l} = \delta_{km} \left(-\frac{1}{2} \alpha_k^* \right) \langle\, \alpha_k \,|\, \alpha_l \,\rangle + \delta_{lm} \left(-\frac{1}{2} \alpha_l^* + \alpha_k^* \right) \langle\, \alpha_k \,|\, \alpha_l \,\rangle \ . \tag{4.48}$$

With this, we can get to the expression

$$\sum_{k,l=1}^{N} \frac{\partial \left(\langle\, \alpha_k \,|\, \alpha_l \,\rangle \right)}{\partial \alpha_m} A_{kl} = \sum_{k \neq m} \left(\left(-\frac{1}{2} \alpha_m^* \right) \langle\, \alpha_m \,|\, \alpha_k \,\rangle A_{mk} + \left(-\frac{1}{2} \alpha_m^* + \alpha_k^* \right) \langle\, \alpha_k \,|\, \alpha_m \,\rangle A_{km} \right) \ . \tag{4.49}$$

We insert this expression as well as the equations of motion (4.36) on the right hand side of (4.43). Using the abbreviations

$$\begin{aligned} C_{km} &= \alpha_k^* \langle\, \alpha_k \,|\, \alpha_m \,\rangle A_{km} \\ D_{mk} &= -\frac{1}{2} \alpha_m^* \Big(\langle\, \alpha_m \,|\, \alpha_k \,\rangle A_{mk} + \langle\, \alpha_k \,|\, \alpha_m \,\rangle A_{km} \Big) + C_{km} \ , \end{aligned} \tag{4.50}$$

we find

$$\frac{d}{dt}\, Y = \sum_m \sum_{k \neq m} \left(i\omega (-\alpha_m C_{km} + \alpha_m^* C_{km}^*) + \frac{p_{\eta_m}}{Q_m} \frac{\alpha_m - \alpha_m^*}{2} (-D_{mk} + D_{mk}^*) \right) \ . \tag{4.51}$$

Fortunately, this expression simplifies considerably, because the first addend in the sum vanishes,

$$\begin{aligned} \sum_m \sum_{k \neq m} (-\alpha_m C_{km} + \alpha_m^* C_{km}^*) &= -\sum_m \sum_{k \neq m} \alpha_m C_{km} + \sum_m \sum_{k \neq m} \alpha_m^* C_{km}^* \\ &= -\sum_m \sum_{k \neq m} \alpha_m C_{km} + \sum_m \sum_{k \neq m} \alpha_k C_{mk} = 0 \ , \end{aligned} \tag{4.52}$$

since we have $\alpha_m^* C_{km}^* = \alpha_k C_{mk}$, see the definition of C_{km}, equation (4.50). The final expression we obtain after a reorganisation of terms reads

$$\begin{aligned} &\frac{d}{dt}\, Y = \\ &\sum_m \frac{p_{\eta_m}}{Q_m} \frac{\alpha_m - \alpha_m^*}{2} \sum_{k \neq m} \left\{ \left(\frac{\alpha_m^*}{2} \Big(\langle\, \alpha_m \,|\, \alpha_k \,\rangle A_{mk} + \text{c.c.} \Big) + \alpha_k \langle\, \alpha_m \,|\, \alpha_k \,\rangle A_{mk} \right) - \text{c.c.} \right\} \ . \end{aligned} \tag{4.53}$$

Lastly, we need

$$\frac{d}{dt}\, Z = -\beta Z \sum_{j=1}^{N} \frac{p_{\eta_j}}{Q_j} \dot{p}_{\eta_j} \ . \tag{4.54}$$

For the right hand side of the generalised Liouville equation, we find

$$\begin{aligned} -f \left(\frac{\partial}{\partial x} \cdot \dot{x} \right) &= -X\, Y\, Z \sum_{m=1}^{N} \left(\frac{\partial \dot{\alpha}_m}{\alpha_m} + \frac{\partial \dot{\alpha}_m^*}{\partial \alpha_m^*} \right) \\ &= X\, Y\, Z \sum_{m=1}^{N} \frac{p_{\eta_m}}{Q_m} \ . \end{aligned} \tag{4.55}$$

Here again, the constraint $\partial \dot{p}_{\eta_m}/\partial p_{\eta_m} = 0$ has been imposed.

We insert equations (4.42), (4.53) and (4.54) into (4.38) and divide both sides of the generalised Liouville equation by $f_-^{(N)} = XYZ$. In the resulting equation, we compare the coefficients of the term p_{η_m}/Q_m, and the following equations of motion for the pseudofriction coefficients are obtained:

$$\begin{aligned}\frac{d}{dt}\, p_{\eta_m} = & \\ & \frac{1}{\beta}\Bigg(-\frac{e^{\beta\hbar\omega}-1}{2}(\alpha_m - \alpha_m^*)^2 - 1 \\ & + \frac{1}{Y}\frac{\alpha_m - \alpha_m^*}{2}\sum_{k\neq m}\left\{\left(\frac{\alpha_m^*}{2}\Big(\langle\,\alpha_m\,|\,\alpha_k\,\rangle A_{mk} + \text{c.c.}\Big) + \alpha_k\langle\,\alpha_m\,|\,\alpha_k\,\rangle A_{mk}\right) - \text{c.c.}\right\}\Bigg)\ .\end{aligned} \tag{4.56}$$

This set of equations of motion gives the analytical generalisation of (4.29) to an arbitrary number N of fermions. Since the coupling of these equations to a sufficient number of chain thermostats to ensure ergodicity is straightforward, there is no doubt that these equations of motion will permit to sample the distribution function $w_-^{(N)}$.

It the case $N = 2$, $m = 1$, (4.56) reduces to

$$\frac{d}{dt}\, p_{\eta_1} = \frac{1}{\beta}\left(-\frac{e^{\beta\hbar\omega}-1}{2}(\alpha_1 - \alpha_1^*)^2 - 1 + \frac{\alpha_1 - \alpha_1^*}{2}\,\frac{(\alpha_1 - \alpha_1^* - \alpha_2 + \alpha_2^*)}{e^{|\alpha_1-\alpha_2|^2}-1}\right)\ , \tag{4.57}$$

which can clearly be identified as the known result (4.29) (with $\varepsilon = -$) written in terms of the complex coherent states parameters α_m.

For reasons of completeness, we give also the final results for the demon method. The equations of motion read

$$\begin{aligned}\frac{d}{dt}\,\alpha_m &= -i\omega\alpha_m - g'_{2m}(\xi_m)F_m(\alpha_m,\alpha_m^*) - i\frac{1}{m\omega}g'_{1m}(\zeta_m)G_m(\alpha_m,\alpha_m^*)\ , \\ \frac{d}{dt}\,\alpha_m^* &= i\omega\alpha_m - g'_{2m}F_m + i\frac{1}{m\omega}g'_{1m}G_m\ ,\end{aligned} \tag{4.58}$$

where we assume the F_m and G_m are real valued functions. The thermal distribution function is given by

$$f_-^{(N)}(\alpha,\alpha^*,\zeta,\xi) = w_-^{(N)}\exp\left(-\beta\sum_{m=1}^{N}\left(\frac{g_{1m}}{\kappa_{1m}} + \frac{g_{2m}}{\kappa_{2m}}\right)\right)\ , \tag{4.59}$$

and from a comparison of coefficients of g'_{1m} we get the equation of motion of ζ_m,

$$\begin{aligned}\frac{d}{dt}\,\zeta_m = \frac{\kappa_{1m}}{\beta}\Bigg(& -i\frac{e^{\beta\hbar\omega}-1}{m\omega}(\alpha_m - \alpha_m^*)G_m \\ & + i\frac{G_m}{m\omega Y}\sum_{k\neq m}\left\{\left(\frac{\alpha_m^*}{2}\Big(\langle\,\alpha_m\,|\,\alpha_k\,\rangle A_{mk} + \text{c.c.}\Big) + \alpha_k\langle\,\alpha_m\,|\,\alpha_k\,\rangle A_{mk}\right) - \text{c.c.}\right\} \\ & + \frac{i}{m\omega}\left(\frac{\partial G_m}{\partial\alpha_m^*} - \frac{\partial G_m}{\partial\alpha_m}\right)\Bigg)\ ,\end{aligned} \tag{4.60}$$

whereas the equation of motion of ξ_m is obtained from a comparison of coefficients of g'_{2m},

$$\begin{aligned}\frac{d}{dt}\,\xi_m = \frac{\kappa_{2m}}{\beta}\Bigg(&-(e^{\beta\hbar\omega}-1)(\alpha_m+\alpha_m^*)F_m \\ &-\frac{F_m}{Y}\sum_{k\neq m}\left\{\left(\frac{\alpha_m^*}{2}\Big(\langle\,\alpha_m\,|\,\alpha_k\,\rangle A_{mk}+\text{c.c.}\Big)+\alpha_k\langle\,\alpha_m\,|\,\alpha_k\,\rangle A_{mk}\right)-\text{c.c.}\right\} \\ &-\left(\frac{\partial F_m}{\partial\alpha_m^*}+\frac{\partial F_m}{\partial\alpha_m}\right)\Bigg)\,.\end{aligned} \tag{4.61}$$

The present subsection impressingly demonstrates the possibility to come to analytical results for fermions. In contrast, a similar treatment for bosons is not possible, since the permanent involved in $w_+^{(N)}$ does not feature a comparable richness of calculational properties as the determinant. However, the practical calculation of thermodynamic properties of many-particle quantum systems, e. g. using Path Integral Monte Carlo methods, is in general easier for bosons, since the calculations for fermionic systems are frequently prevented by the so-called sign problem, see chapter 1. The sign problem in our method occurs in the calculation of the determinants.

5. Results

In the preceding chapter, we have developed schemes that are supposed to produce an isothermal time evolution that gives time averages corresponding to quantum canonical ensemble averages. In the case of a single particle, the quantum methods are closely related to their classical counterparts such that we do not expect new and rich insights; this is why we do not discuss results using the quantum Langevin equation proposed in 2.1. However, since we are able to apply the Nosé-Hoover and related schemes to the unprecedented case of identical particles, we will also present findings for a single particle in order to become familiar with the quantum Nosé-Hoover method.

The key question that needs to be discussed in the following is whether the equations of motion proposed in section 4.2 reliably lead to ergodic behaviour. From the analysis of the classical techniques in section 2.2.4 it is clear that ergodicity is destroyed as soon as there are conserved quantities other that the pseudoenergy H'. Unfortunately, the analytical determination of such conserved quantities from the equations of motion is extremely difficult, so that one has to resort to numerical studies.

As a rule of thumb, it is widely accepted that the more complex a system is, the more probable becomes ergodic behaviour. The effects of Bose-attraction and Pauli-blocking in the case of identical quantum particles effectively act like a many-body-interaction and obviously make the overall dynamics more complex. Hence, we have tested whether it is sufficient to couple only one particle to a thermostat; however, this method fails to produce ergodic behaviour.

Throughout this chapter, we have set the numerical values of the constants m, ω, $\hbar$, and k_B equal to 1. This implies that in our units the energy spacing $\hbar\omega$ of the eigenvalues of the harmonic oscillator Hamiltonian is equal to 1, as well as the temperature T corresponding to the energy $k_B T = \hbar\omega$.

5.1. One particle

5.1.1. Nosé-Hoover method

We start with a discussion of the quantum Nosé-Hoover method for a single particle in a harmonic oscillator potential.

Formally, the transition from the classical Boltzmann distribution, equation (2.11), to the quantum phase space density $w^{(1)}$, equation (3.37), results from replacing the inverse temperature β by the expression $\left(e^{\beta\hbar\omega} - 1\right)/(\hbar\omega)$. This applies analogously on the level of the respective isothermal equations of motion. Since this term is only a c-number that depends on temperature, but not on the coherent states parameters r and p, it is clear that it does not influence the overall characteristics of the dynamics. Therefore, we expect that ergodicity problems in the quantum case will arise under the same circumstances as in the classical case.

We show results for the set of parameters chosen in [24] to enable a direct comparison. We chose $Q = 1$ and the initial conditions $r(0) = 1$, $p(0) = 1$. The numerical integration of the equations of motion (4.4), (4.9) was carried out with a fourth-order Runge-Kutte algorithm using a step size that ensured conservation of the pseudoenergy H' (see eq. (4.12)) to at least

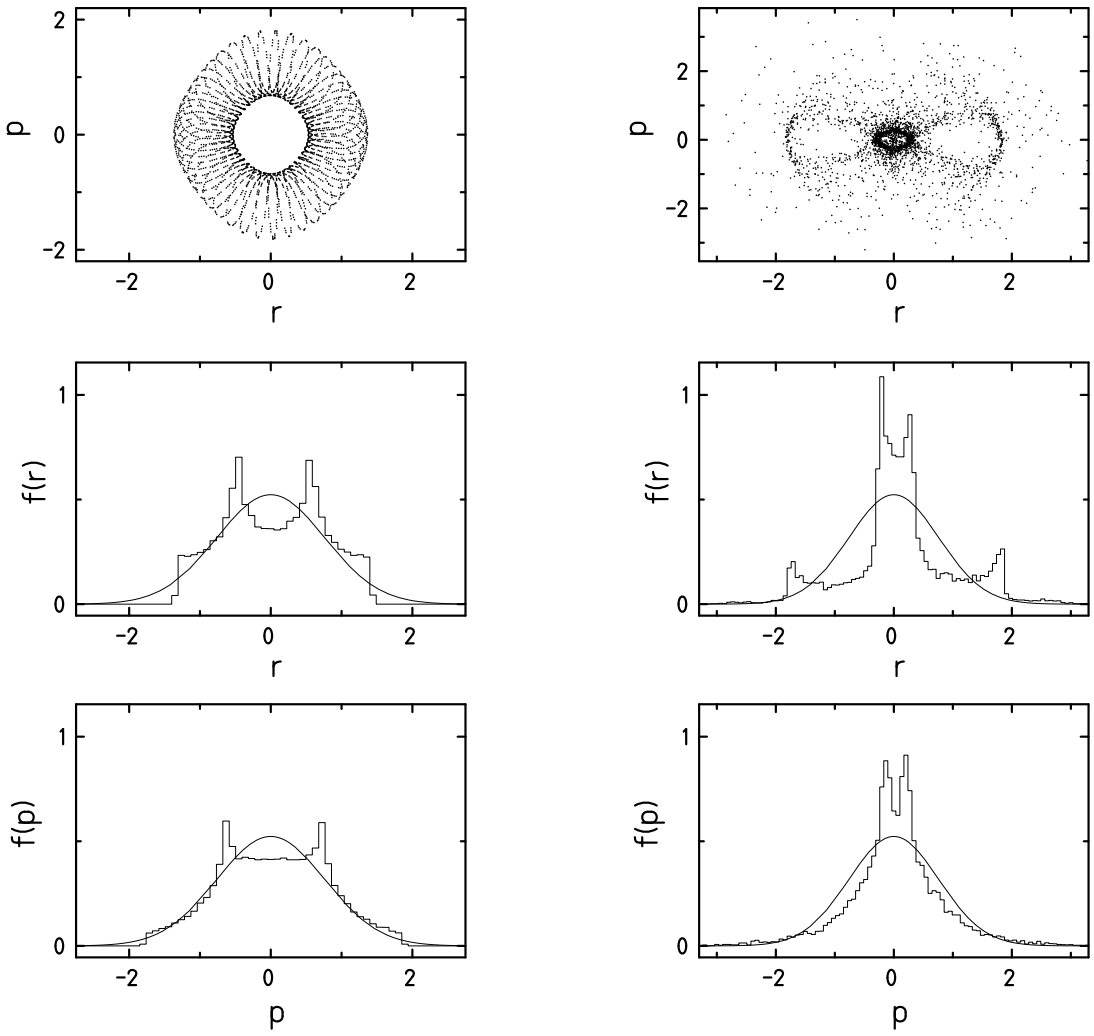

Figure 5.1.: Results of time averaging with a simple Nosé-Hoover scheme, $T = 1$. Left panel: $p_\eta(0) = 1$, right panel: $p_\eta(0) = 10$. From above: (r, p)–density plot, position distribution, momentum distribution. The solid line shows the respective normalised marginal of $w^{(1)}$, e. g. $f(r) = (1/\tilde{Z}^{(1)}) \int (\mathrm{d}p/(2\pi\hbar)) w^{(1)}(r, p)$. The distributions sampled by time averaging are presented as histograms.

six significant figures. All runs were made over a total integration time of $\tau = 2000\,\mathcal{T}$, where the time unit is given by $\mathcal{T} = 2\pi/\omega$.

In figure 5.1, we present results for the case $T = 1$, with the initial condition $p_\eta(0) = 1$ on the left, $p_\eta(0) = 10$ on the right panel. On the left panel, the system performs rotational motions in the (r, p)–parameter space, resulting in a very regularly shaped density plot. On the right panel, the motion looks more chaotic. However, in both cases, the histograms deviate considerably from the respective marginal of $w^{(1)}$. It is also evident that the change of the initial conditions substantially affects the distributions that are sampled. This is unacceptable as an invariant probability distribution is desired.

Figure 5.2 presents results obtained with the initial condition $p_\eta(0) = 10$, but at temperatures $T = 0.1$ on the left and $T = 10$ on the right panel. At the low temperature, the

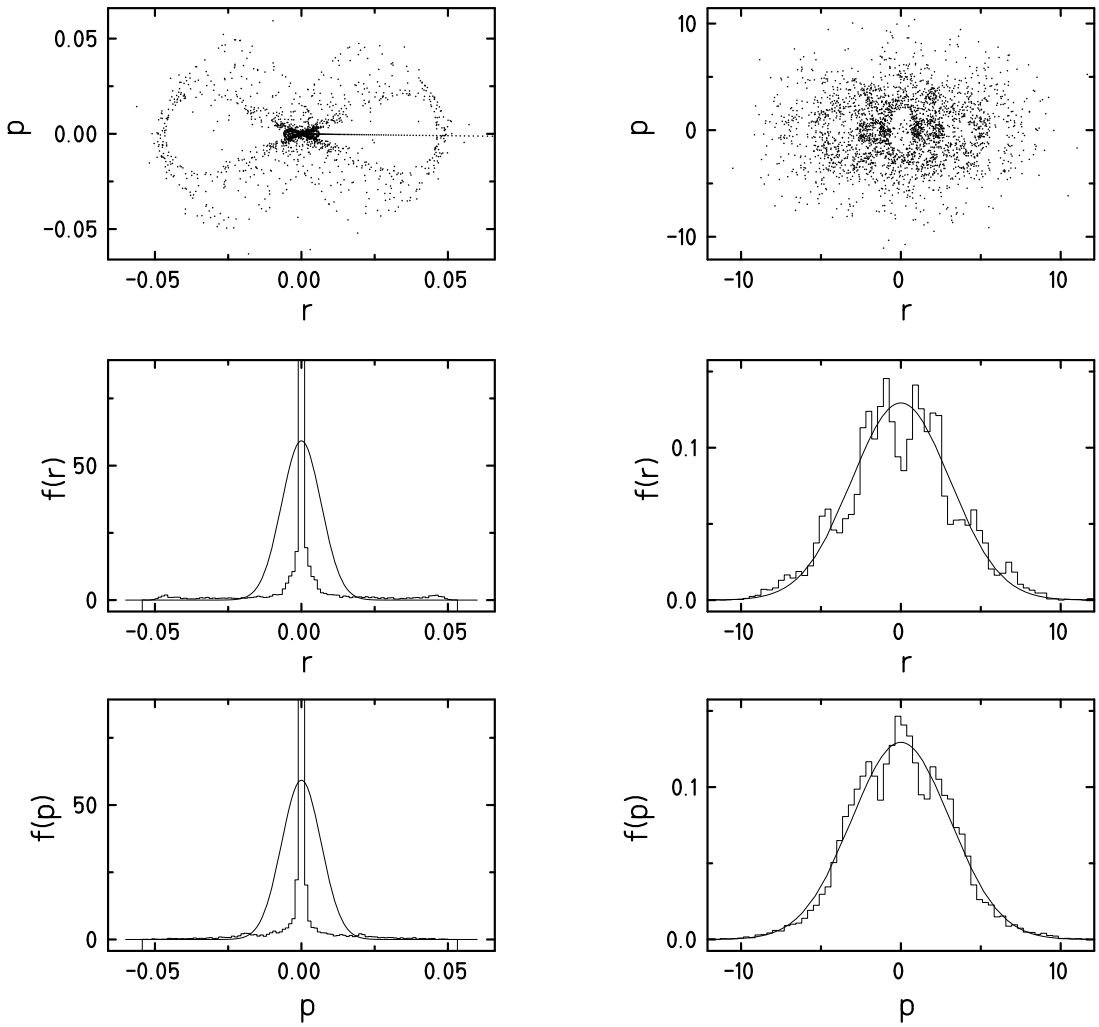

Figure 5.2.: Results of time averaging with a simple Nosé-Hoover scheme at a low temperature ($T = 0.1$, left panel), and at a high temperature ($T = 10$, right panel).

histograms do not at all agree with the respective marginals of $w^{(1)}$. Additional investigations for modified initial conditions and parameter values (e. g., Q) show different patterns in the (r, p)–density plots, but the theoretical distribution function $w^{(1)}$ is not matched. This also applies to the marginal distribution of the pseudofriction coefficient p_η. Altogether, strong non-ergodic behaviour is observed in the low temperature regime.

Although the overall agreement is better in the high temperature regime, the corresponding (r, p)–plot reveals that the histograms do not correspond to Gaussians, since the distribution that is sampled has a depleted probability density at the origin of the harmonic potential which is also prominent in the marginal $f(r)$. From more extensive investigations, it can be inferred that generally speaking, the agreement with the desired distribution improves with temperature. Therefore, it will be necessary to carefully investigate in particular the *low-temperature behaviour* of all dynamical schemes.

The examples given here suffice to illustrate that the simple quantum Nosé-Hoover scheme does not produce ergodic motion for the harmonic oscillator. Hence, this dynamical scheme

will not reproduce all canonical ensemble averages correctly. The sampled histograms strongly depend on temperature and on the initial conditions as well as on the particular parameter values. This general difficulty was to be expected from the classical harmonic oscillator where the simple Nosé-Hoover scheme also fails to sample Gaussian distribution functions. Anticipating the improvements of ergodic behaviour that will be attained in the following for the more refined schemes (e. g., by a temperature dependent adaptation of thermostat masses or coupling constants), we stress that these measures have turned out to be insufficient in the present case. Therefore, alternate methods need to be studied.

5.1.2. Nosé-Hoover chain method

The situation changes radically with the successive introduction of further thermostating variables acting upon the first pseudofriction coefficient p_η, see figure 5.3. We consider chain

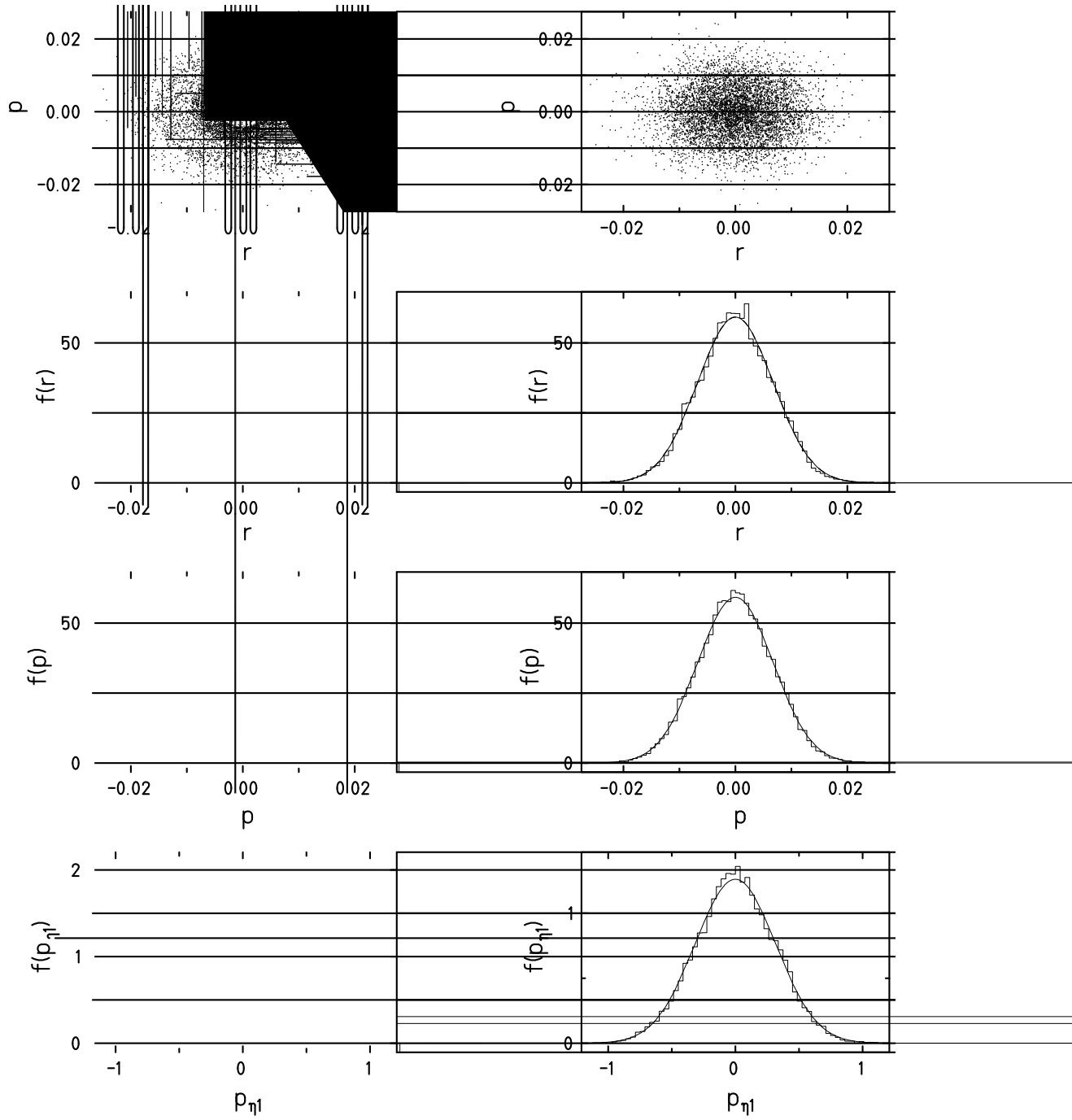

Figure 5.3.: Results of time averaging at $T = 0.1$ using Nosé-Hoover chains of length $M = 2$ (left panel), and $M = 4$ (right panel).

thermostats of length $M = 2$ and $M = 4$ (for the meaning of M, see equation (2.37)) at $T = 0.1$, using in the beginning equal thermostat masses $Q_i = 1$.

The distribution functions sampled by the scheme using a chain thermostat of length $M = 2$ (figure 5.3, left panel) are much closer to the theoretical Gaussian distributions than in the case of the simple Nosé-Hoover scheme, cf. figure 5.2, left panel. Nevertheless, the histograms still deviate noticeably from the theoretical Gaussians, since the feature of a depleted probability density at the origin of the harmonic potential is still visible.

This problem is completely resolved in the case of a chain of length $M = 4$. The histograms reproduce the respective marginals of $w^{(1)}$ extremely well. More detailed investigations show that changes of the initial conditions do not have observable effects on the results. Likewise, the values of the initial conditions may be modified, and further thermostating variables may be added. In all cases, we found that the dynamics generated in this way is ergodic, even at low temperatures.

The following figure 5.4 illustrates the short-time evolution resulting from an ergodic Nosé-Hoover chain dynamics ($M = 4$) in the (r, p)–plane. Instead of rotating clockwise on a circle of constant radius, the parameter trajectory approaches the origin of the harmonic potential on a spiral. This corresponds to *cooling* the particle. At a later time, the radius increases again.

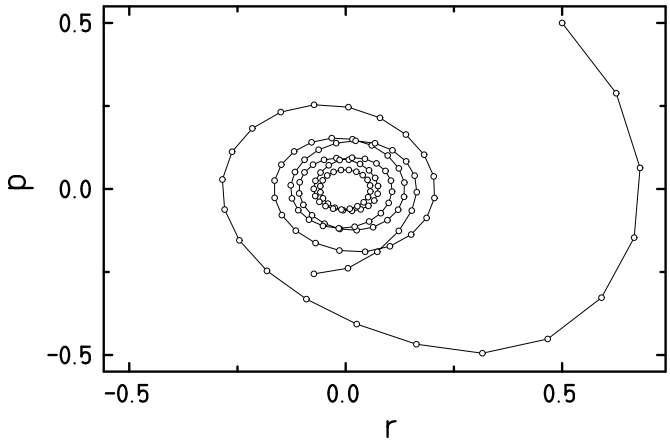

Figure 5.4.: Short-time behaviour of an ergodic Nosé-Hoover chain dynamics. The initial conditions are given by $r(0) = 0.5$, $p(0) = 0.5$, $p_{\eta_i} = 1$, and we have $T = 0.2$. The open circles represent the values of the coherent states parameters at time distances $0.05\,\mathcal{T}$, the total integration time is $6.4\,\mathcal{T}$. The connecting line is drawn to guide the eye.

An alternate way of improving the ergodicity of the scheme consists of an adaptation of the numerical values of the thermostat masses. This idea has first been discussed in the context of the demon method by Kusnezov, Bulgac, and Bauer [23]. They found a rule of thumb for the values of the coupling constants that considerably improves ergodicity (see next section). Adopting this rule, we take $Q_i \approx T^2$, and find that even the chain of length $M = 2$ is ergodic down to a temperature value of $T = 0.05$. Note that in order to avoid numerical difficulties at such low temperatures, the initial state needs to be chosen very close to the ground state.

5.1.3. The demon method

We have also investigated the cubic coupling scheme given by the set of functions (2.32), choosing the initial values $r(0) = 1$, $p(0) = 1$, $\xi(0) = 1$, $\zeta(0) = -1$. The coupling constants were initially chosen to be $\kappa_1 = \kappa_2 = 1$.

At temperatures above $T = 0.3$, no ergodicity problems are encountered. The dynamics provides ergodic behaviour in all examples investigated, and the histograms obtained by time averages converge rapidly against $w^{(1)}$. However, using identical parameter values and initial conditions, but lowering the temperature to $T = 0.2$, the dynamics samples wrong distributions (see figure 5.5, left panel). At even lower temperatures, the agreement becomes progressively worse. This is a striking example that even if a system is ergodic at some temperature, it is

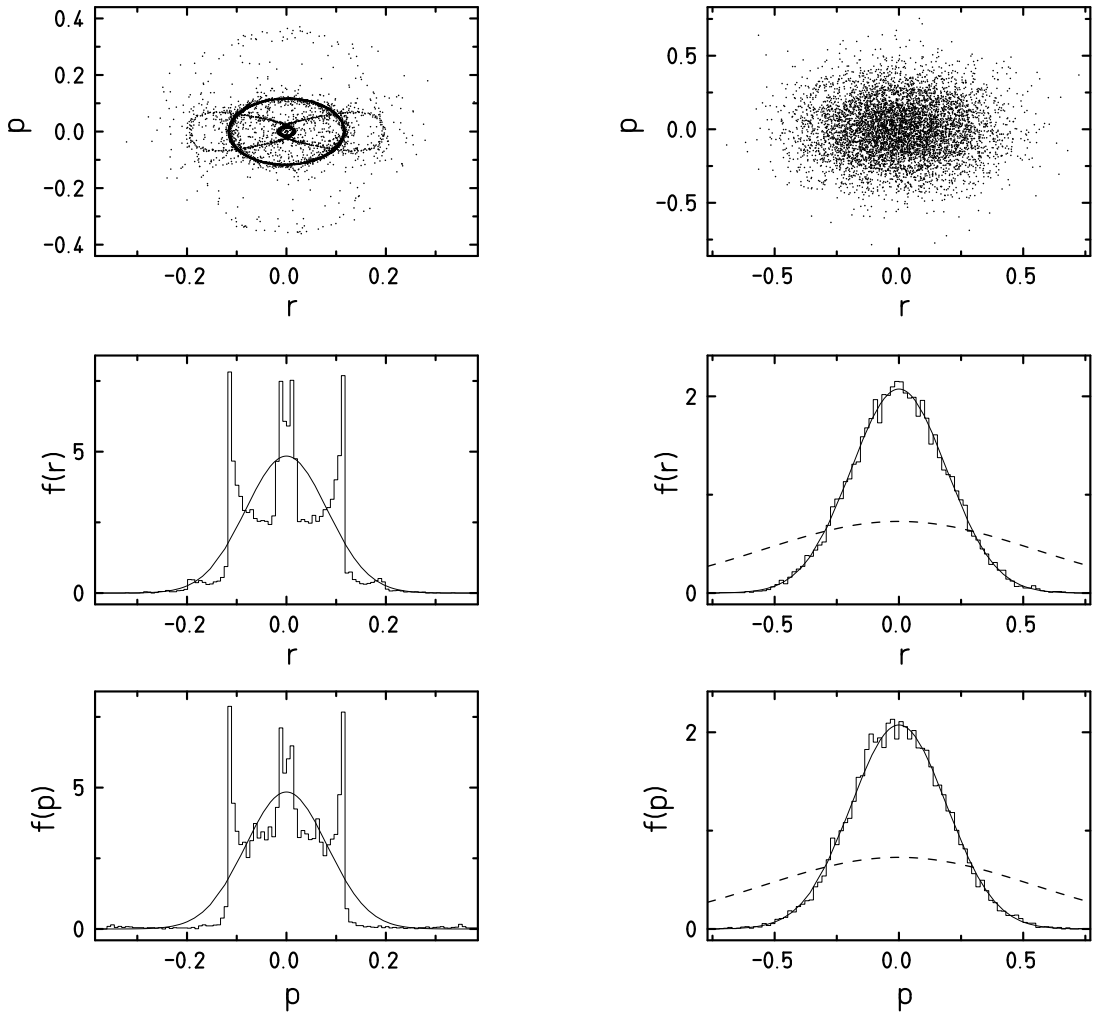

Figure 5.5.: Results of time averaging using the cubic coupling scheme. At $T = 0.3$, we obtain an ergodic dynamics (right panel). The dashed line represents the marginal of the corresponding classical canonical distribution function. The left panel illustrates that at a lower temperature ($T = 0.2$), non-ergodic motion occurs. The trajectories appear to be regular and recurrent and thus do not reproduce $w^{(1)}$.

not necessarily ergodic at a different temperature.

Kusnezov, Bulgac, and Bauer have found this feature also in the classical case [23]. From their own results, they propose to adapt the choice of the coupling constants according to T, $\kappa_1 \approx 1/T$ and $\kappa_2 \approx 1/T^2$, which increases the numerical values of the time derivatives of the demons at low T, cf. (2.28). This increased "mobility" of the demons resolves the problem in the classical case. In the quantum case, we find that the adaptation of the coupling constants is not as successful; it ensures ergodicity only down to a temperature value of $T \approx 0.2$ (not shown).

In comparing the chain thermostat and the demon method in conjuction with the cubic coupling scheme, it appears as an advantage of the chain thermostat that it can easily be made "more complex" if required. The addition of more pseudofriction terms in the chain is simple to perform and numerically inexpensive. Moreover, a convenient choice of the thermostat masses leads to ergodic behaviour at temperature values well below the regime in which the cubic coupling scheme is ergodic. A combination of the demon method and the chain method is of course thinkable and sensible, since the demon method has the advantage of treating the parameters r and p equally.

Finally, we point out that the statistics obtained by time averaging over the modified quantum time evolution is the quantum statistics of the harmonic oscillator. To make this evident, we present on the right hand panel of figure 5.5 plots of $\frac{1}{2\pi\hbar}\, w^{(1)}(r,p)/\tilde{Z}^{(1)}(\beta)$ along with plots of its classical limit

$$\lim_{\frac{e^{\beta\hbar\omega}-1}{\beta\hbar\omega}\to 1} \frac{1}{2\pi\hbar}\frac{1}{\tilde{Z}^{(1)}(\beta)}\, w^{(1)}(r,p) = \frac{\beta\omega}{2\pi}\exp\left(-\beta\Big(\frac{p^2}{2m}+\frac{1}{2}m\omega^2 r^2\Big)\right)\ , \tag{5.1}$$

which is precisely the normalised classical canonical Boltzmann distribution function. Since $\left(e^{\beta\hbar\omega}-1\right)/(\beta\hbar\omega) > 1$ for all β, the quantum distribution function is narrower compared to its classical limit.

5.1.4. Convergence speed

In order to check the convergence speed of the deterministic time averages, we consider the deviation of the histograms from the theoretical marginals of $w^{(1)}$. As an example, we investigate the demon method using the cubic coupling scheme at $T = 1$.

We define the deviation of an $r-$histogram at the sampling time τ (denoted by $f_{hist}(r,\tau)$) to the exact theoretical marginal distribution (in percent) as

$$\Delta_r(\tau) = 100\int_{-\infty}^{\infty} \mathrm{d}r\, |f(r) - f_{hist}(r,\tau)|\ , \tag{5.2}$$

and analogously we have Δ_p, Δ_ξ, Δ_ζ for the parameter p and the demons. The evolution of Δ with time is an indication of the convergence speed of the coupling scheme.

It is well known that the error of the average value of a series of N statistically independent measurements decreases like $N^{-1/2}$. This result is derived by the application of the law of error propagation to the algebraic average. Therefore, in figure 5.6, the bold straight line corresponds to $\Delta \propto \tau^{-1/2}$, according to the case of "optimal sampling", i. e. statistically independent samples. An inspection of figure 5.6 shows that in this case the convergence speed is very close to its theoretical optimum.

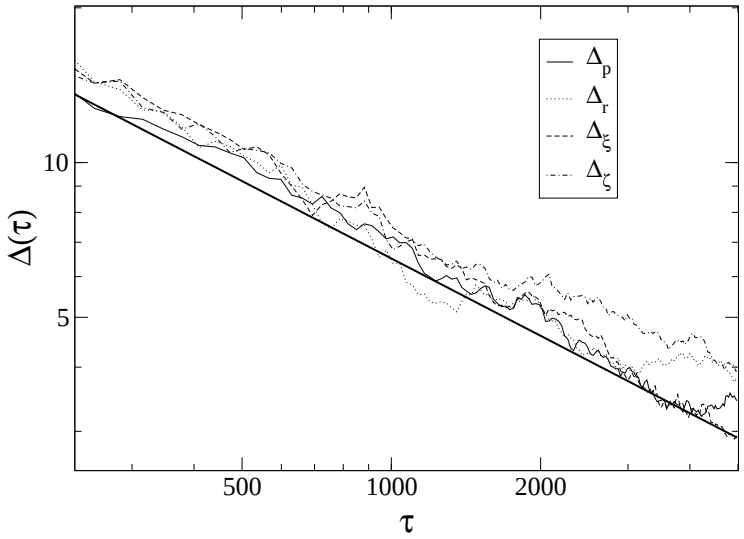

Figure 5.6.: *log – log* – representation of the time evolution of the deviation of the sampled histograms from the respective theoretical distribution using the cubic coupling scheme, $T = 1$. The bold straight line corresponds to $\Delta(\tau) \propto \tau^{-1/2}$.

5.1.5. Mean values of selected observables

It is a priori clear that if the relevant distribution function is correctly sampled during time evolution, the time average of any observable will match its ensemble average. To illustrate this, we investigate two typical observables, the internal energy and its variance. The analytical expressions for the canonical ensemble averages are given by

$$U(\beta) = \langle\langle\ \underset{\sim}{H}\ \rangle\rangle = \frac{\hbar\omega}{2} + \frac{\hbar\omega}{e^{\beta\hbar\omega} - 1} = \frac{\hbar\omega}{2} \coth\left(\frac{1}{2}\beta\hbar\omega\right) \ , \tag{5.3}$$

$$\mathrm{var}(\underset{\sim}{H}) = \langle\langle\ \underset{\sim}{H}^2\ \rangle\rangle - \langle\langle\ \underset{\sim}{H}\ \rangle\rangle^2 = \left(\frac{\hbar\omega}{2\sinh(\frac{1}{2}\beta\hbar\omega)}\right)^2 \ . \tag{5.4}$$

Interestingly, in the expression for the internal energy, we find again that – apart from the non-zero ground state energy – the replacement of β by $(e^{\beta\hbar\omega} - 1)/\hbar\omega$ leads from the classical to the quantum statistical mechanics result.

In order to calculate the respective time averages, the following matrix elements are needed:

$$\langle\, \alpha \,|\, \underset{\sim}{H} \,|\, \alpha \,\rangle = \hbar\omega \left(|\alpha|^2 + \frac{1}{2}\right) = \frac{1}{2}\hbar\omega + \frac{p^2}{2m} + \frac{1}{2}m\omega^2 r^2 \ , \tag{5.5}$$

$$\langle\, \alpha \,|\, \underset{\sim}{H}^2 \,|\, \alpha \,\rangle = \hbar^2\omega^2 \left(\left(|\alpha|^2 + \frac{1}{2}\right)^2 + |\alpha|^2\right) \ . \tag{5.6}$$

These matrix elements have to be regarded as phase space functions in the sense of equation (3.39). Figure 5.7 shows results obtained by time averaging using the cubic coupling scheme with a total sampling time $\tau = 1000\,\mathcal{T}$. The agreement with the exact results is excellent. We observe only small deviations that are of statistical origin.

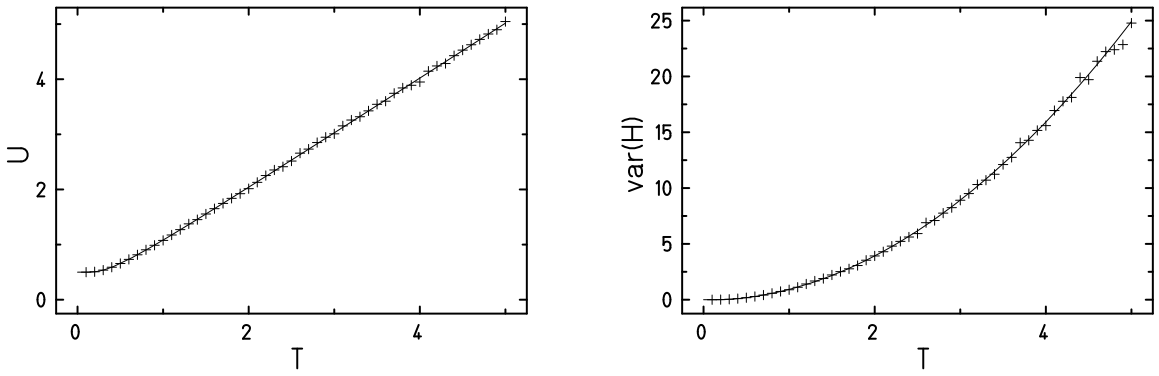

Figure 5.7.: Values of the internal energy and its variance for the harmonic oscillator obtained from time averaging with a KBB dynamics (crosses) compared to the exact quantum canonical ensemble result (solid line).

In closing this section, we remark that the question whether a given scheme of isothermal dynamics produces ergodic motion or not cannot be answered in closed form. The numerical values of the temperature and the free parameters (like coupling constants or thermostat masses), and the choice of functions in the KBB-scheme affect this question in an unpredictable manner. However, the problems occur only if the value of T lies an order of magnitude below the typical energy unit of the considered system; and even in this case, simple modifications of the dynamics like an extension of the chain or adapted values of the coupling constants resolve the problem reliably. Moreover, in all examples we studied, non-ergodic motion could easily be detected by monitoring the marginals of the pseudofriction coefficients. We found that if and only if the marginals of the pseudofriction coefficients were sampled correctly, the marginals $f(r)$ and $f(p)$ were sampled correctly. Although the condition of ergodic sampling in the subspace of the additional degrees of freedom is only necessary for ergodicity on the whole space, we did not encounter a counterexample and therefore consider such a case – ergodicity of the pseudofriction coefficients, non-ergodicity of the original system – as highly exceptional.

5.2. Two particles

In the preceding section, we have presented results of the quantum Nosé-Hoover and related methods for a single particle. We briefly studied questions of ergodicity and convergence, stressing the close relation to the classical case.

Now, considering two identical quantum particles, we enter an entirely new field that does not have a classical counterpart. The quantum distribution functions $w_\varepsilon^{(2)}$ are entangled and do not have the form of a product of two functions depending separately on the parameters of one particle. Therefore, the isothermal equations of motion derived in section 4.2 postulating that $w_\varepsilon^{(2)}$ be a stationary solution of the generalised Liouville equation contain additional terms. The impact of these terms on the dynamics will be studied in the following sections.

5.2.1. Bose-attraction and Pauli-blocking

The different signs for bosons and fermions in the equations of motion of the pseudofriction coefficients stem from the factor $\langle A_\varepsilon \,|\, A_\varepsilon \rangle$ included in $w_\varepsilon^{(2)}$. We investigate the consequences for the movements of the particles. Obviously, the effects of Bose-attraction and Pauli-blocking will be most pronounced at low temperatures, when both particles tend to occupy the one-particle ground state and thereby get close to one another in phase space.

As a simple example, we examine the Nosé-Hoover scheme, see equation (4.20) and (4.29). When two fermions approach in phase space, $V = |\alpha_1 - \alpha_2|^2$ becomes very small and the factor $1/(e^V - 1)$ grows like $1/V$, overcompensating the linear decrease of the prefactor $p_1 - p_2$. This causes a strong acceleration of p_{η_1} and p_{η_2}, and thereby of p_1 and p_2. The directions of the accelerations of the momenta are opposed due to different signs: In case p_1 and p_2 approach the origin of the harmonic potential with the same sign, the signs in equation (4.29) in front of the additional term are opposite; in case p_1 and p_2 approach the origin with different signs, the opposite directions of the acceleration stem from the equations of motion (4.20) where p_1 and p_2 appear in front of p_{η_1} and p_{η_2}. Effectively, a close approach of the particles in phase space, corresponding to $V \to 0$, is avoided by the dynamics. This may be regarded as the dynamical consequence of the exclusion principle. In the case of fermions, the additional terms in the equations of motion (4.29) act like a repulsive force. Hence, we will refer to these terms as *statistical interaction forces*.

In the case of bosons, the opposite signs in the equations (4.29) cause an acceleration of the parameters into the direction of one another, favouring a "meeting" of the particles in phase space. Moreover, if $V = 0$, the factor $(p_1 - p_2)/(e^V + 1)$ vanishes, and the statistical interaction forces vanish at this point. So the case $V = 0$ is not excluded at all; on the contrary, it is aimed at by the boson version of the dynamics.

Figure 5.8 illustrates the simple Nosé-Hoover dynamics of two fermions at low temperature. Initially, both particles are cooled and move to the origin of the potential, i. e. to states of lower energy. But immediately after approaching closely, the fermions are strongly driven away from each other. Figure 5.9 illustrates the short-time behaviour of two bosons at low temperature. After cooling, the bosons are located close to each other and stay at the origin of the potential for a considerable period, and only after $t \approx 8\,\mathcal{T}$, they are again driven away from the origin. These different short-time appearances will obviously lead to different thermal distribution functions.

We remark that the repulsive or attractive statistical interaction forces occur although we are treating a system of non-interacting particles. The interaction is purely a consequence of the quantum statistics of a system of identical particles and is mediated by the influence of the

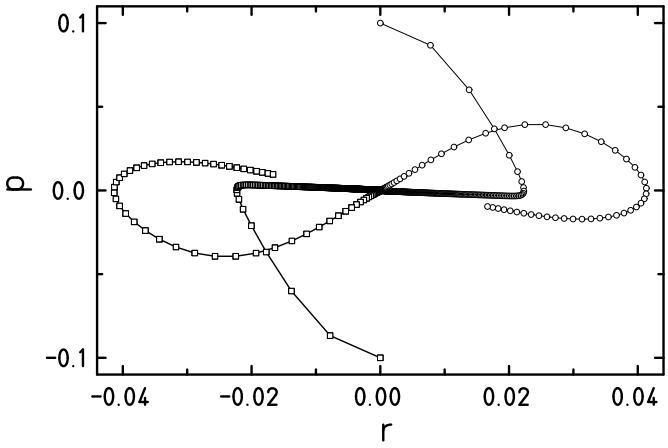

Figure 5.8.: Isothermal Nosé-Hoover dynamics of two identical fermions. The initial values of $\{r_1, p_1, r_2, p_2, p_{\eta_1}, p_{\eta_2}\}$ are $\{0, -0.1, 0, 0.1, 0, 0\}$, the value of the temperature is $T = 0.1$, and $Q_1 = Q_2 = 0.5$. The time distance between the symbols is $0.013\,\mathcal{T}$, and the total integration time is $6.5\,\mathcal{T}$. The two fermions reach their closest position after $t \approx 5.5\,\mathcal{T}$ and are driven away from each other immediately.

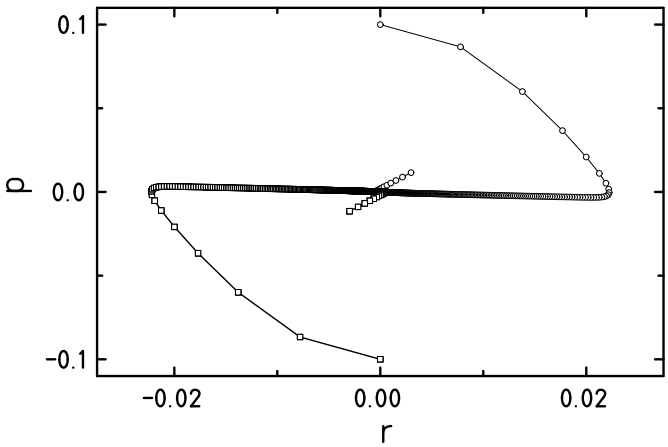

Figure 5.9.: Isothermal Nosé-Hoover dynamics of two identical bosons. All values are chosen as in figure 5.8. However, the total integration time is $8.1\,\mathcal{T}$, since the bosons do not separate earlier.

pseudofrictional forces.

As we will see in section 5.2.2, the simple Nosé-Hoover scheme that has been used here to visualise the effects of the statistical interaction forces fails to produce ergodic motion in the low temperature regime. Nevertheless, we have chosen this scheme for the present illustrative purpose since the effects of Bose-attraction and Pauli-blocking are most lucid in this elementary version of the equations of motion. The schemes that lead to ergodic behaviour have a slightly different short-time appearance with more pronounced rotational movements around the origin that are reminiscent of figure 5.4.

5.2.2. Ergodicity investigations for two fermions

The impact of quantum mechanical indistiguishability on the thermostated dynamics of identical particles effectively looks like an attractive or repulsive interaction. One may anticipate that this interaction which is most pronounced at low temperature values influences the complexity and thereby the ergodicity of the dynamics. One may hope that this leads to improvements, especially in the low temperature range where the demon method shows non-ergodic behaviour, cf. section 5.1.3. Furthermore, one could think of linking only one particle to a thermostat and hope that the second one thermalises "sympathetically" due to the statistical interaction. This will be discussed in section 5.2.2.1.

In order to check the ergodicity of the different methods, we will study marginal distributions of the thermal weight function $w_\varepsilon^{(2)}$. Algebraically, it is more convenient and elegant to determine the marginal distributions written in terms of the relative and the center-of-mass coordinate (i. e., switch to $\alpha_+ = \frac{1}{\sqrt{2}}(\alpha_1 + \alpha_2)$, $\alpha_- = \frac{1}{\sqrt{2}}(\alpha_1 - \alpha_2)$, as indicated for the calculation of the two-particle partition function, equation (3.56)). However, to avoid a reformulation of the equations of motion in terms of new coordinates and to be able to compare the histograms of the thermalised variables directly to the correct respective distributions, we prefer to stick to the representation in terms of r_1, p_1, r_2, p_2. As an example, we give the analytical expressions obtained for the normalised marginal distributions of r_1 and p_1:

$$
\begin{aligned}
f_\varepsilon(r_1) &= \frac{1}{\tilde{Z}_\varepsilon^{(2)}} \int \frac{\mathrm{d}p_1}{2\pi\hbar} \frac{\mathrm{d}r_2\,\mathrm{d}p_2}{2\pi\hbar}\; w_\varepsilon^{(2)}(r_1, r_2, p_1, p_2) \qquad (5.7)\\
&= \frac{1}{\tilde{Z}_\varepsilon^{(2)}} \sqrt{\frac{m\omega}{8\pi\hbar}} \left(\sqrt{\frac{1}{(e^{\beta\hbar\omega}-1)^3}}\; e^{-\frac{m\omega}{2\hbar}(e^{\beta\hbar\omega}-1)r_1^2} \right.\\
&\qquad \left. + \varepsilon \sqrt{\frac{1}{e^{2\beta\hbar\omega}-1}} \sqrt{\frac{1}{e^{\beta\hbar\omega}}} e^{-\frac{m\omega}{\hbar}\sinh(\beta\hbar\omega) r_1^2} \right),\\
f_\varepsilon(p_1) &= \frac{1}{\tilde{Z}_\varepsilon^{(2)}} \int \frac{\mathrm{d}r_1}{2\pi\hbar} \frac{\mathrm{d}r_2\,\mathrm{d}p_2}{2\pi\hbar}\; w_\varepsilon^{(2)}(r_1, r_2, p_1, p_2) \qquad (5.8)\\
&= \frac{1}{\tilde{Z}_\varepsilon^{(2)}} \sqrt{\frac{1}{8\pi m\hbar\omega}} \left(\sqrt{\frac{1}{(e^{\beta\hbar\omega}-1)^3}}\; e^{-\frac{p_1^2}{2m}(e^{\beta\hbar\omega}-1)/(\hbar\omega)} \right.\\
&\qquad \left. + \varepsilon \sqrt{\frac{1}{e^{2\beta\hbar\omega}-1}} \sqrt{\frac{1}{e^{\beta\hbar\omega}}} e^{-\frac{1}{m\hbar\omega}\sinh(\beta\hbar\omega) p_1^2} \right).
\end{aligned}
$$

5.2.2.1. Nosé-Hoover method

To start with, we present results obtained by averaging over trajectories generated by the equations of motion (4.20) along with (4.29). At low temperature values $T \lesssim 1.0$, an extensive study shows that the scheme exhibits non-ergodic behaviour, just as in the one-particle case. An example is given in figure 5.10, left panel. For the given set of initial values and parameters, we obtain histograms that strongly resemble the left panel of figure 5.1. An adaptation of the thermostat masses according to the known rule $Q_i \approx T^2$ does not resolve the problem.

However, if the scheme is investigated at higher temperature values, the agreement between the sampled histograms and the theoretical marginals becomes gradually better. In the temperature range $T \gtrsim 1.2$, we find very good agreement; the right hand panel of figure 5.10 gives an example. This should be contrasted with the one-particle case, where non-ergodicity was found in the simple Nosé-Hoover scheme even for very high temperatures, cf. figure 5.2, right

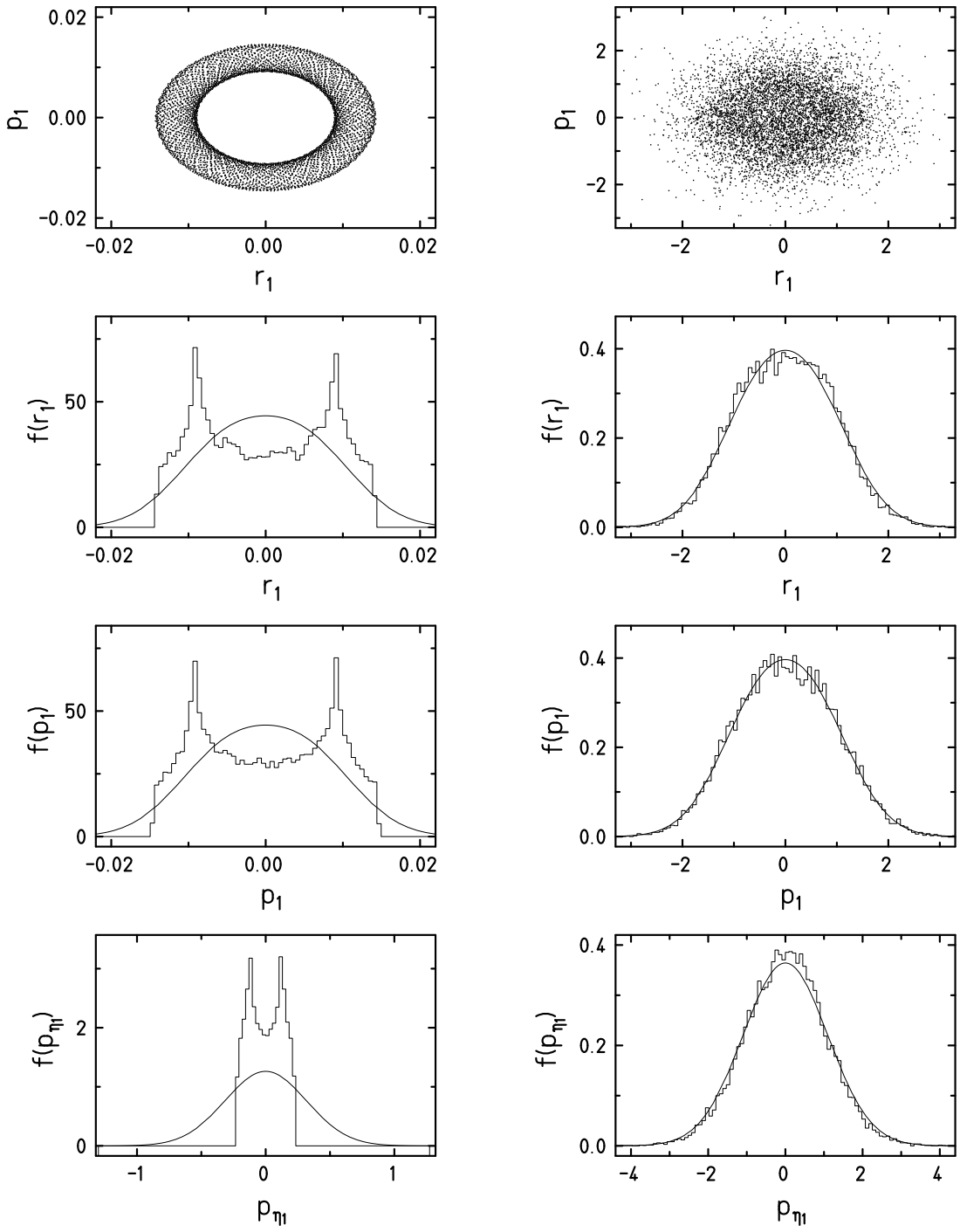

Figure 5.10.: Results of time averaging with the simple Nosé-Hoover scheme for two fermions, left panel: $T = 0.1$, right panel: $T = 1.2$. In both cases, we used identical initial conditions, $r_1(0) = -r_2(0) = 0.01$, $p_1(0) = -p_2(0) = 0.01$, $p_{\eta_1}(0) = -p_{\eta_2}(0) = 0.01$, $Q_1 = Q_2 = 1.0$. We present density plots and histograms for r_1, p_1, and p_{η_1}; the respective results for r_2, p_2, and p_{η_2} look similar.

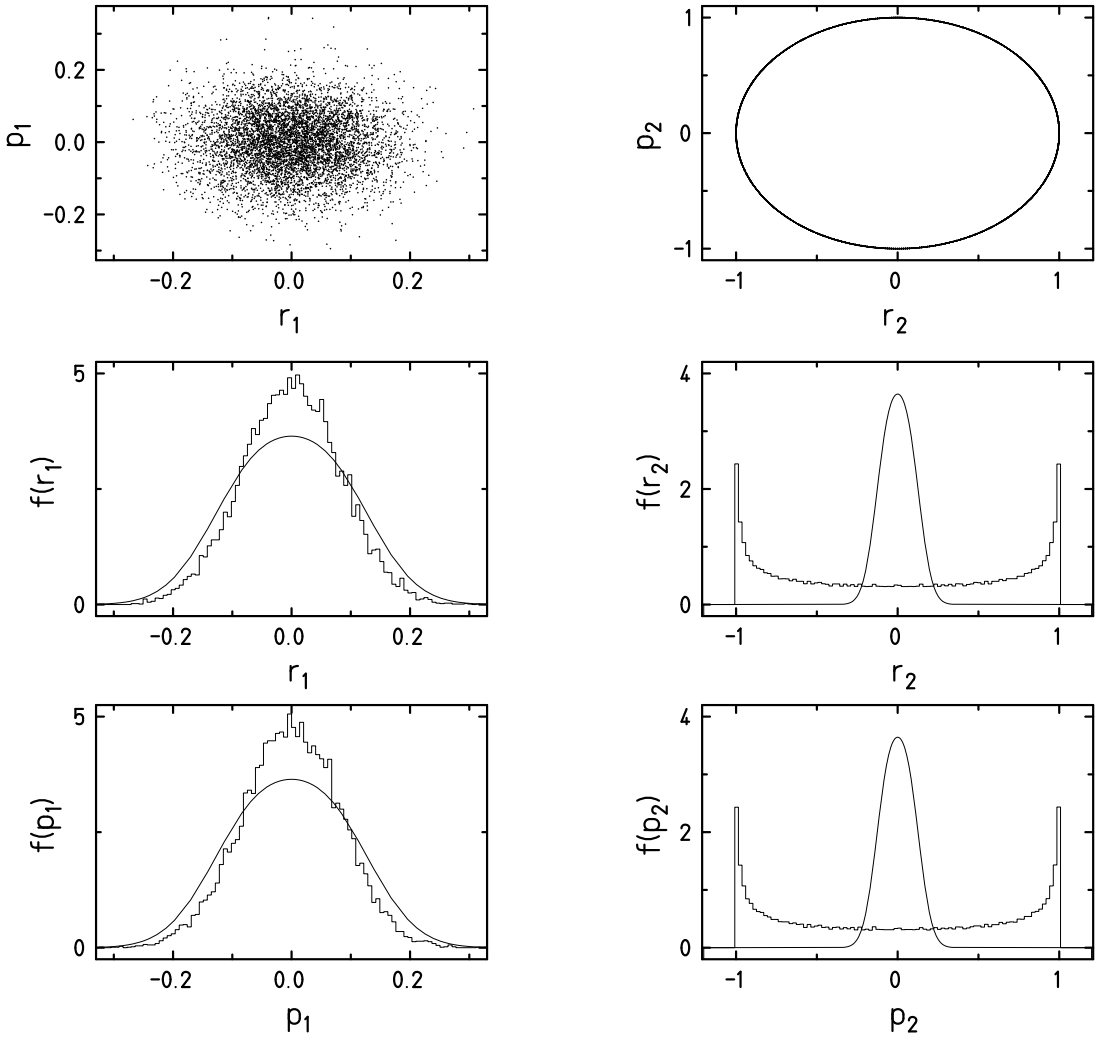

Figure 5.11.: Density plots and marginal distributions at $T = 0.2$ for a Nosé-Hoover scheme in which only particle 1 is coupled to a chain thermostat of length $M = 2$. The equations of motion of particle 2 have not been modified. Note that on the right panel, different scales have been used on all axes.

panel. We attribute this improved ergodicity to the increased complexity of the two-particle dynamics due to the statistical interaction force.

The problem of non-ergodic behaviour at low temperatures is resolved by a scheme involving the coupling of a Nosé-Hoover chain of length $M = 2$ to both p_1 and p_2. If in addition the values of the parameters Q_1 and Q_2 are adapted according to the rule of thumb $Q_i \approx T^2$, ergodic behaviour is found over the entire temperature range investigated that reaches down to $T = 0.04$. A study of even lower temperatures was prohibited by numerical difficulties.

We note that it is not sufficient to couple a second thermostating pseudofriction coefficient to only one parameter, say p_{η_1}. In this case, the marginals of p_{η_2} are not sampled correctly at temperature values $T \lesssim 0.3$. This illustrates the limits of the improved ergodicity due to the statistical interaction.

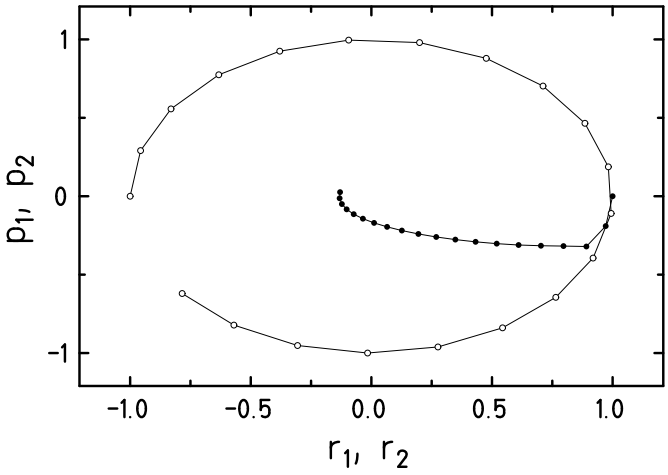

Figure 5.12.: Short-time behaviour of the scheme in which only one particle is coupled to a chain thermostat, $T = 0.2$. The initial conditions are $r_1(0) = -r_2(0) = 1.0$, $p_1(0) = p_2(0) = 0$, and the total integration time is $0.9\mathcal{T}$. It is nicely visible that particle 1 is cooled by the Nosé-Hoover chain, while particle 2 performs an undisturbed oscillatory motion in the harmonic potential.

More drastically, if only p_1 is coupled to a Nosé-Hoover chain of length $M = 2$, the dynamics of the parameters r_2 and p_2 is not affected at all. Hence, the energy of particle 2 is an additional conserved quantity. Although the parameters of particle 2 influence the motion of particle 1 via the value of V, there is no feedback mechanism in the opposite direction. Consequently, only particle 1 experiences the statistical interaction (which remains very weak, since the two fermions stay a considerable distance apart in phase space), whereas particle 2 rotates uniformly on a circle of constant radius, corresponding to the unperturbed motion of a particle in a harmonic oscillator potential. The resulting marginal distributions are shown in figure 5.11. Although the marginal distributions of r_1 and p_1 are not sampled exactly, the deviation is fairly small, and vanishes completely at higher temperature values (not shown). In contrast, the uniform rotation of the second particle leads to a microcanonical distribution. Figure 5.12 illustrates the short-time behaviour of this dynamical scheme.

5.2.2.2. The demon method

We have also applied the cubic coupling scheme (2.32) to the case of two fermions, using the rules of thumb for the adjustment of the coupling constants that have been presented in section 5.1.3. These adaptation rules turn out to be very efficient in providing ergodic motion in the present two-particle case, in contrast to what has been observed for a single particle. Yet, at temperature values below $T \approx 0.1$, we find the following feature unprecedented in the classical applications of the method: The pseudofriction coefficients ξ_1 and ξ_2 "freeze", i. e., they remain very close to their initial value, see figure 5.13. Although the marginals of the original system are still sampled with good precision, the distributions of ξ_1 and ξ_2 are narrowly peaked around their initial value and therefore completely wrong. This deficiency is not cured by choosing modified values for the coupling constants κ_{r_1} and κ_{r_2}. However, since we find that the marginals of the coefficients ζ_1 and ζ_2 are well matched, we attribute it to the *linear* coupling of ξ_1 and ξ_2 in the two-particle version of the equations of motion (4.19).

Therefore, we have also investigated the following set of equations of motion,

$$
\begin{aligned}
\frac{d}{dt}\, r_1 &= \frac{p_1}{m} - \xi_1^3 r_1 \ , \\
\frac{d}{dt}\, p_1 &= -m\omega^2 r_1 - \zeta_1^3 p_1 \ , \\
\frac{d}{dt}\, r_2 &= \frac{p_2}{m} - \xi_2^3 r_2 \ , \\
\frac{d}{dt}\, p_2 &= -m\omega^2 r_2 - \zeta_2^3 p_2 \ , \\
\frac{d}{dt}\, \xi_1 &= \frac{\kappa_{r_1}}{\beta} \left(m\omega^2 r_1^2 \frac{e^{\beta\hbar\omega} - 1}{\hbar\omega} - 1 - m\omega^2 r_1 \frac{r_1 - r_2}{\hbar\omega} \frac{1}{e^V - 1} \right) \ , \\
\frac{d}{dt}\, \xi_2 &= \frac{\kappa_{r_2}}{\beta} \left(m\omega^2 r_2^2 \frac{e^{\beta\hbar\omega} - 1}{\hbar\omega} - 1 + m\omega^2 r_2 \frac{r_1 - r_2}{\hbar\omega} \frac{1}{e^V - 1} \right) \ , \\
\frac{d}{dt}\, \zeta_1 &= \frac{\kappa_{p_1}}{\beta} \left(\frac{p_1^2}{m} \frac{e^{\beta\hbar\omega} - 1}{\hbar\omega} - 1 - \frac{p_1}{m} \frac{p_1 - p_2}{\hbar\omega} \frac{1}{e^V - 1} \right) \ , \\
\frac{d}{dt}\, \zeta_2 &= \frac{\kappa_{p_2}}{\beta} \left(\frac{p_2^2}{m} \frac{e^{\beta\hbar\omega} - 1}{\hbar\omega} - 1 + \frac{p_2}{m} \frac{p_1 - p_2}{\hbar\omega} \frac{1}{e^V - 1} \right) \ ,
\end{aligned}
\tag{5.9}
$$

in which ξ_1 and ξ_2 are cubically coupled to the equations of motion, just as ζ_1 and ζ_2. Choosing all coupling constants to be of the order of magnitude $1/T$, we found ergodic behaviour down to $T = 0.05$ for this scheme, see figure 5.13, right panel.

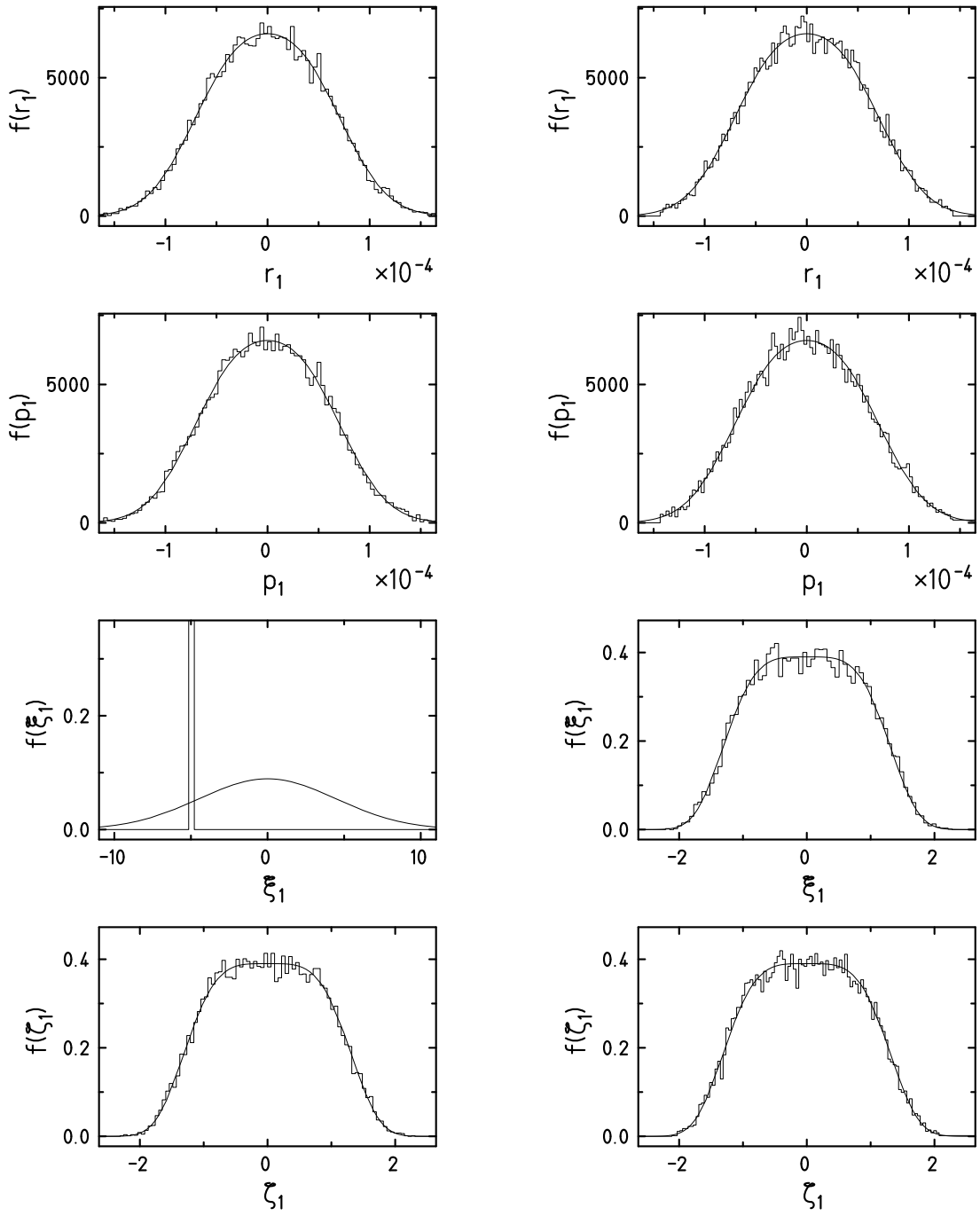

Figure 5.13.: Marginal distributions obtained at $T = 0.05$ with a cubic coupling scheme (left panel), and with the scheme described by the set of equations of motion (5.9). The initial value of ξ_1 on the left panel is $\xi_1(0) = -5.1$, and the "freezing" is striking. Surprisingly, all other marginals are well reproduced. The right panel illustrates that the problem is resolved by the modified scheme (5.9).

5.2.3. Ergodicity investigations for two bosons

The extensive study of the preceding section 5.2.2 may be repeated for the two-boson system. Basically, it turns out that the main features are preserved, which is why we give only a brief survey of the results.

5.2.3.1. Nosé-Hoover method

Like in the fermionic case, the simple Nosé-Hoover scheme is not ergodic in the temperature range $T \lesssim 1.0$. Above that value, with the known adaptation of the thermostat masses, the agreement between the sampled histograms and the theoretical marginals becomes satisfying.

The scheme with two Nosé-Hoover chains of length $M = 2$ is found to be ergodic over the entire temperature range. The smallest temperature value that has been investigated is $T = 0.025$.

5.2.3.2. The demon method

Employing the cubic coupling scheme, we find again that the pseudofriction coefficients ξ_1 and ξ_2 that are linearly coupled to the equations of motion of r_1 and r_2, respectively, "freeze" at temperatures below $T \approx 0.1$. As can be inferred from figure 5.14, this problem is cured by coupling ξ_1 and ξ_2 cubically, in analogy to the scheme (5.9).

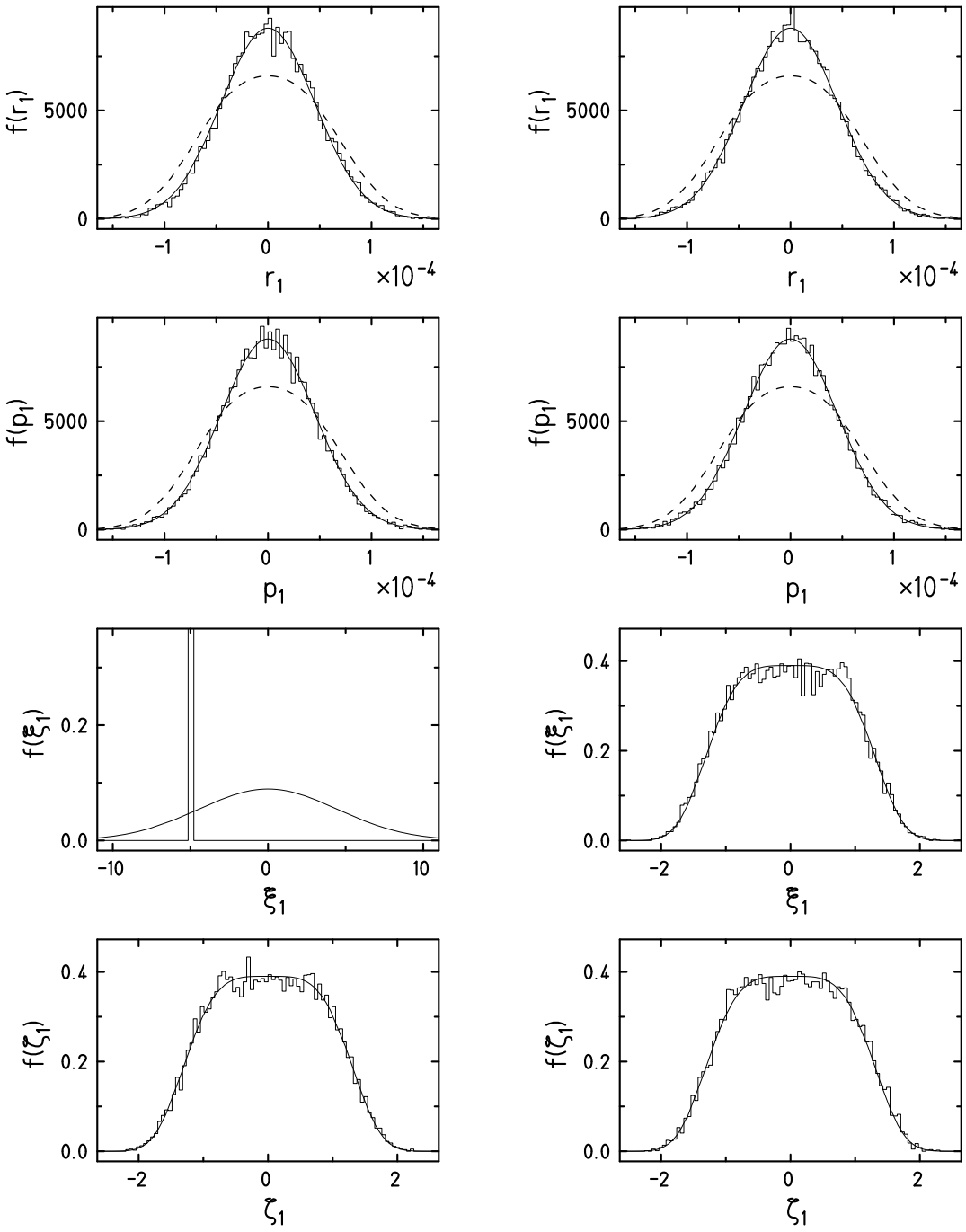

Figure 5.14.: Same figure as 5.13, but for a two-boson system. The figure is given to exemplify the statement that the key features of the dynamics are preserved in the boson case. The dashed lines in the upper four figures correspond to the respective fermionic marginals.

5.2.4. Convergence speed

Figure 5.15 shows in analogy to figure 5.6 that the convergence speed of the histograms to the exact theoretical marginal distributions in the two-fermion case is again close to its theoretical optimum. The result in the bosonic case is similar.

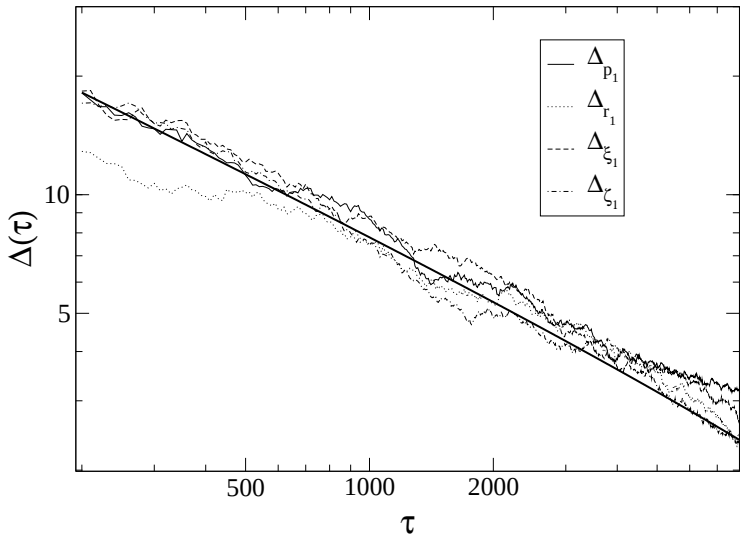

Figure 5.15.: *log – log* – representation of the time evolution of the deviation of the sampled histograms from the respective theoretical distribution using the scheme (5.9) at $T = 0.05$. The bold straight line corresponds to $\Delta(\tau) \propto \tau^{-1/2}$.

5.2.5. Mean values of typical observables

As in the case of a single particle, we compare time averages obtained with our method to the analytically accessible canonical ensemble averages.

The matrix element that is needed for the calculation of the internal energy for fermions reads

$$\frac{\langle\, A_- \,|\, \underset{\sim}{H}^{(2)} \,|\, A_- \,\rangle}{\langle\, A_- \,|\, A_- \,\rangle} = \hbar\omega \left(\frac{1}{2}|\alpha_1 + \alpha_2|^2 + \frac{1}{2} \coth\left(\frac{1}{2}|\alpha_1 - \alpha_2|^2\right)|\alpha_1 - \alpha_2|^2 + 1 \right) \ , \tag{5.10}$$

where $\underset{\sim}{H}^{(2)}$ denotes the Hamiltonian of two non-interacting particles in an external harmonic oscillator potential, (3.52). For two bosons, we obtain

$$\frac{\langle\, A_+ \,|\, \underset{\sim}{H}^{(2)} \,|\, A_+ \,\rangle}{\langle\, A_+ \,|\, A_+ \,\rangle} = \hbar\omega \left(\frac{1}{2}|\alpha_1 + \alpha_2|^2 + \frac{1}{2} \tanh\left(\frac{1}{2}|\alpha_1 - \alpha_2|^2\right)|\alpha_1 - \alpha_2|^2 + 1 \right) \ . \tag{5.11}$$

For the variance of the internal energy, $\mathrm{var}(\underset{\sim}{H}^{(2)}) = \langle\langle\, \underset{\sim}{H}^{(2)\,2} \,\rangle\rangle - \langle\langle\, \underset{\sim}{H}^{(2)} \,\rangle\rangle^2$, one also needs the matrix element of $\underset{\sim}{H}^{(2)\,2}$,

$$\frac{\langle\, A_\varepsilon \,|\, \underset{\sim}{H}^{(2)\,2} \,|\, A_\varepsilon \,\rangle}{\langle\, A_\varepsilon \,|\, A_\varepsilon \,\rangle} \ . \tag{5.12}$$

The result for the numerator reads

$$\begin{aligned}\langle\, \alpha_1,\alpha_2 \,|\, \underset{\sim}{S}_\varepsilon \underset{\sim}{H}^{(2)\,2} \,|\, \alpha_1,\alpha_2 \,\rangle = \qquad\qquad (5.13)\\ \frac{1}{2}\hbar^2\omega^2\Big(\Big(|\alpha_1|^2+\frac{1}{2}\Big)^2+|\alpha_1|^2+\Big(|\alpha_2|^2+\frac{1}{2}\Big)^2+|\alpha_2|^2+2\Big(|\alpha_1|^2+\frac{1}{2}\Big)\Big(|\alpha_2|^2+\frac{1}{2}\Big)\\ +\varepsilon\Big((\alpha_2^*\alpha_1)^2\langle\,\alpha_1\,|\,\alpha_2\,\rangle+(\alpha_1^*\alpha_2)^2\langle\,\alpha_2\,|\,\alpha_1\,\rangle\\ +e^{-|\alpha_1-\alpha_2|^2}\big(2|\alpha_1|^2|\alpha_2|^2+3(\alpha_1^*\alpha_2+\alpha_2^*\alpha_1)+1\big)\Big)\Big)\,.\end{aligned}$$

The analytical expressions for the ensemble averages of the internal energy and its variance are easily derived from the respective partition function $Z_\varepsilon^{(2)}$ (cf. equation (3.56)) via the relations

$$U_\varepsilon^{(2)}(T) = \langle\langle\, \underset{\sim}{H}^{(2)} \,\rangle\rangle(T) = -k_B T^2 \frac{\partial}{\partial T} \ln Z_\varepsilon^{(2)}(T)\,, \tag{5.14}$$

$$\mathrm{var}(\underset{\sim}{H}^{(2)})_\varepsilon(T) = k_B^2 T^4 \,\frac{\partial^2}{\partial T^2} \ln Z_\varepsilon^{(2)}(T)\,. \tag{5.15}$$

Note that if we used the modified partition function $\tilde{Z}_\varepsilon^{(2)} = e^{-\beta\hbar\omega} Z_\varepsilon^{(2)}(T)$ in relation (5.14), we would obtain a function $\tilde{U}_\varepsilon^{(2)}(T)$ satisfying

$$\tilde{U}_\varepsilon^{(2)}(T) = U_\varepsilon^{(2)}(T) + \hbar\omega\,.$$

The result for $\mathrm{var}(\underset{\sim}{H}^{(2)})_\varepsilon$ is not affected.

We restrict ourselves to the presentation of results for the fermionic case, see figure 5.16, since the resulting curves for the two-boson system are identical (variance of the internal energy) or very similar (the internal energy of two bosons differs only by a total shift due to a different ground state energy)[1].

Another interesting and more complex observable that we investigate in the following is the two-particle density denoted by $\rho_\varepsilon^{(2)}(x_1,x_2)$. It gives the conditional probability to find one particle within the interval $[x_2, x_2+\mathrm{d}x_2]$ on the x-axis provided that the other particle is located within $[x_1, x_1+\mathrm{d}x_1]$. Of course, $\rho_\varepsilon^{(2)}(x_1,x_2)$ is given by the thermal average of the absolute square of the normalised two-particle wavefunction,

$$\rho_\varepsilon^{(2)}(x_1,x_2) = \langle\langle\, \frac{|\langle\, x_1,x_2 \,|\, A_\varepsilon\,\rangle|^2}{\langle\, A_\varepsilon \,|\, A_\varepsilon\,\rangle} \,\rangle\rangle\,, \tag{5.16}$$

which can be calculated analytically by the evaluation of the integral

$$\rho_\varepsilon^{(2)}(x_1,x_2) = \frac{1}{\tilde{Z}_\varepsilon^{(2)}} \iint \frac{\mathrm{d}r_1\,\mathrm{d}p_1}{2\pi\hbar}\frac{\mathrm{d}r_2\,\mathrm{d}p_2}{2\pi\hbar}\, w_\varepsilon^{(2)}(r_1,p_1,r_2,p_2)\, \frac{|\langle\, x_1,x_2 \,|\, A_\varepsilon\,\rangle|^2}{\langle\, A_\varepsilon \,|\, A_\varepsilon\,\rangle}\,. \tag{5.17}$$

Since the thermal weight function $w_\varepsilon^{(2)}$ contains the factor $\langle\, A_\varepsilon \,|\, A_\varepsilon\,\rangle$ in the numerator, this term cancels and all integrations can be carried out. We give the exact result of the thermal average

[1] Given the phase space functions (5.10) and (5.11) and the respective thermal weight functions $w_\varepsilon^{(2)}$, both insights are somewhat noteworthy. Note that they imply that ideal Fermi and Bose gases contained in a one-dimensional harmonic oscillator potential have the same specific heat [40].

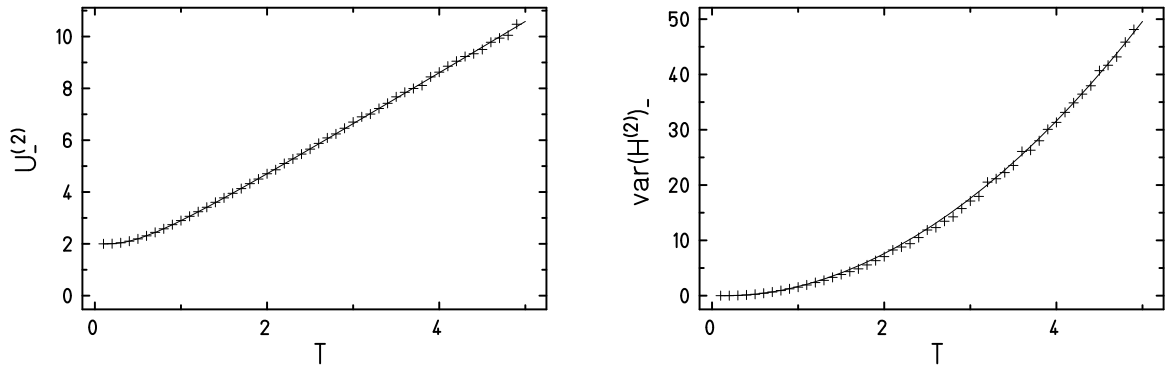

Figure 5.16.: Results of time averages for the internal energy and its variance for two fermions using the cubic coupling scheme (crosses). The solid lines correspond to the respective exact analytical result. The values of the coupling constants have been adapted to temperature according to the rule of thumb $\kappa_i \approx 1/T$, and the sampling time was $\tau = 2000\,\mathcal{T}$ for every temperature value.

of the two-particle density for bosons and fermions in terms of the relative and center-of-mass variables $x_- = \frac{1}{\sqrt{2}}(x_1 - x_2)$, $x_+ = \frac{1}{\sqrt{2}}(x_1 + x_2)$,

$$\rho_\varepsilon^{(2)}(x_-, x_+) = \frac{1}{\tilde{Z}_\varepsilon^{(2)}} \frac{m\omega}{2\pi\hbar} \frac{1}{e^{2\beta\hbar\omega} - 1} \exp\left(-\frac{m\omega}{\hbar} \tanh\left(\frac{1}{2}\beta\hbar\omega\right)(x_+^2 + x_-^2)\right) \cdot \left(1 + \varepsilon \exp\left(-4\frac{m\omega}{\hbar} \frac{e^{\beta\hbar\omega}}{e^{2\beta\hbar\omega} - 1}\, x_-^2\right)\right) . \quad (5.18)$$

As a consequence of the Pauli exclusion principle, the fermionic two-particle density vanishes for $x_- = 0$, whereas for bosons, small values of the relative coordinate have an increased probability density.

In order to give a useful representation of our findings, we present results of time averages along with the respective analytical results for fixed values of x_+ that have been chosen arbitrarily. Figure 5.17 shows an excellent agreement.

Finally, we compare the mean occupation numbers $\langle\langle\ n\ \rangle\rangle(T)$ of the nth oscillator eigenstate in the canonical ensemble at temperature T for the two-fermion system. For *finite* Fermi systems, the grand canonical limit is not applicable, and the mean occupation numbers differ from the Fermi distribution function. Therefore, in order to display the exact results, we have used a recursion relation due to Schönhammer [41]. Figure 5.18 displays again an excellent agreement between time averages and ensemble averages.

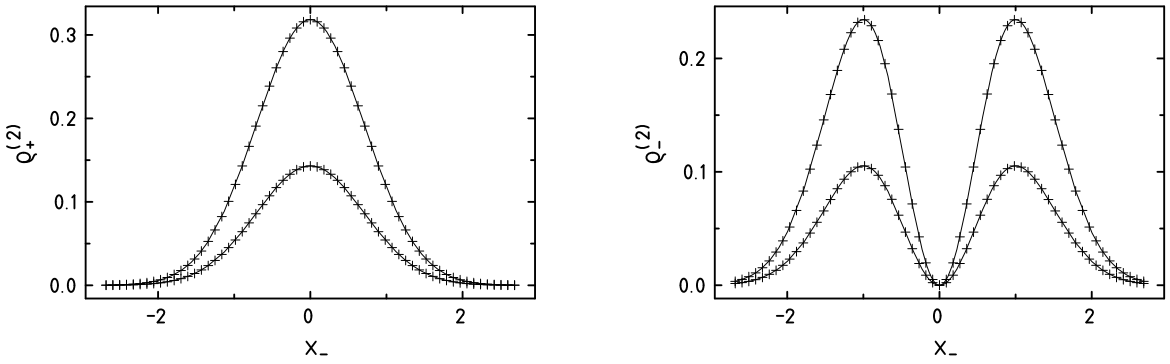

Figure 5.17.: Results of time averages for the bosonic (left figure) and fermionic (right figure) two-particle density. The solid curves correspond to the respective analytical results as given by equation (5.18). The crosses are obtained from the simulations that gave the right hand panels of figure 5.13 and figure 5.14. While the upper line has been obtained by setting $x_+ = 0$, the lower line corresponds to the value $x_+ = 0.894$.

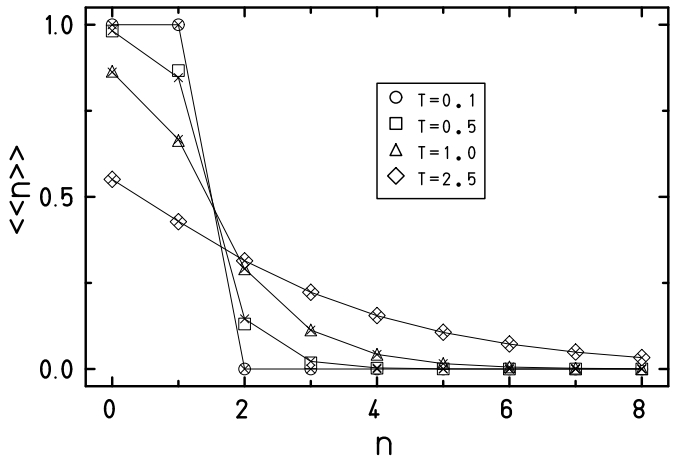

Figure 5.18.: Mean occupation numbers for a two-fermion system at various temperature values. The results obtained by a time average employing the scheme (5.9) (total sampling time $\tau = 1000\,\mathcal{T}$) are displayed by symbols, whereas the exact occupation numbers are given by crosses ($\times$) that are linked by straight lines to guide the eye.

6. Summary and discussion

In this work, we have presented an extension of the powerful techniques of heat bath coupling in classical MD simulations to the quantum harmonic oscillator. The particular framework provided by coherent states allows an immediate access that is able to yield valid isothermal equations of motion both in the elementary case of a single quantum particle and in the more involved cases of indistinguishable particles. Time averages can be performed by direct numerical integration of these equations. For the quantum Nosé-Hoover and related techniques, we have shown that the results thus obtained are in agreement with the respective analytical canonical ensemble averages. Problems of non-ergodic behaviour are a constant topic of concern, but we have proposed and tested a number of effective remedies, like adjustment of coupling constants or addition of further degrees of freedom. These measures can be transferred directly from the classical case, since the thermalising additional degrees of freedom remain essentially classical variables. Moreover, in the case of indistinguishable quantum particles, we observe that due to the statistical interaction the ergodicity of the dynamics improves (see 5.2.2.1). This confirms the widespread opinion that the more involved a dynamics is, the less important ergodicity problems become.

Compared to the approaches of Grilli and Tosatti [17] and Kusnezov [19], substantial progress in basic methodology has been made. On the one hand, the quantum Nosé-Hoover method is more reliable and easier to handle than the Grilli-Tosatti method, and on the other hand, its range of application reaches well beyond the practial scope of Kusnezov's method which is restricted to finite-dimensional quantum systems. Moreover, although deduced in close analogy to classical approaches, the method turns out to be suitable for the sampling of quantum entangled distribution functions. This unexpected feature is a distinction of the quantum Nosé-Hoover method over the approach using a Langevin equation.

However, the present development stage of the method does not yet permit the investigation of quantum systems other than the harmonic oscillator that are not solvable with more traditional methods. It is not clear how an isothermal dynamics scheme can be devised for systems for which the phase space distribution is unknown. Another serious drawback of the entire idea of isothermal quantum dynamics is that it requires that the time evolution of the quantum system is computable, which is just not the case for complicated many-body quantum systems. Put differently, if the time evolution of a quantum system is known, the calculation of its thermodynamical properties is usually also feasible, since the operator of time evolution and the statistical density operator are both exponentials of the Hamiltonian operator of the system. So the solution of the Schrödinger equation and the calculation of the partition function usually amount to the same problem.

The most promising prospect that our method offers lies in a combination with approximate quantum dynamics schemes. A variety of such schemes is available some of which are based on the time-dependent quantum variational principle,

$$\delta \int_{t_1}^{t_2} \mathrm{d}t \, \langle \, Q(t) \, | \, i\hbar \frac{d}{dt} \; - \underset{\sim}{H} \, | \, Q(t) \, \rangle = 0 \; , \tag{6.1}$$

which allows to derive approximations to the time-dependent Schrödinger equation. Typically,

the trial states $|\, Q(t) \,\rangle$ are given in terms of parameters, and (6.1) is used to determine the equations of motion of these parameters. In the method of Fermionic Molecular Dynamics (FMD) [10], $|\, Q(t) \,\rangle$ is a Slater determinant of single-particle Gaussian wave packets parametrised by mean position, mean momentum, and complex width[1]. FMD has been developed and successfully employed in nuclear physics, e. g. for the description of the nuclear liquid-gas phase transition [42]. Beyond, its statistical properties have been studied extensively [43], and even a thermostating method using a thermometer and a feedback mechanism has been developed (cf. chapter 1).

Given the availability of these powerful approximate quantum dynamics schemes, a new field of possible research opens. How can we combine the thermostating method developed in this work with, e. g., FMD in order to obtain an isothermal dynamical scheme for a complex interacting fermion system? This question is very timely in view of recent experiments investigating the behaviour of trapped Fermi gases. In view of the fact that at low temperatures, the trapped fermions form an ideal gas and the trapping potential may be considered harmonic, the isothermal quantum dynamics scheme developed in the present work can be considered a good starting point for a perturbative treatment that is correct in the limit of vanishing interaction and a harmonic confining potential.

Another idea of combining FMD with a thermostat is to cool the system of interest "sympathetically", i. e. via an interaction between particles that are kept at a constant temperature by a quantum Nosé-Hoover-chain and the physical system under investigation. This corresponds precisely to the experimental technique of "sympathetic cooling" currently employed to investigate ultracold fermionic gases [13]. Again, the thermalising of the particles coupled to a Nosé-Hoover chain would correspond to a thermalising of non-interacting particles, which is only approximately correct since we need to employ an interaction to enable the sympathetic cooling.

Despite these difficulties, an important asset of an isothermal MD scheme is that it can possibly provide temporal information, in particular time correlation functions. Although it is not clear to which degree the extended system methods realistically mimic the heat bath interaction, the underlying equations of motion are physically reasonable. Therefore, in principle, this method is tailor-made to model the particle dynamics at constant temperature in a magnetic trap. Employing a two-body interaction and FMD, the resulting trajectory is a well-defined approximation of the exact quantum time development which is determined by forces and the heat bath interaction, providing a good picture of temporal correlations. This is to be contrasted to MC calculations where no dynamical equations are solved and the resulting MC trajectories are unphysical.

It is noteworthy that our method offers in combination with FMD a new perspective for the calculation of fermionic systems at low temperatures, while the path-integral MC methods have been very successful for bosons. Hence, our method may be regarded as complementary to MC approaches also in this respect.

In summary, the developments of the present work offer a variety of new approaches in the simulation of quantum systems at finite temperature. In combination with the ongoing investigations of ultracold trapped quantum gases, new and rich physical insights are to be expected in this field.

[1] These wave packets are frequently referred to as *squeezed states* and may be regarded as generalisations of coherent states. Therefore, an application of the thermostats developed in the present work to FMD appears feasible.

A. The Grilli-Tosatti thermostat

This appendix gives a brief general review of the quantum thermostat method proposed by Grilli and Tosatti [17] along with a discussion of the problems encountered when applying it to the harmonic oscillator.

The method is based on the following theorem. Consider a general quantum Hamiltonian $\underset{\sim}{H}$,

$$\underset{\sim}{H}(\underset{\sim}{r},\underset{\sim}{p}) = \sum_{i=1}^{N} \frac{\underset{\sim}{p}_i^2}{2m_i} + V(\underset{\sim}{r}) \ . \tag{A.1}$$

The thermal average of a quantum observable $\underset{\sim}{B}$, which is supposed to be some function of the operators of position and momentum,

$$\langle\langle\ \underset{\sim}{B}(\underset{\sim}{r},\underset{\sim}{p})\ \rangle\rangle = \frac{\mathrm{Tr}\,(\underset{\sim}{B}e^{-\beta\underset{\sim}{H}})}{\mathrm{Tr}\,e^{-\beta\underset{\sim}{H}}} \ , \tag{A.2}$$

is equal to the following *microcanonical* average

$$\langle\langle\ \underset{\sim}{B}\ \rangle\rangle_{mc} = \frac{\iint \mathrm{d}p_s\mathrm{d}s\,\mathrm{Tr}\left(\underset{\sim}{B}(s\underset{\sim}{r},\underset{\sim}{p}/s)\delta(E-\underset{\sim}{H}_{ext})\right)}{\iint \mathrm{d}p_s\mathrm{d}s\,\mathrm{Tr}\left(\delta(E-\underset{\sim}{H}_{ext})\right)} \ , \tag{A.3}$$

where $\underset{\sim}{H}_{ext}$ denotes the extended Hamiltonian

$$\underset{\sim}{H}_{ext} = \underbrace{\sum_{i=1}^{N} \frac{\underset{\sim}{p}_i^2}{2m_i s^2} + V(s\underset{\sim}{r})}_{\underset{\sim}{H}_s = \underset{\sim}{H}(s\underset{\sim}{r},\underset{\sim}{p}/s)} + \frac{p_s^2}{2Q} + k_B T \ln s \ , \tag{A.4}$$

where $\underset{\sim}{H}_s$ is obtained from the original Hamiltonian by a scaling of the operators $\underset{\sim}{r}$ and $\underset{\sim}{p}$ to $s\underset{\sim}{r}$ and $\underset{\sim}{p}/s$, respectively.

The proof of the theorem is based on the fact that this scaling leaves the trace of any operator $\underset{\sim}{B}(\underset{\sim}{r},\underset{\sim}{p})$ invariant. This is seen most easily if one considers that the following unitary operator[1],

$$\underset{\sim}{U}_s = \exp\left(\frac{i}{2}\ln s(\underset{\sim}{r}\underset{\sim}{p} + \underset{\sim}{p}\underset{\sim}{r})\right) \ , \tag{A.5}$$

precisely performs the scalings

$$\underset{\sim}{U}_s\underset{\sim}{r}\,\underset{\sim}{U}_s^\dagger = s\underset{\sim}{r} \ , \qquad \underset{\sim}{U}_s\underset{\sim}{p}\,\underset{\sim}{U}_s^\dagger = \underset{\sim}{p}/s \ . \tag{A.6}$$

[1] $\hbar$ has been set equal to 1 in this appendix.

As a result, we have

$$\underset{\sim}{U}_s \underset{\sim}{H} \underset{\sim}{U}_s^\dagger = \underset{\sim}{H}_s \ , \tag{A.7}$$

and any unitary transformation is obviously trace-invariant. Therefore, the numerator of (A.3) can be transformed into

$$\iint \mathrm{d}p_s \mathrm{d}s \, \mathrm{Tr}\left(\underset{\sim}{B}(s\underset{\sim}{r}, \underset{\sim}{p}/s)\delta(E - \underset{\sim}{H}_s)\right) = \tag{A.8}$$
$$\iint \mathrm{d}p_s \mathrm{d}s \int \mathrm{d}x \, \langle\, x \,|\, \underset{\sim}{B}(\underset{\sim}{r}, \underset{\sim}{p})\delta(E - \underset{\sim}{H}(\underset{\sim}{r}, \underset{\sim}{p}) - \frac{p_s^2}{2Q} - k_B T \ln s) \,|\, x \,\rangle \ ,$$

where we have dropped the unitary scaling of $\underset{\sim}{H}$ and used a representation of the identity operator $\underset{\sim}{\mathbf{1}} = \int \mathrm{d}x \ |\, x \,\rangle\langle\, x \,|$ (with $|\, x \,\rangle$ being the eigenstates of $\underset{\sim}{r}$, i. e., $\underset{\sim}{r} \,|\, x \,\rangle = x \,|\, x \,\rangle$) to evaluate the trace. An analogous calculation holds for the denominator. Now the integrations over the variables s and p_s inside the δ-function can be carried out, and after cancelling overall prefactors, we obtain the result

$$\langle\langle\, \underset{\sim}{B} \,\rangle\rangle_{mc} = \frac{\int \mathrm{d}x \, \langle\, x \,|\, \underset{\sim}{B} e^{-\beta \underset{\sim}{H}} \,|\, x \,\rangle}{\int \mathrm{d}x \, \langle\, x \,|\, e^{-\beta \underset{\sim}{H}} \,|\, x \,\rangle} \ , \tag{A.9}$$

where the right hand side corresponds to the usual quantum canonical average.

The theorem of Grilli and Tosatti is potentially very powerful since – contrary to the quantum Nosé-Hoover method developed for the harmonic oscillator in this work – it applies to *any* Hamiltonian of the general form (A.1).

However, the practical application of the theorem turns out to be delicate. In order to be able to replace the microcanonical average of equation (A.3) by a time average, a dynamical scheme is needed that samples the microcanonical distribution function $\delta(E - \underset{\sim}{H}_s)$ on the mixed quantum-classical state space consisting of quantum states $|\, \Psi \,\rangle$ and two real numbers s, p_s. In other words, the equations of motion have to conserve the quantity

$$E' = \langle\, \Psi \,|\, \underset{\sim}{H}_s \,|\, \Psi \,\rangle + \frac{p_s^2}{2Q} + k_B T \ln s \tag{A.10}$$

and need to be ergodic. Grilli and Tosatti have proposed the following set of equations of motion,

$$\begin{aligned} i\frac{d}{dt} \ |\, \Psi(t) \,\rangle &= \underset{\sim}{H}_s \,|\, \Psi(t) \,\rangle \ , \\ \frac{d}{dt} \, s &= \frac{p_s}{M} \ , \\ \frac{d}{dt} \, p_s &= -\frac{T}{s} - \langle\, \Psi(t) \,|\, \left(\frac{\partial}{\partial s} \underset{\sim}{H}_s\right) \,|\, \Psi(t) \,\rangle \ . \end{aligned} \tag{A.11}$$

In the following, we show that in the case of the harmonic oscillator, this dynamical scheme does not produce ergodic motion, which means that the method unfortunately fails in this elementary, but ubiquitous model. For simplicity, we consider the motion of a single particle in a one-dimensional harmonic oscillator. The eigenstates of the original

$$\underset{\sim}{H} = \frac{1}{2m} \underset{\sim}{p}^2 + \frac{1}{2} m\omega^2 \underset{\sim}{r}^2 \tag{A.12}$$

and the scaled Hamilton operator

$$\underset{\sim}{H}_s = \frac{1}{2ms^2}\underset{\sim}{p}^2 + \frac{1}{2}ms^2\omega^2\underset{\sim}{r}^2 \tag{A.13}$$

are, respectively,

$$\underset{\sim}{H}\,|\,n\,\rangle = E_n\,|\,n\,\rangle\ , \quad \underset{\sim}{H}_s\,|\,n,s\,\rangle = E_n\,|\,n,s\,\rangle\ . \tag{A.14}$$

Since in the case of the harmonic oscillator the scaling corresponds to a scaling of the mass, $m \to ms^2$, it is particularly evident that the eigenvalues $E_n = \omega(n+1/2)$ are not affected by the scaling, i. e., $\underset{\sim}{H}$ and $\underset{\sim}{H}_s$ are isospectral. Moreover, the following relation for the wavefunctions of the eigenstates holds:

$$\langle\, x\,|\,n,s\,\rangle = \sqrt{s}\,\langle\, sx\,|\,n\,\rangle\ . \tag{A.15}$$

The time-dependent quantum state $|\,\Psi(t)\,\rangle$ can be represented with respect to the basis $\{\,|\,n,s(t)\,\rangle\}$, which itself is time-dependent through the time-dependence of s:

$$|\,\Psi(t)\,\rangle = \sum_{n=0}^{\infty} c_n(t)\,\mathrm{e}^{-iE_nt}\ |\,n,s(t)\,\rangle\ . \tag{A.16}$$

Then the left hand side of the Grilli-Tosatti dynamical equation for the quantum state reads

$$\begin{aligned} i\frac{d}{dt}\ |\,\Psi(t)\,\rangle = i\Bigg(&\sum_n (-iE_n)c_n(t)e^{-iE_nt}E_n\,|\,n,s\,\rangle \\ &+ \sum_n \dot{c}_n(t)e^{-iE_nt}\,|\,n,s\,\rangle \\ &+ \sum_n c_n(t)e^{-iE_nt}\Big(\frac{d}{dt}\ |\,n,s\,\rangle\Big)\Bigg)\ , \end{aligned} \tag{A.17}$$

and for the right hand side we obtain

$$\underset{\sim}{H}_s\,|\,\Psi(t)\,\rangle = \sum_n E_n\,c_n(t)e^{-iE_nt}\,|\,n,s\,\rangle\ . \tag{A.18}$$

The equation of motion simplifies since two sums cancel. The term $d/dt\,|\,n,s\,\rangle$ can be calculated in a straightforward manner. With the obvious notation (using the dimensionless operators $\underset{\sim}{\hat{r}}$ and $\underset{\sim}{\hat{p}}$ of equation (3.1))

$$\underset{\sim}{a}_s = \frac{1}{\sqrt{2}}(s\underset{\sim}{\hat{r}} + i\underset{\sim}{\hat{p}}/s)\ , \tag{A.19}$$

we obtain

$$\begin{aligned} \frac{d}{dt}\ |\,n,s\,\rangle &= \frac{d}{dt}\ \left(\frac{1}{\sqrt{n!}}(a_s^\dagger)^n\,|\,0,s\,\rangle\right) \\ &= \frac{1}{\sqrt{n!}}\left(\Big(\frac{d}{dt}\ (a_s^\dagger)^n\Big)\,|\,0,s\,\rangle + (a_s^\dagger)^n\frac{d}{dt}\ |\,0,s\,\rangle\right)\ . \end{aligned} \tag{A.20}$$

Using

$$\frac{d}{dt}\, a_s^\dagger = \dot{s}\, \frac{\partial}{\partial s} \left(\frac{1}{\sqrt{2}} (s \underset{\sim}{r} - i \underset{\sim}{p}/s) \right) = \frac{\dot{s}}{s}\, a_s \ , \tag{A.21}$$

we find

$$\left(\frac{d}{dt}\, (a_s^\dagger)^n \right) |\, 0, s \,\rangle = \frac{\dot{s}}{s} \frac{n(n-1)}{2} \sqrt{(n-2)!}\, |\, n-2, s \,\rangle \ . \tag{A.22}$$

We also have

$$\frac{d}{dt}\ |\, 0, s \,\rangle = -\frac{\dot{s}}{\sqrt{2}\, s}\, |\, 2, s \,\rangle \ . \tag{A.23}$$

Therefore, we arrive at

$$\frac{d}{dt}\ |\, n, s \,\rangle = \frac{\dot{s}}{2s} \big(\sqrt{n(n-1)}\, |\, n-2, s \,\rangle - \sqrt{(n+1)(n+2)}\, |\, n+2, s \,\rangle \big) \ . \tag{A.24}$$

Altogether, we obtain an equation of motion for the expansion coefficients which reads

$$\frac{d}{dt}\, c_n = \frac{\dot{s}}{2\, s} \left(c_{n-2} \sqrt{n(n-1)} - c_{n+2} \sqrt{(n+1)(n+2)} \right) \ . \tag{A.25}$$

Equation (A.24) implies that in this case, the Grilli-Tosatti time evolution conserves the inital partition of probability among states of even and odd parity, since occupation probability is transferred either among basis states with even n (even parity) or odd n (odd parity). This is not surprising since $\underset{\sim}{H}_s$ in the equation of motion of the quantum state (A.11) commutes with the parity operation. Clearly, this additional conservation law is incompatible with ergodicity. This result is corroborated by numerical investigations which show that neither the quantum system attains the desired temperature nor that the marginal of the variable p_s is accurately sampled.

In order to break this conservation law, consider the shifted harmonic oscillator potential (r_0 being a fixed real number),

$$\underset{\sim}{H} = \frac{1}{2m} \underset{\sim}{p}^2 + \frac{1}{2} m\omega^2 (\underset{\sim}{r} - r_0)^2 \ , \tag{A.26}$$

which is not symmetric with respect to the parity operation. Extensive numerical investigations have shown that the sampling of the marginal of the variable p_s is improved, but still, the quantum system does not equilibrate [44].

Nonetheless, we stress that the theorem provided by Grilli and Tosatti appears extremely powerful and deserves further reflection. It will be necessary to devise a dynamical scheme that reliably leads to ergodicity both for elementary and more involved systems.

B. Position representation of the canonical density operator

As an example for the usefulness of the formula (3.41),

$$\langle\langle\ \underset{\sim}{B}\ \rangle\rangle = \frac{1}{\tilde{Z}^{(1)}(\beta)} \int \frac{\mathrm{d}r\,\mathrm{d}p}{2\pi\hbar}\ w^{(1)}(r,p)\ \mathcal{B}(r,p)\ , \tag{B.1}$$

with

$$\mathcal{B}(r,p) = \langle\, r,p \,|\, \underset{\sim}{B} \,|\, r,p \,\rangle\ , \tag{B.2}$$

we present here an elementary and straightforward calculation of the position representation of the density operator

$$\underset{\sim}{\rho} = \frac{1}{Z^{(1)}(\beta)} \sum_{n=0}^{\infty} \exp(-\beta E_n)\ |\, n \,\rangle\langle\, n \,|\ \ , \tag{B.3}$$

i. e., we calculate the matrix elements

$$\rho(x,x') = \langle\, x \,|\, \underset{\sim}{\rho} \,|\, x' \,\rangle\ . \tag{B.4}$$

Note that the probability distribution of the position of a particle in a harmonic oscillator potential at temperature T,

$$g(x) = \frac{1}{Z(\beta)} \sum_{n=0}^{\infty} \exp(-\beta E_n)\ |\langle\, x \,|\, n \,\rangle|^2\ , \tag{B.5}$$

is equal to the diagonal matrix element $\langle\, x \,|\, \underset{\sim}{\rho} \,|\, x \,\rangle$ of the density operator. Moreover, $g(x)$ is closely related to the Wigner function $W(x,p)$ of the thermal state (B.3), since the marginal distribution of the variable x of the Wigner function corresponds to $g(x)$,

$$g(x) = \int \mathrm{d}p\, W(x,p)\ . \tag{B.6}$$

$\rho(x,x')$ may be calculated by an immediate evaluation of the expression (B.4) using the representation (B.3) for $\underset{\sim}{\rho}$. For this direct calculation, an elaborate relation for Hermite polynomials that is accessible from an integral representation of the Hermite polynomials is indispensable [35]. Another approach which works only for the diagonal matrix element consists of solving a differential equation for $\langle\, x \,|\, \underset{\sim}{\rho} \,|\, x \,\rangle$ [45]. In addition to these known approaches, we propose here to rephrase $\rho(x,x')$, which is in general a complex number, as the thermal expectation

value of a non-hermitian operator,

$$\begin{aligned}\rho(x,x') &= \frac{1}{Z^{(1)}(\beta)}\sum_{n=0}^{\infty}\exp(-\beta E_n)\langle\, x\,|\,n\,\rangle\langle\, n\,|\,x'\,\rangle \\ &= \frac{1}{Z^{(1)}(\beta)}\sum_{n=0}^{\infty}\exp(-\beta E_n)\langle\, n\,|\,x'\,\rangle\langle\, x\,|\,n\,\rangle \\ &= \langle\langle\ |\,x'\,\rangle\langle\, x\,|\ \rangle\rangle\ ,\end{aligned} \tag{B.7}$$

and to use (B.1) for the calculation of the thermal average. The evaluation of the integral

$$\rho(x,x') = \frac{1}{\tilde{Z}^{(1)}(\beta)}\int\frac{\mathrm{d}r\,\mathrm{d}p}{2\pi\hbar}\,w^{(1)}(r,p)\,\langle\, r,p\,|\,x\,\rangle\langle\, x'\,|\,r,p\,\rangle \tag{B.8}$$

is straightforward. The integration over p is trivial, and the integration over r can be carried out directly by addition and subtraction of the quadratic completion in the exponent. Using the identities

$$\frac{2}{e^{\beta\hbar\omega}-1} = \coth\left(\frac{1}{2}\beta\hbar\omega\right) - 1\ , \tag{B.9}$$

$$\text{and}\quad -\frac{2}{e^{\beta\hbar\omega}+1} = \tanh\left(\frac{1}{2}\beta\hbar\omega\right) - 1\ , \tag{B.10}$$

we finally obtain the result

$$\begin{aligned}\rho(x,x') = &\sqrt{\frac{m\omega}{\hbar\pi}\tanh\left(\frac{1}{2}\beta\hbar\omega\right)} \\ &\cdot\exp\left(-\frac{m\omega}{4\hbar}\tanh\left(\frac{1}{2}\beta\hbar\omega\right)(x+x')^2 - \frac{m\omega}{4\hbar}\coth\left(\frac{1}{2}\beta\hbar\omega\right)(x-x')^2\right)\ ,\end{aligned} \tag{B.11}$$

in agreement with the direct evaluation of (B.4) [35]. The spatial probability density of a particle on the x-axis is

$$\rho(x,x) = g(x) = \sqrt{\frac{m\omega}{\hbar\pi}\tanh\left(\frac{1}{2}\beta\hbar\omega\right)}\ \exp\left(-\frac{m\omega}{\hbar}\tanh\left(\frac{1}{2}\beta\hbar\omega\right)x^2\right)\ . \tag{B.12}$$

We stress that compared to the other known approaches this calculation has the pedagogical advantage of being very simple and straightforward.

C. Sinusoidal oscillations of displaced harmonic oscillator eigenfunctions[1]

The remarkably simple time evolution of a coherent state in a harmonic oscillator potential, equation (3.25), initially found by Schrödinger [33], is at the heart of the translation of the classical Nosé-Hoover method to quantum dynamics. It implies that the mean position and the mean momentum of the Gaussian wavepacket follow the solutions of the equations of motion of the corresponding classical oscillator, and, moreover, that the shape of the wavepacket remains constant.

This behaviour is a special case of a more general equation found in 1954 by I. R. Senitzky [46]. He has shown that in a harmonic oscillator potential, all the various eigenfunctions $u_n(x) = \langle\, x \,|\, n \,\rangle$, if displaced in coordinate and momentum space, oscillate sinusoidally in time while maintaining a fixed shape, i. e.

$$|\psi(x,t)|^2 = |u_n(x - q_0(t))|^2 \ , \quad q_0(t) = a\cos(\omega t + \theta) \ , \tag{C.1}$$

where a and θ are arbitrary constants. The time evolution of a coherent state is a special case of this equation which is obtained by setting $n = 0$.

Senitzky derived this result by performing an elegant analysis of the time-dependent Schrödinger equation in the coordinate representation. The purpose of this appendix is to present two alternate instructive methods for proving Senitzky's result, the first using coherent states, the second using the displacement operator.

In section 3.2 we have expressed the time evolution of a coherent state as follows:

$$\begin{aligned} e^{-\frac{i}{\hbar}\underset{\sim}{H}t}\,|\,\alpha\,\rangle &= e^{-i\omega t(\underset{\sim}{a}^\dagger\underset{\sim}{a}+\frac{1}{2})}\underset{\sim}{D}(\alpha)\,|\,0\,\rangle \\ &= e^{-i\omega t\frac{1}{2}}\,|\,e^{-i\omega t}\alpha\,\rangle \\ &= e^{-i\omega t\frac{1}{2}}\underset{\sim}{D}(e^{-i\omega t}\alpha)\,|\,0\,\rangle \ . \end{aligned} \tag{C.2}$$

Using the notation of the displacement operator, Senitzky's finding, (C.1), that *any* initially displaced eigenfunction undergoes sinusoidal oscillations while maintaining constant shape, may be rephrased as

$$e^{-i\omega t(\underset{\sim}{a}^\dagger\underset{\sim}{a}+\frac{1}{2})}\underset{\sim}{D}(\alpha)\,|\,n\,\rangle = e^{-i\omega t(n+\frac{1}{2})}\underset{\sim}{D}(e^{-i\omega t}\alpha)\,|\,n\,\rangle \ . \tag{C.3}$$

We will prove this form of the theorem first by means of an expansion of $|\,n\,\rangle$ into coherent states, thereby arriving at a very straightforward calculation. Secondly, we will derive a general relation, (C.9), between the displacement and the time evolution operators, from which (C.3) follows immediately.

[1] This appendix is similar to a part of the article "Almost-periodic wave packets and wave packets of invariant shape" that has been submitted to American Journal of Physics, in collaboration with Prof. M. Luban, Ames Laboratory, Ames, Iowa, USA.

a. Our first method of establishing the theorem of (C.3) exploits the fact that the general energy eigenstate $|\,n\,\rangle$ may be expanded as an integral over the coherent states $|\,\beta\,\rangle$ defined on a circle in the complex plane with radius $|\beta| = \beta_0$, where β_0 is an arbitrary positive number. In order to find this expansion, we start with the familiar expansion of a coherent state $|\,\alpha\,\rangle$ in an infinite series of oscillator eigenstates $|\,m\,\rangle$,

$$|\,\alpha\,\rangle = e^{-\frac{1}{2}|\alpha|^2} \sum_{m=0}^{\infty} \frac{\alpha^m}{\sqrt{m!}}\,|\,m\,\rangle\ . \tag{C.4}$$

Writing $|\beta|e^{i\theta}$ for α, multiplying both sides of this equation by $e^{-in\theta}$ and integrating on θ from $-\pi$ to π one obtains

$$|\,n\,\rangle = \mathcal{N}_n(|\beta|) \int_{-\pi}^{\pi} \mathrm{d}\theta e^{-in\theta}\,|\,|\beta|e^{i\theta}\,\rangle\ , \tag{C.5}$$

the normalization factor $\mathcal{N}_n(|\beta|)$ being

$$\mathcal{N}_n(|\beta|) = \frac{1}{2\pi} e^{\frac{1}{2}|\beta|^2} \frac{\sqrt{n!}}{|\beta|^n}\ . \tag{C.6}$$

Using the well-known formula [32, p. 40] $e^{\underset{\sim}{A}+\underset{\sim}{B}} = e^{\underset{\sim}{A}} e^{\underset{\sim}{B}} e^{-[\underset{\sim}{A},\underset{\sim}{B}]/2}$ which applies if both $\underset{\sim}{A}$ and $\underset{\sim}{B}$ commute with $[\underset{\sim}{A}, \underset{\sim}{B}]$, one easily obtains the following identity for the displacement operator:

$$\underset{\sim}{D}(\alpha+\beta) = \underset{\sim}{D}(\alpha)\underset{\sim}{D}(\beta)e^{i\,\mathrm{Im}(\alpha^*\beta)}\ . \tag{C.7}$$

Using equations (C.2), (C.5), and (C.7), the following calculation is straightforward:

$$\begin{aligned}
e^{-i\omega t\underset{\sim}{a}^\dagger \underset{\sim}{a}}\,\underset{\sim}{D}(\alpha)\,|\,n\,\rangle &= \mathcal{N}_n(|\beta|) \int_{-\pi}^{\pi} \mathrm{d}\theta e^{-in\theta} e^{-i\omega t\underset{\sim}{a}^\dagger \underset{\sim}{a}} \underset{\sim}{D}(\alpha)\underset{\sim}{D}(\beta)\,|\,0\,\rangle \\
&= \mathcal{N}_n(|\beta|) \int_{-\pi}^{\pi} \mathrm{d}\theta e^{-in\theta} e^{i\mathrm{Im}(\alpha\beta^*)}\,\underset{\sim}{D}(e^{-i\omega t}(\alpha+\beta))\,|\,0\,\rangle \\
&= \mathcal{N}_n(|\beta|) \int_{-\pi}^{\pi} \mathrm{d}\theta e^{-in\theta} \underset{\sim}{D}(e^{-i\omega t}\alpha)\underset{\sim}{D}(e^{-i\omega t}\beta)\,|\,0\,\rangle \\
&= \underset{\sim}{D}(e^{-i\omega t}\alpha)\mathcal{N}_n(|\beta|) \int_{-\pi}^{\pi} \mathrm{d}\theta e^{-in\theta}\,|\,e^{-i\omega t}\beta\,\rangle \\
&= e^{-in\omega t}\underset{\sim}{D}(e^{-i\omega t}\alpha)\mathcal{N}_n(|\beta|) \int_{-\pi}^{\pi} \mathrm{d}\theta e^{-in(\theta-\omega t)}\,|\,e^{i(\theta-\omega t)}|\beta|\,\rangle \\
&= e^{-in\omega t}\underset{\sim}{D}(e^{-i\omega t}\alpha)\,|\,n\,\rangle\ .
\end{aligned} \tag{C.8}$$

This provides our first proof of the theorem of (C.3).

b. A second method for proving (C.3) consists of the following. Inspecting the final result of (C.8), one is led to conjecture the operator identity

$$e^{-i\omega t\underset{\sim}{a}^\dagger \underset{\sim}{a}}\underset{\sim}{D}(\alpha) = \underset{\sim}{D}(e^{-i\omega t}\alpha)e^{-i\omega t\underset{\sim}{a}^\dagger \underset{\sim}{a}}\ , \tag{C.9}$$

which immediately implies the claimed identity (C.3). To prove it, we define the three operators

$$\begin{aligned} \underset{\sim}{A} &= \underset{\sim}{a}^\dagger \underset{\sim}{a} \ , \\ \underset{\sim}{B}_+(\alpha) &= \alpha \underset{\sim}{a}^\dagger + \alpha^* \underset{\sim}{a} \ , \\ \underset{\sim}{B}_-(\alpha) &= \alpha \underset{\sim}{a}^\dagger - \alpha^* \underset{\sim}{a} \ . \end{aligned} \tag{C.10}$$

These satisfy the following commutation relations:

$$\begin{aligned} [\underset{\sim}{A}, \underset{\sim}{B}_\pm(\alpha)] &= \underset{\sim}{B}_\mp(\alpha) \ , \\ [\underset{\sim}{B}_+(\alpha), \underset{\sim}{B}_-(\alpha)] &= 2|\alpha|^2 \underset{\sim}{\mathbb{1}} \ , \\ [\underset{\sim}{A}, [\underset{\sim}{A}, \underset{\sim}{B}_-(\alpha)]] &= \gamma \underset{\sim}{B}_-(\alpha) \ , \end{aligned} \tag{C.11}$$

with $\gamma = 1$. Because of the third commutation relation we may use the standard theorem, valid for any c-number λ [32],

$$e^{\lambda \underset{\sim}{A}} \underset{\sim}{B}_-(\alpha) e^{-\lambda \underset{\sim}{A}} = \underset{\sim}{B}_-(\alpha) \cosh(\lambda\sqrt{\gamma}) \ + \ \frac{[\underset{\sim}{A}, \underset{\sim}{B}_-(\alpha)]}{\sqrt{\gamma}} \sinh(\lambda\sqrt{\gamma}) \ . \tag{C.12}$$

Setting $\lambda = -i\omega t$ and using the first equation of (C.11) as well as the definition of $\underset{\sim}{B}_-(\alpha)$ we obtain

$$e^{-i\omega t \underset{\sim}{A}} \underset{\sim}{B}_-(\alpha) e^{i\omega t \underset{\sim}{A}} = \underset{\sim}{B}_-(\alpha e^{-i\omega t}). \tag{C.13}$$

It then follows that

$$\begin{aligned} e^{-i\omega t \underset{\sim}{A}} (\underset{\sim}{B}_-(\alpha))^2 e^{i\omega t \underset{\sim}{A}} &= e^{-i\omega t \underset{\sim}{A}} \underset{\sim}{B}_-(\alpha) e^{i\omega t \underset{\sim}{A}} e^{-i\omega t \underset{\sim}{A}} \underset{\sim}{B}_-(\alpha) e^{i\omega t \underset{\sim}{A}} \\ &= (\underset{\sim}{B}_-(\alpha e^{-i\omega t}))^2 \end{aligned} \tag{C.14}$$

and thus

$$e^{-i\omega t \underset{\sim}{A}} e^{\underset{\sim}{B}_-(\alpha)} e^{i\omega t \underset{\sim}{A}} = e^{\underset{\sim}{B}_-(\alpha e^{-i\omega t})} \ . \tag{C.15}$$

But we have $e^{\underset{\sim}{B}_-(\alpha)} = \underset{\sim}{D}(\alpha)$, so that (C.15) is the conjectured identity (C.9).

We remark that the harmonic oscillator does not possess any other wave packets of constant shape. This follows from the fact that if one tried to replace the eigenket $|\, n \,\rangle$ in (C.3) by a linear combination, $|\, \psi \,\rangle$, of two or more eigenkets, the right-hand side could not be written as a single time-dependent factor multiplying $\underset{\sim}{D}(e^{-i\omega t}\alpha)\, |\, \psi \,\rangle$.

Bibliography

[1] R. P. Feynman. *Statistical Mechanics.* W. A. Benjamin, Inc., Reading, MA, 1972.

[2] N. Metropolis, A. W. Rosenbluth, M. N. Rosenbluth, A. H. Teller, and E. Teller. *J. Chem. Phys.*, 21:1087, 1953.

[3] M. C. Wang and G. E. Uhlenbeck. *Rev. Mod. Phys.*, 17:323, 1945.

[4] S. Nosé. *J. Chem. Phys.*, 81:511, 1984.

[5] J. Grotendorst, D. Marx, and A. Muramatsu, editors. *Quantum Simulations of Complex Many-Body Systems: From Theory to Algorithms*, volume 10 of *NIC Series.* John von Neumann Institute for Computing (NIC), 2002. p. 211, Chapter "Classical Molecular Dynamics" by G. Sutmann.

[6] Chr. Schröder. *Numerische Simulationen zur Thermodynamik magnetischer Strukturen mittels deterministischer und stochastischer Wärmebadankopplung.* PhD thesis, Universität Osnabrück, 1999.

[7] M. E. Tuckerman and A. Hughes. *Proc. CECAM conference on "Computer simulation of rare events and quantum dynamics in condensed phase systems"*, page 311, 1997. Chapter 14, "Path integral molecular dynamics: A computational approach to quantum statistical mechanics".

[8] D. M. Ceperley. *Rev. Mod. Phys.*, 67:279, 1995.

[9] W. Krauth. *Phys. Rev. Lett.*, 77:3695, 1996.

[10] H. Feldmeier and J. Schnack. *Rev. Mod. Phys.*, 72:655, 2000.

[11] M. H. Anderson, J. R. Ensher, M. R. Matthews, C. E. Wieman, and E. A. Cornell. *Science*, 269:198, 1995.

[12] K. B. Davis, M.-O. Mewes, M. R. Andrews, N. J. van Druten, D. S. Durfee, D. M. Kurn, and W. Ketterle. *Phys. Rev. Lett.*, 75:3969, 1995.

[13] B. DeMarco and D. S. Jin. *Phys. Rev. A*, 58:R4267, 1998.

[14] B. DeMarco and D. S. Jin. *Science*, 285:1703, 1999.

[15] W. Ketterle, D. S. Durfee, and D. M. Stamper-Kurn. *cond-mat/9904034*, 1999.

[16] H. T. C. Stoof, M. Houbiers, C. A. Sackett, and R. G. Hulet. *Phys. Rev. Lett.*, 76:10, 1996.

[17] M. Grilli and E. Tosatti. *Phys. Rev. Lett.*, 62:2889, 1989.

[18] F. Mauri, R. Car, and E. Tosatti. *Europhys. Lett.*, 24:431, 1993.

[19] D. Kusnezov. *Phys. Lett. A*, 184:50, 1993.

[20] J. Schnack. *Physica A*, 259:49, 1998.

[21] F. Reif. *Statistische Physik und Theorie der Wärme.* Walter de Gruyter, Berlin, 3rd edition, 1987.

[22] W. G. Hoover. *Phys. Rev. A*, 31:1695, 1985.

[23] D. Kusnezov, A. Bulgac, and W. Bauer. *Ann. of Phys.*, 204:155, 1990.

[24] G. J. Martyna, M. L. Klein, and M. Tuckerman. *J. Chem. Phys.*, 97:2635, 1992.

[25] S. Nosé. *Prog. Theor. Phys. Suppl.*, 103:1, 1991.

[26] M. E. Tuckerman, C. J. Mundy, and G. J. Martyna. *Europhys. Lett.*, 45:149, 1999.

[27] A. Bulgac and D. Kusnezov. *Phys. Rev. A*, 42:5045, 1990.

[28] M. E. Tuckerman, Y. Liu, G. Ciccotti, and G. J. Martyna. *J. Chem. Phys.*, 115:1678, 2001.

[29] H. G. Schuster. *Deterministic Chaos.* Physik-Verlag, Weinheim, 1984.

[30] B. Diu, C. Guthmann, D. Lederer, and B. Roulet. *Physique statistique.* Hermann, Paris, 1995.

[31] R. J. Glauber. *Phys. Rev.*, 131:2766, 1963.

[32] E. Merzbacher. *Quantum Mechanics.* John Wiley & Sons Inc., New York, 3rd edition, 1998.

[33] E. Schrödinger. *Naturwiss.*, 14:664, 1926.

[34] V. Bargmann, P. Butera, L. Girardello, and J. R. Klauder. *Rep. Math. Phys.*, 2:221, 1971.

[35] W. P. Schleich. *Quantum Optics in Phase Space.* Wiley-VCH, Berlin, 2001.

[36] J. Schnack. *Europhys. Lett.*, 45:647, 1999.

[37] H.-J. Schmidt and J. Schnack. *Physica A*, 265:584, 1999.

[38] D. Mentrup and J. Schnack. *Physica A*, 297:337, 2001.

[39] I. S. Gradshteyn and I. M. Ryzhik. *Table of integrals, series, and products.* Academic Press, San Diego, 4th edition, 1992.

[40] H.-J. Schmidt and J. Schnack. *Physica A*, 260:479, 1998.

[41] K. Schönhammer. *Am. J. Phys.*, 68:1032, 2000.

[42] J. Schnack and H. Feldmeier. *Phys. Lett. B*, 409:6, 1997.

[43] J. Schnack and H. Feldmeier. *Nucl. Phys. A*, 601:181, 1996.

[44] J. Schnack, D. Mentrup, and H. Feldmeier. *Revision of the Grilli-Tosatti quantum thermostat method*, in preparation.

[45] C. Cohen-Tannoudji, B. Diu, and F. Laloë. *Mécanique quantique.* Hermann, Paris, 1995.

[46] I. R. Senitzky. *Phys. Rev.*, 95:1115, 1954.

Acknowledgements

This thesis has been prepared during the past three years in the group "Makroskopische Systeme und Quantentheorie" at the physics department of the University of Osnabrück. I thank all group members for the open and fruitful working atmosphere.

In particular, I am very grateful to PD Dr. J. Schnack who supported the project with both powerful ideas and his unmatched enthusiasm. His ongoing encouragement was very helpful, and I enjoyed working with him very much. He also raised the funds for the project "Isotherme Dynamik kleiner Quantensysteme", giving me the occasion to prepare my thesis in Osnabrück. Financial support of this project by the DFG is gratefully acknowledged.

Prof. K. Bärwinkel and Prof. H.-J. Schmidt provided both support and freedom which helped making my research enjoyable and successful. I also appreciate the collaboration with Dipl.-Phys. F. Homann, his extensive computer support, and his sorcerous inspiration in many respects.

In addition, I would like to express my thanks to Prof. M. Luban who agreed to be an external referee for the present work. I have been working with him for several years on magnetic molecules, but our contact reaches far beyond that. I am especially grateful for the kind hospitality during my stays at the Ames Lab, and for a large number of helpful and enjoyable discussions.

Last but not least, I thank Dr. C. Schröder for a lot of support, advice and guidance over the years, and many helpful and delightful discussions.